Regulation of $CD4^+$ T cell inflammatory response following hematopoietic transplantation.

By

Nikhila Sham Sunder Bharadwaj

A dissertation submitted in partial fulfillment of

the requirements for the degree of

Doctor of Philosophy

(Comparative Biomedical Sciences)

at the

UNIVERSITY OF WISCONSIN-MADISON

2022

Date of final oral examination: 08/22/2021

The dissertation is approved by the following members of the Final Oral Committee:

Jenny E. Gumperz, Professor, SMPH

Christian Mathew Capitini, Associate Professor, SMPH/Pediatrics

Eric Christian Johannsen, Associate Professor, SMPH/School of Medicine

Suresh Marulasiddappa, Professor; Associate Dean for research, Veterinary medicine

Christine M. Seroogy, Professor, SMPH/Pediatrics

Abstract:

Immune complications like graft failure are disproportionately associated with umbilical cord blood (UCB) transplants that limits its clinical use. Excessive activation of donor graft derived T cells following transplantation into a lymphopenic environment is a central driver of graft failure. We have found that co-transplanting human invariant natural killer T (iNKT) cells along with UCB grafts results in markedly enhanced immune engraftment in immunodeficient mice, and this appears to be due to a silencing effect of iNKT cells on expansion and inflammatory activation of UCB T cells. This dissertation aims to investigate pathways that regulate inflammatory activation of T cells in the context of transplantation and mechanisms by which iNKT cells limit T cell inflammation and promote engraftment.

We first sought to investigate how naïve T cells get activated in response to homeostatic signals encountered in a lymphopenic environment. We observed that homeostatic signals provided by autologous monocytes led a fraction of $CD4^+$ T cells to upregulate Th1 associated markers and were able to rapidly make IFNγ. Mechanistic studies revealed that this acquisition of a pathogen-independent memory phenotype (MP) was dependent on self MHC II and ICAM-1. Although generation of a memory phenotype was dependent on T cells receiving a TCR stimulation, LFA-1 ligation by plate bound ICAM-1 alone promoted elevated aerobic glycolysis and mitochondrial activation leading to enhanced IFNγ response to subsequent TCR stimulation while retaining a naïve and stem like phenotype.

Specific pathways employed by iNKT cells to improve engraftment was investigated using complementary in-vitro experiments to our in-vivo hematopoietic engraftment model. We discovered that iNKT cells interact with monocytes to limit MP cell differentiation. Mechanistically, iNKT cells induced monocytes to secrete PGE_2, an eicosanoid lipid mediator, which suppressed the T cell's ability to produce inflammatory cytokines like IFNγ.

Additionally, the crosstalk between iNKT cells, monocytes and T cells induced secretion of pro-hematopoietic cytokines IL-3 and GMCSF that directly enhanced expansion and differentiation of hematopoietic stem and progenitor cells.

In summary, these results demonstrate the importance of homeostatic signals in transforming naïve T cells into pro-inflammatory effector cells independent of a pathogenic stimulation and provides new insight into how iNKT cells interact with monocytes to impact T cell inflammation and improve engraftment

Introduction

Hematopoietic transplantation

Hematopoietic stem cell transplantation (HSCT) is a process by which donor derived hematopoietic stem cells are infused into lymphopenic hosts in order to regenerate an entire immune system. Use of HSCT as a successful cancer therapeutic agent has been on the rise and successfully used to treat many malignancies with over 19,000 procedures in 2020 alone (1). Major graft sources that are used clinically include adult bone marrow (BM), mobilized peripheral blood (PB) and umbilical cord blood (CB). In adults, majority transplants are performed using either BM or PB with very low CB transplants. Although, cord blood as a graft source offers many advantages, including higher tolerance to human leukocyte antigen (HLA) mismatches and the ability to maintain a reliable source of graft that is readily available in cases where there are no other matched donors (2), its use in the clinics has been on the decline (1). Reduced/delayed engraftment or graft failure is one of the major limitations of CB transplants that limit its use (3,4). The failures associated with CB transplants was often attributed to low numbers of stem cells found within the graft. So early efforts were focused on increasing cell dose by implementing double CB transplants (DCBT), which would mean higher number of hematopoietic stem cells (HSCs) and therefor improve engraftment outcome. However, DCBTs showed no significant advantages compared to single CB transplants but also came with its own set of risks like increased graft versus host disease (GVHD) (5**,** 6).

In contrast to what the name implies, stem cells obtained from these grafts often contains a significant number of other immune cells including T cells that can be extremely important in terms of offering protective immunity against infections and play an important role in anti-

tumor effects and therefore prevent disease relapse. However, T cell derived inflammation can be a key player in driving pathogenic graft versus host disease. While inflammatory cytokines such as IFNγ or TNFα is critical in T cell mediated immunity, it can negatively regulate engraftment and impact the ability of HSC's self-renewal capacity (7,8). Finding strategies to improve clinical outcome by tackling T cell driven inflammation has been an important area of research.

In addition, a major cause of mortality post HSCT using any graft source has been due to primary disease indicating lack of effective graft versus leukemia (GVL) effect. Organ failure is another major cause of death which can be caused due to graft versus host disease (GVHD) (1). Therefore, it is extremely important to better understand factors that regulate T cell function in the context of HSCT that could be used to effectively manage their response toward a favorable target such as the tumor and away from attacking host tissue.

Invariant natural killer T (iNKT) cells

iNKT cells are a highly conserved subset of innate lymphocytes that are known to mediate a diverse range of immune responses. Like conventional T cells (T_{CON}), iNKT cells undergo TCR rearrangement and express a semi-invariant TCRα (Vα24Jα18 in humans, Vα14Jα18 in mice) chain that is paired with limited range of beta chain. They also express surface markers associated with NK cells (which is usually not associated with T_{CON}) (3). iNKT cells are able to recognize self and foreign derived lipid antigens presented by non-polymorphic MHC class 1 like molecule called CD1d (9-11). Functionally, they are anything but similar to conventional T cells. They exhibit many characteristics that are commonly associated with innate immune cells. iNKT cells are cytokine competent as they exit the thymus and are in a primed state that can respond to immunogenic signals in a rapid manner. Additionally, they

are one of the early responders to a potential immunological threat and can rapidly respond by secreting large amounts of cytokines that potently impact activation status of other innate immune cells and dictate the course of the immune response (12-14).

Previous studies have specifically shown that iNKT cells in the context of solid organ transplant promote immunological tolerance (15,16). They also mediate immunoregulatory functions in autoimmune disease models (17-19). Additionally, iNKT cells are associated with lower incidences of graft versus host disease (GVHD) and better graft versus leukemia (GVL) responses in HSCT cases (20-23). The fact that iNKT cells are able to mediate such potent tolerogenic outcome in these various disease models makes them a favorable candidate for cellular immunotherapy.

In mice, iNKT cells can be functionally categorized into distinct subsets based on transcription factors and their cytokine profile. NKT1, NKT2, NKT17 and NKT10 that primarily make IFN-γ, IL-4, IL-17 and IL-10 respectively are the four major functional groups described (24). NKT2 and NKT10 subsets are thought to be important in mediating tolerogenic pathways. In humans, however, these subsets are not as well defined. Interestingly, human derived CD4 iNKT cells when stimulated can secrete a wide range of cytokines including IFN-γ and IL-4.

Specifically, importance of Th2 cytokines produced by iNKT cells are thought to be important in mediating tolerogenic outcome in the context of autoimmune disease or GVH mouse models (25-27). iNKT cells mediated immunoregulatory functions in the context of GVHD has mostly been studied using Ja18 KO mouse models or by testing iNKT cells from IL-4 KO hosts. However, using an allogeneic transplant model, it was recently shown that

administration of NKT cells that make Th2 cytokines significantly suppressed GVHD and improved survival (25).

In humans, many observational studies have linked better transplant outcome to iNKT cells. But it is unclear how the same subset that can make both pro and anti-inflammatory cytokine mediate a tolerogenic function. Although prior studies have pointed to factors that can influence differential functional responses by these cells, specific mechanistic pathways that result in T cell suppression post HSCT is not well understood.

Pathogen independent activation of T cells

It is now well established that pathogen independent mechanisms can drive differentiation of naïve T cell into memory-like cells. Naïve T cells when transplanted into a lymphopenic environment undergo rapid expansion and differentiate into an effector memory like population independent of a pathogenic stimulation. There is now growing evidence to show that antigen independent memory like cells can be identified even under lymphoreplete conditions that are classified as virtual memory (VM) cells with respect to $CD8^+$ T cells or memory phenotype (MP) cells with respect to $CD4^+$ T cells (28-30).

Specifically, the differentiation of CD4 MP cells has been associated with expression of T_{H1} markers. They are able to make IFNγ in response to IL-12 and also express T-bet, a signature Th1 transcription factor (29-31). Prior work has pointed to a role for TCR stimulation in generating CD4 MP cells (32). However, the requirement for a TCR signal or recognition of self-antigens for generation of MP cells can be debated. Results from MHC II KO and CD28 KO models show that generation of CD4 memory-like cells under lymphoreplete conditions are only partially dependent on these signals (29). A subset of CD4 memory like T cells were found in naïve germ-free mice (33). There is also evidence to support importance for

cytokines like IL-7 in driving homeostatic activation of CD4 (34-36). Since most of these studies that focus on understanding the signals that contribute to the generation of these memory-like cells are primarily done using a lymphopenic system, the idea of space and niche availability is considered to be important in promoting such differentiation.

In terms of functionality, prior work has shown that these pathogen independent memory cells that show elevated effector responses compared to their naïve counterpart. Results from mouse studies have suggested that these memory-like cells that are activated independent of a pathogen can mount efficient anti-tumor response and offer protection against infectious agents either in an antigen specific manner or via non-specific pathways (29,37,38).

The overarching goal of my thesis was to delineate factors that influence this MP cell differentiation in humans and explore pathways that could be employed by iNKT cells to suppress such inflammatory differentiation.

Chapter I: Homeostatic signals drive differentiation of naïve T cells into memory phenotype CD4 T cells

Nikhila S. Bharadwaj, Nicholas A. Zumwalde, Kelsey Smith, Arvinder Kapur, Manish Patankar, Akshat Sharma, Jenny E. Gumperz

This chapter was co-written with Dr. Jenny Gumperz.

ABSTRACT

Homeostatic signals are sufficient to drive naïve $CD4^+$ T cells to transition into memory phenotype (MP) cells that mediate rapid effector responses, yet processes involved in the differentiation of these pathogen-independent T cells remain poorly understood. We show here that LFA-1/ICAM-1 interactions induce metabolic changes in naïve human $CD4^+$ T cells that are associated with an enhanced ability to produce IFN-g in response to weak TCR stimulation from transformed target cells. In contrast to MP-like cells that differentiated in an MHC class II-dependent manner through interactions with autologous monocytes, naïve T cells exposed to ICAM-1 alone did not acquire a memory phenotype and did not upregulate T_{H1} markers. However, similar to MP-like cells, ICAM-1-exposed T cells showed increased rates of glycolysis and greater resilience to oxidative stress. These results indicate that LFA-1 ligation leads to metabolic changes in naïve T cells that promote their ability to mount T_{H1}-effector responses.

INTRODUCTION

Upon completing thymic maturation and entering into circulation naïve $CD4^+$ T cells initially produce little IFN-g, a key cytokine involved in both host defense and immune-mediated pathologies (1-3). The classic paradigm is that naïve $CD4^+$ T cells are activated to acquire effector functions through antigenic stimulation in the presence of co-stimulatory signals, and

that specialization for IFN-g production is induced by IL-12p70, a T_{H1}-polarizing cytokine produced by dendritic cells (4-7). According to this paradigm, the conditions required for naïve T cells to gain efficient IFN-g functionality mainly occur in the context of infection by a pathogen, since this is the situation where antigenic stimulation, co-stimulatory signals, and IL-12p70 are all concurrently available. However, it has become clear that naïve $CD4^+$ T cells can also transition to an IFN-g producing phenotype independently of pathogen exposure (8). $CD4^+$ T cells that transition to an effector status in a pathogen-independent manner have been termed "memory phenotype" (MP) cells (9, 10). IFN-g producing MP cells may play important roles in host defense (11, 12), and may also contribute to immune-mediated pathologies (13-16). Moreover, pathogen-independent T cells that are capable of producing an initial burst of IFN-g in the early stages of infection may play an important role in promoting the differentiation of antigen-dependent T_{H1} cells, since it has long been clear that the presence of "early" IFN-g promotes antigen-specific T_{H1} immunity (17). Thus, determining the signals that facilitate pathogen-independent acquisition of IFN-g functionality by naïve T cells has important implications for understanding immune responses in a variety of contexts.

Prior studies have established that the acquisition of pathogen-independent T_{H1} effector status is associated with homeostatic proliferation (18). Models involving transplantation of naïve T cells into syngeneic lymphopenic hosts have delineated two distinct types of homeostatic proliferation, one involving rapid proliferation and one in which proliferation occurs more slowly (8, 19). Slow homeostatic proliferation is not associated with the acquisition of effector functions by naïve T cells, whereas T cells that undergo rapid homeostatic proliferation under lymphopenic conditions gain the ability to rapidly produce IFN-g and upregulate cell surface markers indicating immunological experience. Differentiation of T_{H1}

cells via lymphopenia-induced rapid homeostatic proliferation is dependent on antigen presenting cells expressing self MHC class II molecules and is facilitated by peptide antigens from commensal microbes (19-24). Importantly, while lymphopenic conditions efficiently give rise to pathogen-independent T cells, it has recently become clear that similar $CD4^+$ T cells can also be identified under lymphoreplete conditions in non-transplanted healthy mice (9, 12, 25, 26). Hence, it seems that the generation of pathogen-independent T_{H1} cells probably occurs physiologically even during the steady-state, and the process is probably greatly upregulated by exposure to the abundant niche-space found in lymphopenic environments.

Lymphopenia is a central feature of a number of clinical settings. For example, lymphodepleting induction therapies are commonly performed prior to hematopoietic transplantation protocols, in order to prevent rejection of the graft by the patient's lymphocytes (27). Thus, pathogen-independent effector T cells are probably often generated from naïve T cells during immune reconstitution following hematopoietic transplantation, though little is known about the functional impact of these cells. Since their TCR repertoire was not selected to respond to specific foreign pathogens, such T cells might be particularly prone to mediating graft-versus-host-disease (GVHD). Consistent with this, studies in murine models have shown that transplanting naïve T cells leads to more severe GVHD than transplantation of memory T cells (28-30). Additionally, since T cell IFN-g production plays a key role in tumor control following hematopoietic transplantation (31, 32), the ability of pathogen-independent T cells to produce "early" IFN-g may contribute to the initiation of graft-versus-tumor (GVT) responses (33). To investigate the potential for naïve human $CD4^+$ T cells to contribute to anti-tumor responses following hematopoietic transplantation, in this study we investigated IFN-g production by human umbilical cord blood T cells.

Surprisingly, compared to T cells that had acquired effector status in the presence of strong TCR stimulation, homeostatically differentiated MP cells showed elevated IFN-g secretion in response to low levels of TCR stimulation and correspondingly also mediated stronger responses to transformed autologous and allogeneic B lymphocytes.

RESULTS

CD4+ T cells from human umbilical cord blood are recent thymic emigrants that lack the ability to produce effector cytokines.

We used human umbilical cord blood to investigate IFN-g production by naïve human $CD4^+$ T cells. In contrast to adult peripheral blood where only about 50% of the $CD4^+$ T cells have a $CD45RA^+CD45RO^-$ naïve phenotype, nearly 100% of the $CD4^+$ T cells in human umbilical cord blood are $CD45RA^+CD45RO^-$ (Fig. 1A). Moreover, we consistently found that over 80% of the $CD4^+$ T cells in cord blood expressed CD31, indicating they are recent thymic emigrants (RTEs) (*34*), whereas the frequency of $CD31^+$ cells in the naïve $CD4^+$ T cell population of adult samples was highly variable (Fig. 1A). Prior studies have established that human umbilical cord blood $CD4^+$ T cells show reduced effector cytokine production compared to naïve T cells from adults (*35, 36*). It is not clear whether this is due to suppression (e.g. as a result of exposure to inhibitory factors or regulatory T cells) or whether this simply reflects their highly naïve status. To clarify this, we compared cytokine production by cord $CD4^+$ T cells to that of adult $CD4^+$ RTEs in response to 4-6 hours of PMA and ionomycin stimulation. Intracellular cytokine staining analysis revealed little or no production of IFN-g, IL-4, IL-13, IL- 17A, or IL-10 by either cord blood $CD4^+$ T cells or adult $CD4^+$ RTEs, although adult $CD4^+$

RTEs contained slightly higher frequencies of IFN-g producing cells than cord blood, and

cord $CD4^+$ T cells showed slightly higher frequencies of IL-17A producing cells than adult $CD4^+$ RTEs (Fig. 1B). In contrast, substantial populations of RTEs producing TNF-a, IL-8, and IL-2 were detectable in both cord and adult blood, with no significant differences in frequency between the two sets of samples (Fig. 1B). Thus, the cytokine profile of $CD4^+$ T cells from umbilical cord blood appeared similar to that of adult RTEs in that they generally lack the ability to rapidly produce effector cytokines, but they readily produce IL-2 and the inflammatory cytokines TNF-a and IL-8. Analysis of Treg frequencies ($CD4^+$ T cells with a $CD25^+CD127^{lo}$ surface phenotype and elevated intracellular expression FoxP3) did not reveal a significant difference between cord blood samples and adult PBMCs (Fig. 1C). Since these results indicated that umbilical cord blood is enriched for highly naïve T cells that have not yet acquired effector cytokine capabilities, we used cord blood as the source of T cells for subsequent experiments.

Transplanted naïve human CD4+ T cells acquire effector characteristics in a pathogen-independent manner. (*Results shown in Figure 2 was generated by Dr. Nicholas Zumwalde)*

We next sought to visualize the dynamics of naïve $CD4^+$ T cell transition into IFN-g producing effector cells following transplantation. To do this, we transplanted human cord blood mononuclear cells (CBMCs) into non-conditioned NOD/SCID/$gc^{-/-}$ (NSG) mice, allowing for analysis of human T cell activation in a lymphopenic environment in the absence of damage- associated inflammation (*37, 38*). In parallel, we similarly transplanted CBMCs that were briefly exposed to Epstein-Barr virus (EBV), a human-specific virus that infects B cells within the CBMC sample and drives their neoplastic transformation *in vivo* over the course of 3-4 weeks (*39*). Splenocytes were harvested after one, three, or five weeks, and human $CD4^+$ T cells were analyzed flow cytometrically for intracellular cytokine expression

after 4h of PMA/ionomycin treatment. As expected, in the presence of EBV infection the frequency of $CD4^+$ T cells capable of rapidly producing IFN-g increased over the first 3 weeks following transplantation (Fig. 2A and B). Remarkably, the $CD4^+$ T cells from mice transplanted with uninfected CBMCs showed

a similar increase in IFN-g producing $CD4^+$ T cells (Fig. 2A). In contrast, the frequency of TNF- a producing T cells did not markedly increase (Fig. 2A), and there was little or no detectable production of type 2 cytokines such as IL-13 in either condition (Fig. S1). Thus, in both the uninfected and virally infected conditions, transplanted cord blood derived $CD4^+$ T cells selectively acquired an IFN-g producing phenotype.

Further investigation of the dynamics of T cell activation following transplantation of uninfected CBMCs into NSG mice revealed that both $CD4^+$ and $CD8^+$ T cells underwent a linear rate of doubling over the first 4 weeks (Fig. 2B). During this time, nearly all of the $CD4^+$ T cells transitioned to an experienced cell surface phenotype characterized by loss of both CD45RA and CD62L (Fig. 2C and D). Together, these findings indicated that damage-associated inflammation and pathogen exposure were not required for human cord blood $CD4^+$ T cells to lose their highly naïve phenotype and acquire IFN-g functionality following transplantation into a lymphopenic environment. However, the role of microbial or xenoantigenic stimulation in this model remains unclear.

Exposure to homeostatic signals is sufficient to induce transition to memory phenotype.

To assess whether the T cell changes we observed in the uninfected condition were due to the xenotransplant system, we used an *in vitro* model where we could better control the stimulation given to the T cells. To do this, $CD4^+$ T cells from cord blood were cultured in

parallel in three different conditions as follows: *i*) with homeostatic cytokines but without antigenic stimulation (i.e. T cells alone in medium containing IL-7 and IL-2); *ii)* with homeostatic cytokines and self-antigenic stimulation (T cells co-cultured with autologous monocytes in medium containing IL-7 and IL-2); or *iii*) with homeostatic cytokines and strong TCR stimulation (T cells co-cultured with autologous monocytes and the bacterial superantigen staphylococcus enterotoxin C in medium containing IL-7 and IL-2). After 3-5 days of culture in these conditions, the T cells were removed and then rested in IL-2/IL-7 medium alone for an additional 5-7 days prior to analysis at day 10 for cell surface phenotype and amount of cell division. Nearly all of the T cells that had been exposed to autologous monocytes in the presence of bacterial superantigen gained an experienced phenotype (loss of CD45RA, acquisition of CD45RO, and loss of CD31) and underwent many rounds of proliferation (Fig. 3A, right). In contrast, T cells that were kept in IL-7/IL-2 medium alone typically underwent several rounds of proliferation but maintained a naïve phenotype in that they retained CD45RA, did not acquire CD45RO, and showed little or no down-regulation of CD31 (Fig. 3A, left). A fraction of the T cells that had been exposed to autologous monocytes without superantigen (self- antigenic stimulation) underwent many rounds of proliferation, and about half typically lost their naïve cell surface phenotype (CD45RA and CD31) and gained CD45RO (Fig. 3A, middle). This suggested that in the presence of IL-7 and IL-2, exposure to autologous monocytes might be inducing a fraction of the naïve $CD4^+$ T cells to differentiate into MP cells.

To investigate this further, we assessed IFN-g production after 4-6h PMA/ionomycin stimulation. As expected, a large fraction of the T cells that had proliferated following exposure to monocytes and superantigen were able to produce IFN-g (Fig. 3B, right panel), whereas T cells that were kept in IL-2/IL-7 alone still showed little or no IFN-g production

(Fig. 3B, left panel). Importantly, T cells that underwent proliferation after exposure to self-antigenic stimulation did acquire the capacity to produce IFN-g (Fig. 3B, middle). Moreover, these T cells began to show an ability to produce IFN-g after undergoing even a single round of cell division and showed increasing frequencies of IFN-g^+ cells with each successive round of division, such that within the population that underwent at least 7 rounds of cell division the fraction of T cells that was able to produce IFN-g was similar to that for T cells that had received strong TCR stimulation from superantigen-treated monocytes (compare plots in Fig. 3B and 3C). In contrast, the T cells that were kept in IL-2/IL-7 medium alone remained almost completely unable to produce IFN-g in response to 4-6h PMA/ionomycin stimulation, even after undergoing 5-6 rounds of cell division (Fig. 3C). Thus, exposure to autologous monocytes led to increased capacity to produce IFN-g in T cells that underwent cell division, and this did not occur in T cells that proliferated during culture in IL-2/IL-7 medium alone.

To investigate whether changes specifically associated with TH1 polarization had occurred, we evaluated intracellular expression of the transcription factor T-bet and cell surface expression of the IL-12 receptor b2 chain (IL12RB2). T-bet expression is required for TH1 differentiation, while expression of IL12RB2 is upregulated by T-bet and is known to play a critical role in promoting TH1 status (*40, 41*). T cells kept in IL-2/IL-7 alone showed little or no expression of intracellular T-bet or cell surface IL12RB2, whereas exposure to autologous monocytes resulted in clearly increased expression of both T-bet and IL12RB2, and this was not further increased by exposure to superantigen (Fig. 3D). Together these results demonstrated that exposure to autologous monocytes in the presence of IL-2 and IL-7 is sufficient to induce a fraction of the $CD4^+$ cord T cell population to acquire MP status.

Role of stimulation through TCR and LFA-1 in MP differentiation.

We observed that superantigen stimulated $CD4^+$ T cells showed clearly upregulated levels of cell surface CD69 after 24h, whereas there was little or no evidence of CD69 upregulation by T cells that were exposed to self-antigen or kept in IL-2/IL-7 alone (Fig. 4A). Since CD69 is upregulated by TCR stimulation in a dose-dependent manner (34), their lack of CD69 upregulation suggested that T cells exposed to autologous monocytes had not received a strong TCR signal. We therefore investigated whether binding to MHC class II molecules during differentiation was required for MP cells to acquire the ability to rapidly produce IFN-g. $CD4^+$ T cells were differentiated by co-culture with autologous monocytes in IL-2/IL-7 medium alone, or in the presence of anti-MHC class II blocking or isotype control antibodies and tested for intracellular IFN-g expression after PMA/ionomycin stimulation. Addition of an anti-MHC class II blocking mAb during differentiation led to significantly reduced frequencies of IFN-g producing cells, whereas the presence of an isotype control mAb had no significant effect (Fig. 4B). Thus, while the stimulation resulting from exposure to autologous monocytes was not sufficient to cause upregulation of CD69, signals from self MHC class II molecules were nevertheless important for MP cells to acquire the ability to rapidly produce IFN-g. We also found that disrupting LFA-1 interaction with ICAM-1 blocked MP cell acquisition of IFN-g functionality. MP cells were differentiated through exposure to autologous monocytes in the presence of a blocking antibody against ICAM-1 or a negative control antibody, or in the presence of a small molecule antagonist of LFA-1 or a negative control compound and tested for intracellular IFN-g after PMA/ionomycin stimulation. Similar to blockade of MHC-II, interrupting LFA-ICAM interactions resulted in markedly reduced frequencies of IFN-g producing cells (Fig. 4B).

MP cells show elevated responsiveness to weak TCR stimulation.

We next investigated IFN-g secretion by the T cells in response to challenge by B-lymphoblastoid cells (cord B cells neoplastically transformed by EBV). $CD4^+$ cord T cells were differentiated into MP cells by exposure to autologous monocytes, or in parallel were super- antigenically stimulated or kept in IL-2/IL-7 medium alone (undifferentiated). Each T cell type was rested for 5-7 days in IL-2/IL-7 medium alone, and then challenged by exposure to autologous lymphoblastoid cell lines (LCLs), or allogeneic LCLs, or superantigen-treated allogeneic LCLs. After 24-48 hours culture supernatants were tested for IFN-g by ELISA. Superantigen-differentiated T cells showed significantly greater IFN-g responses to superantigen- treated LCLs than either the MP cells or the undifferentiated T cells (Fig. 5A). Remarkably, however, the MP cells produced significantly greater amounts of IFN-g than either the undifferentiated or the superantigen-differentiated T cells in response to autologous or allogeneic LCLs in the absence of superantigen (Fig. 5A). These results suggested that MP cells had an enhanced ability to respond to the weaker TCR stimulation provided by LCLs in the absence of superantigen.

To test this, we assessed responses to titrated TCR stimulation using a soluble anti-CD3/anti-CD28 multimer. CD4+ cord T cells were differentiated as described above and then exposed to titrated doses of anti-CD3/anti-CD28 multimer for 24h, and culture supernatants were tested for IFN-g concentration. MP cells produced significantly greater amounts of IFN-g than either undifferentiated T cells or superantigen-differentiated T cells (Fig. 5B), suggesting they had heightened efficiency of responses to TCR stimulation. To investigate further, we assessed the kinetics of ERK phosphorylation in response to a suboptimal (5 μL) dose of the antiCD3/anti-CD28 multimer. This analysis revealed that ERK phosphorylation occurred more quickly in MP cells compared to either the undifferentiated T cells or the

superantigen differentiated T cells (Fig. 5C). Analysis of ZAP-70 phosphorylation similarly demonstrated that MP cells showed a higher level of phosphorylation after 2 minutes of suboptimal CD3/CD28 stimulation than either undifferentiated or superantigen-differentiated T cells (Fig. 5D). Thus, MP differentiation was associated with elevated TCR signaling at early timepoints following a sub-optimal stimulus.

MP differentiation is associated with enhanced mitochondrial activation that promote subsequent effector responses

We observed that in addition to phenotypic and functional changes, MP differentiation was also associated with changes to their metabolic profile. Seahorse phenotype test was performed and changes in mitochondrial respiration and glucose metabolism was assessed simultaneously. MP cells showed significantly higher aerobic glycolysis compared to undifferentiated T cells indicated by increase in basal and maximal oxygen consumption rate (OCR) and extracellular acidification rate (ECAR) (Fig 6A). Overall, we found that rates of aerobic respiration and glycolysis were substantially elevated in both MP cells and super antigen treated T cells compared to undifferentiated T cells (Fig. 6B). However, spare respiratory capacity (SRC), which is a measure of the cell's ability to meet sudden energy demand was also significantly higher in MP cells, SRC values for T cells stimulated in presence of super antigen was variable and showed no increase compared to undifferentiated T cells in most cases (Fig 6B).

To this effect, we further investigated the status of mitochondria in MP cells compared to undifferentiated T cells. MP cells showed increased level of active mitochondria (Fig 6D) assessed by fluorescent imaging. We also observed that after 5 days in culture, MP cells had higher levels of intracellular ATP (Fig 6D).

Previously, we saw that ICAM-LFA interaction was important in promoting IFNg response. We wanted to confirm that this pathway is important in metabolic activation of MP cells. The addition of a small molecule inhibitor of LFA-1 during monocyte-induced differentiation of MP cells largely prevented the increase in OCR and ECAR (Fig. 6H), suggesting that LFA-1/ICAM-1 interaction during MP cell differentiation contributes to their elevated metabolic rates.

We also tested the impact of inhibiting oxidative or glycolytic metabolic pathways. ICAM-exposed or undifferentiated T cells were stimulated with titrated doses of anti-CD3/CD28 complex in the presence or absence of 2-Deoxy-D-glucose (2-DG), a glucose analog that competitively inhibits glucose uptake and consequently abrogates glycolysis, or in the presence or absence of the ATP synthase inhibitor oligomycin A, which prevents the generation of ATP through oxidative phosphorylation. There was a remarkable reduction in IFNγ levels when the cells are unable to use glycolysis. Interestingly, oligomycin treatment caused an increase in cytokine response specifically at weaker concentration of TCR stimulation by MP cells (Fig 6G). This might indicate that during mitochondrial stress, MP cells were able to employ other compensatory mechanisms. An increased capacity to mediate glycolysis might offer a feasible explanation.

DISCUSSION

T cell reconstitution remains a central problem in patients who undergo severe lymphopenia during clinical protocols such as hematopoietic transplantation or intensive chemotherapy, and in particular the $CD4^+$ T cell compartment is typically very slow to recover (*45, 46*). While later T cell recovery may depend mainly on *de novo* differentiation from precursor cells, homeostatic proliferation is probably a major mechanism driving the initial recovery of

T cells following lymphopenia (*27*). It is now well established from murine models that MHC class II-dependent rapid homeostatic proliferation of naïve $CD4^+$ T cells is associated with the acquisition of a T_H1 memory phenotype, whereas IL-7-dependent slow homeostatic expansion maintains $CD4^+$ T cells in a naïve state (*18*). Less is known about homeostatically expanded human T cells, and in particular it is not clear whether they contribute to protective immunity. We show here that human MP cells generated through exposure to autologous monocytes actually mediate stronger IFN-g responses to autologous or allogeneic transformed B cells than either naïve T cells or effector T cells generated through exposure to strong TCR stimulation. Thus, MP cells that arise through rapid homeostatic proliferation may provide a key source of IFN-g for anti-tumor responses at early timepoints during T cell reconstitution.

An intriguing aspect of the effector functions we observed for MP cells is that they showed heightened IFN-g production in response to weak TCR stimulation, but they did not compare favorably when it came to responding to target cells that provided a strong TCR stimulus. We hypothesize that their elevated IFN-g production is a consequence of the homeostatically activated T cells having greater metabolic reserves (Fig. 6C and E), and that this allows them to rapidly switch to glycolysis to produce IFN-g upon receiving low or moderate TCR stimulation. However, their reserves may rapidly become exhausted by the demands of stronger stimulation, and thus they are not able to mediate greatly elevated IFN-g production in response to target cells that present a strong TCR ligand such as a bacterial superantigen (Fig. 5A). If this is the case, MP cells might be able to produce IFN-g comparatively well in response to self or allo-antigens in hypoxic or low glucose environments (such as are commonly found in tumors), but they may not show similarly elevated responses to high-affinity foreign antigens.

A key unresolved question about homeostatically expanded T cells relates to the nature of their antigen specificity. It has been previously observed that lymphopenia-associated homeostatic proliferation leads to expansion of autoreactive T cells (*13*). Since the generation of MP cells was blocked by antibodies against MHC class II molecules (Fig. 4B), it is possible that the T cells that give rise to MP cells have TCRs with comparatively high affinity for self-antigens, providing stimulation that allows for proliferation under homeostatic conditions. However, based on our results, it is not clear if the pool of responding cells in the IL-2+IL-7 and MP culture conditions are different. It is possible that T cells that were cultured in the presence of autologous monocytes simply proliferated more rapidly, such that they underwent more rounds of proliferation in the time span of our analysis (Fig. 3A). If so, the differentiation of MP cells in our system may be due to cell-intrinsic features that promote T cell proliferation, rather than being due to TCR specificity for particular antigens. Mouse studies have shown that differential expression of CD5 is an indicator of sensitivity to tonic TCR signaling and have the highest propensity to differentiate into pathogen independent memory cells. Additional markers such as transcription factor Eomes and IL-15Rβ have been used to isolate CD8 T cells that preferentially differentiate into memory T cells independent of antigen stimulation. However, translation of these markers to human CD4 T cells has not been successful.

In summary, results from our current study establish that in addition to weak TCR signals provided by self MHC molecules, ICAM- LFA stimulation is important in MP cell differentiation. Additionally, we show that higher metabolic activity and substantial spare respiratory capacity allows MP cells to mediate enhanced effector response to relatively weak TCR stimulation.

Author contributions:

Conceptualization: NSB, NAZ, AS, JEG

Data curation and formal analysis: NSB

Methodology: NSB, NAZ, AS, KS, AK, MP, JEG

Investigation: NSB, NAZ

Visualization: NSB, JEG

Supervision: MP, JEG

Validation: NSB

Visualization: NSB, JEG

Writing – original draft: NSB

Writing – review & editing: JEG

FIGURES

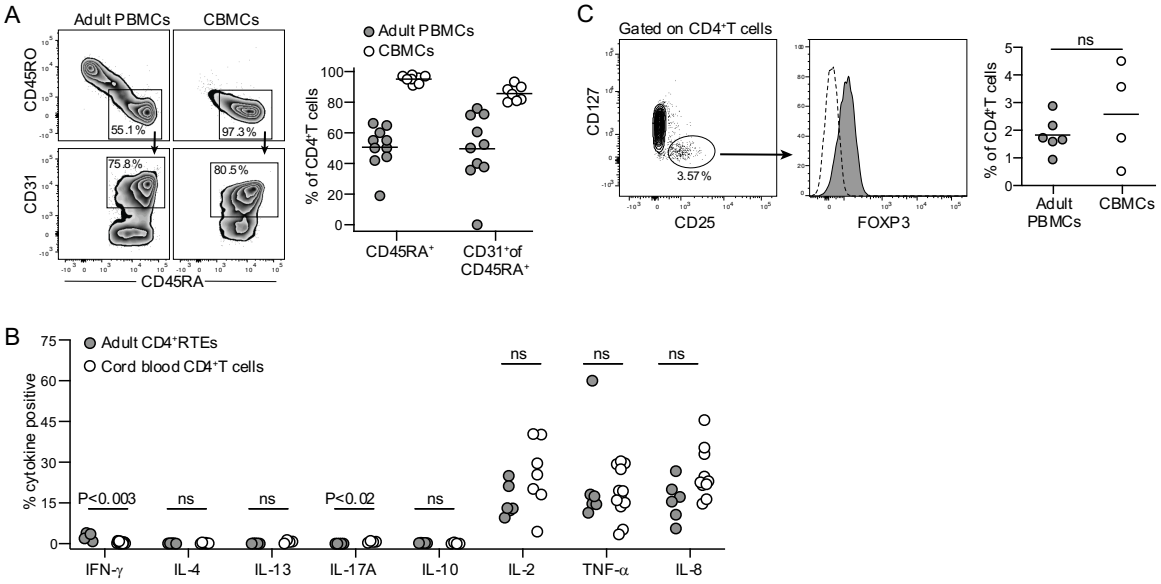

Figure 1. **CD4 T cells from cord blood are enriched for recent thymic emigrants and do not produce effector cytokines.** (A) Representative flow cytometric staining of $CD4^+$ T cells isolated from human umbilical cord blood or adult peripheral blood. CD45RA and CD45RO were used to identify naïve cells (top row); CD31 expression within the naïve population was assessed to identify recent thymic emigrants (RTEs). Scatter plot on right shows aggregated results from 10 PBMC and 8 cord blood samples. (B) Analysis of intracellular cytokine expression by $CD4^+$ T cells from cord blood, or $CD4^+$ RTE population from adult blood, after PMA/ionomycin stimulation. P values determined using Mann-Whitney analysis. (C) Representative flow cytometric staining of cord blood T cells showing identification of T_{regs} ($CD25^+CD127^{lo}$), and FoxP3 expression (filled histogram) of the gated population compared to isotype (dotted line). Plot on right shows percent T_{regs} detected in different samples.

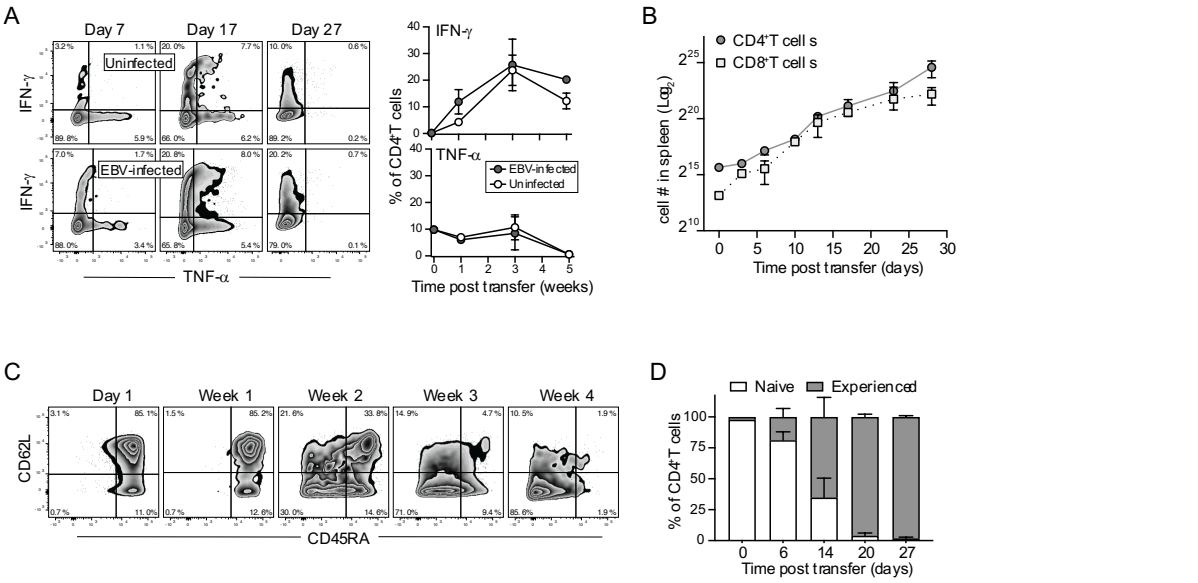

Figure 2. Transplanted naïve human CD4$^+$ T cells acquire effector characteristics in a pathogen-independent manner. EBV-infected or mock-treated CBMCs were administered to NSG mice. (A) Murine splenocytes were harvested at indicated times after transplantation and stimulated with PMA/ionomycin. Representative flow cytometric staining is shown for intracellular IFN-g and TNF-a. Plots on right show means and standard deviations for 2-3 mice. (B) Quantitation of the total numbers of human CD4$^+$ and CD8$^+$ T cells in the murine spleen following transplantation of uninfected CBMCs. (C) Representative flow cytometric staining showing CD45RA and CD62L expression by human CD4$^+$ T cells in murine spleen at the indicated times post-transplant. (D) Proportions of naïve (CD45RA$^+$) and experienced (CD45RA$^-$) human CD4$^+$ T cells at each time point. Plot shows means and standard deviations from 3 replicate mice.

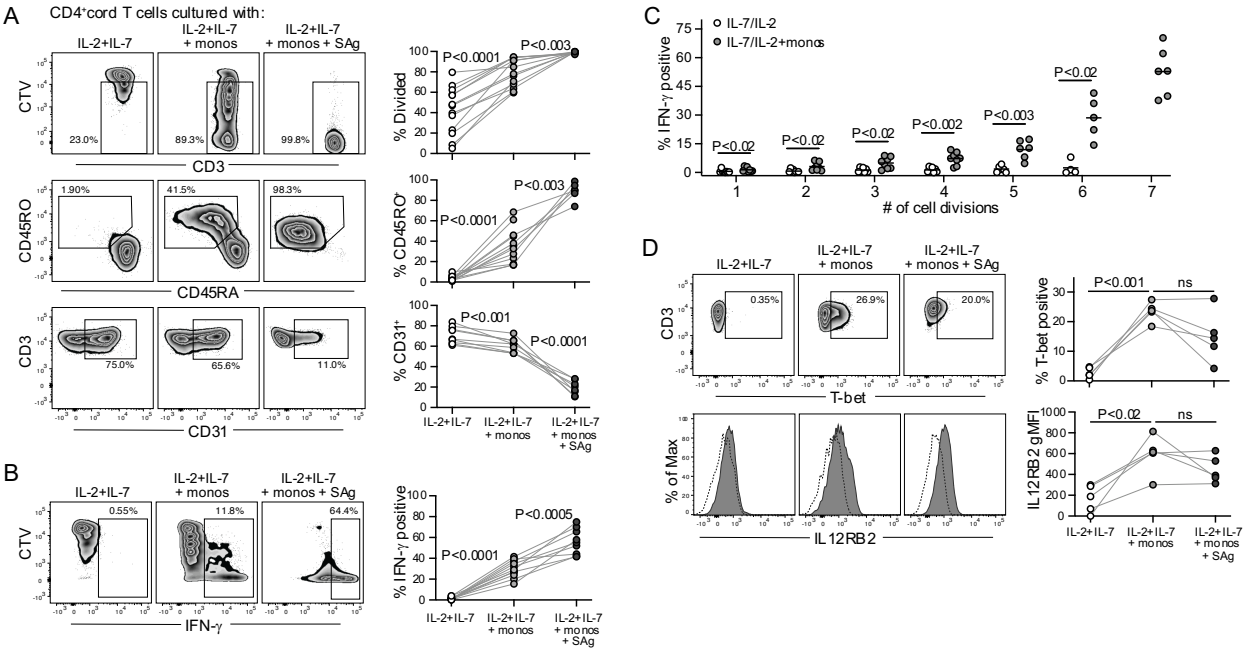

Figure 3. A fraction of cord T cells differentiate into MP cells through exposure to homeostatic signals. $CD4^+$ T cells were cultured in medium containing IL-2 and IL-7 alone, or with autologous monocytes in the presence or absence of bacterial superantigen (SAg) for 3-5 days, then rested in IL-2/IL-7 medium alone for 7 days. (A) Top row: T cell proliferation assessed by dilution of cell trace violet (CTV); middle row: experience assessed by CD45RA and CD45RO; bottom row: loss of RTE status assessed by CD31. (B) Intracellular IFN-g expression after PMA/ionomycin stimulation. (C) Percent IFN-g^+ cells as a function of number of cell divisions. (D) Top row: intracellular expression of T-bet; bottom row: cell surface expression of IL12RB2. P values in panels (A, B, and D) determined using two-tailed parametric paired t-test; P values in panel (C) determined using Mann-Whitney analysis.

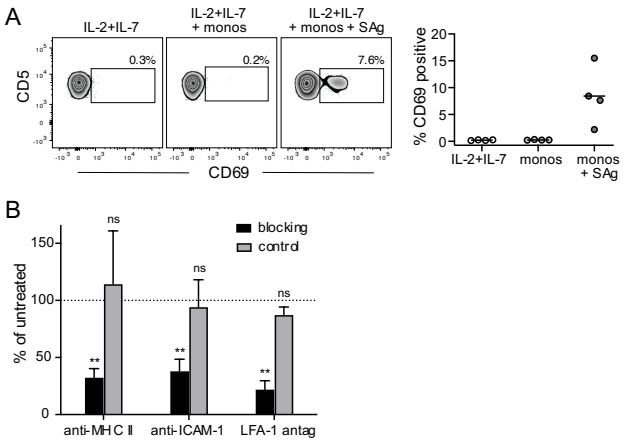

Figure 4. MP differentiation depends on self MHCII and LFA-1/ICAM-1 interaction.

(A) $CD4^+$ T cell expression of CD69 after 24h of incubation in IL-2/IL-7 medium alone, or with autologous monocytes in the presence or absence of bacterial superantigen (SAg). (B) T cells were cultured with autologous monocytes in the presence of blocking antibodies against MHC class II or ICAM-1 or isotype-matched negative controls, or in the presence of the LFA-1 small molecule antagonist (BI-1950) or the negative control compound (BI-9446). Plot shows IFN-g production as a fraction of the amount produced by positive control T cells that were co-cultured in parallel with autologous monocytes in the absence of any blocking reagents. Bars show means + SEM from 4-7 independent experiments; P values calculated by one-sample t-test compared to a theoretical mean of 100.

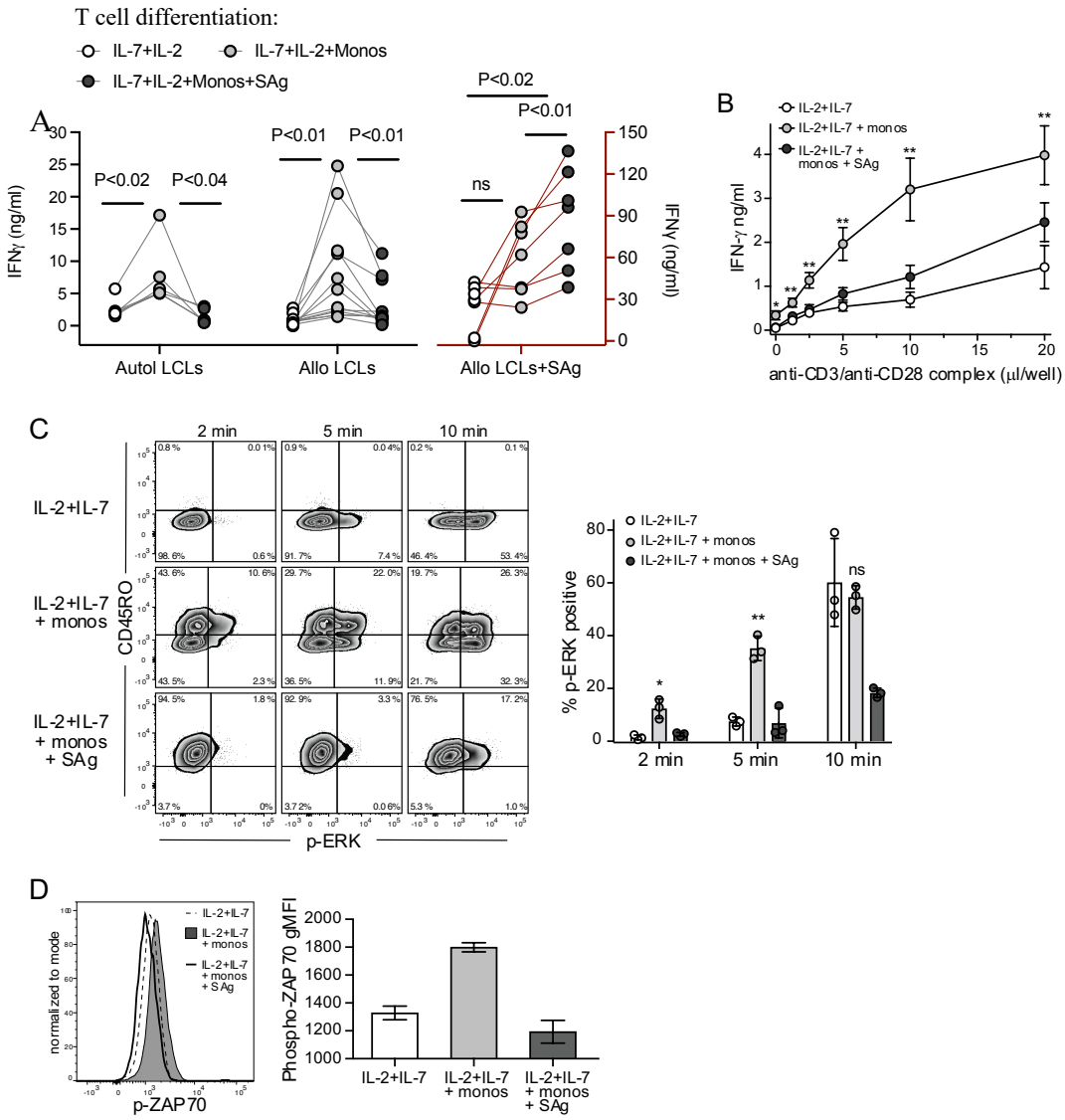

Figure 5. MP cells show elevated responsiveness to weak TCR stimulation. (A) MP cells and control T cells were co-incubated with autologous LCLs, or allogeneic LCLs with or without SAg, and IFN-g in the culture supernatant was quantitated after 24-48h. Plot shows results from 7 independent experiments; P values calculated by two-tailed parametric paired t-test. (B) T cells were stimulated with an anti-CD3/anti-CD28 antibody complex and secreted IFN-g was quantitated after 24h. Plot shows means + SEM of 8 independent experiments; asterisks indicate statistical comparison of MP cells (IL-2/IL-7+monos) with undifferentiated T cells (IL-2+IL-7). (C) T cells were stimulated with 5 µl anti-CD3/anti-

CD28 antibody complex for the indicated times, and ERK phosphorylation was assessed by flow cytometry. P values calculated by unpaired t-test with Welch's correction. (D) Phospho-ZAP70 after 2 minutes stimulation with 5 µl anti-CD3/anti-CD28 antibody complex. Bar plot shows means + SD of two replicates.

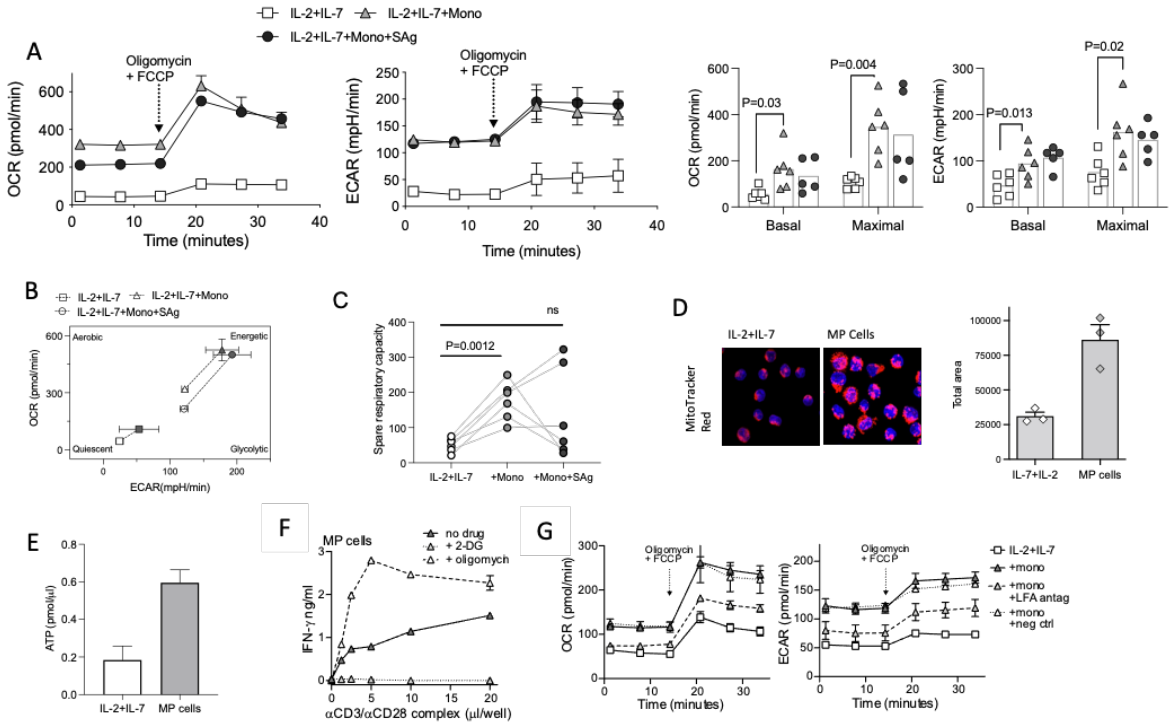

Figure 6. Differentiation of MP cells is associated with mitochondrial activation and increased metabolic reserve (ATP). $CD4^+$ T cells were cultured in medium containing IL-2 and IL-7 alone (undifferentiated), or with autologous monocytes (MP cells) in the presence or absence of bacterial superantigen (SAg) for 3-5 days, then rested in IL-2/IL-7 medium alone for 7 days. (A) Representative plot showing rates of oxygen consumption rate (OCR) and extracellular acidification rate (ECAR) (Left two plots). Aggregated results of OCR and ECAR from at least 5 different samples (rRght two plots). P values calculated using a two-tailed parametric paired t-test. (B) Plot comparing overall metabolic profiles of undifferentiated T cells, MP cells and SAg exposed T cells. Light symbols show basal and

dark symbols show maximal metabolic rates. (C) T cell spare respiratory capacity calculated from OCR analysis. (D) Representative image of undifferentiated or MP cells labelled with nuclear dye DAPI and MitoTracker Red dye. Bar graph represents total area of mitochondrial dye quantified from three independent cord samples using imaging software. (E) Quantitation of ATP in T cells after 5 days of culture. (F)Impact of 2-DC and oligomycin on IFN-g production by MP cells. (G) Representative plots showing OCR and ECAR for MP cells differentiated in the presence or absence of BI-1950 (an LFA-1 antagonist) or BI-9446 (a negative control compound), compared to undifferentiated T cells (IL-2+IL-7). Similar results were observed using T cells from 4 different cord samples.

MATERIALS AND METHODS

Study Design. This study investigated functional properties of naïve human T cells that were exposed to distinct stimulation pathways. For each experiment, $CD4^+$ T cells were isolated from a primary human umbilical cord blood sample, and cells from the same sample were exposed in parallel to distinct test conditions. Experiments were repeated multiple times using unrelated cord blood samples, and results from like treatment conditions were aggregated for analysis.

Human tissue samples and cellular isolation. Human tissue samples were acquired and handled in accordance with UW-Madison Minimal Risk IRB protocol 2018-0304. De-identified human umbilical cord blood samples were obtained from the Obstetrics and Gynecology department at Meriter Hospital, Madison, WI, or from commercial sources. Peripheral blood samples were acquired by venipuncture from healthy adult volunteers. Mononuclear cells were isolated by density gradient centrifugation using Ficoll-plaque PLUS (GE Healthcare). $CD14^+$ monocytes were positively isolated using magnetic beads (Miltenyi Biotec). $CD4^+$ T cells were magnetically isolated by positive selection using anti-CD4 beads, or by negative selection using a CD4 T cell isolation kit (Miltenyi Biotec) or EasySep CD4 T cell isolation kit (Stemcell technologies).

Flow cytometric analysis. Cells were resuspended in phosphate buffered saline (PBS) containing 5% bovine calf serum (BCS), 20% human AB serum and 0.1% sodium azide, then labeled with fluorescent antibodies for 20 min at 4°C. Cells were phenotyped using the following antibodies: CD3 (HIT3a, Biolegend), CD14 (63D3, Biolegend), CD45RO (UCHL1, Biolegend), CD45RA (HI100, Biolegend), CD31 (WM59, Biolegend), CD69 (FN50, Biolegend), IL-12Rβ2 (2B6/12beta2, BD Biosciences). For analysis of proliferation,

T cells were labelled with 5 μM Cell Trace Violet (CTV) proliferation dye (ThermoFisher Scientific) prior to culture. For intracellular analysis of IFN-g (4S.B3; Biolegend), IL-4 (8D4-8, Biolegend), IL-13 (JES10-5A2, Biolegend), IL-17A (N49-653, BD Biosciences), IL-10 (JES3-9D7, Biolegend), IL-2 (MQ1- 17H12, Biolegend), TNF-a (Mab11, Biolegend), IL-8 (BH0814, Biolegend), and T-bet (04-46, BD Biosciences), T cells were stimulated with PMA/ionomycin in the presence of brefeldin A for 4-6h, then fixed and permeabilized (Cyto-Fast Fix/Perm buffer set, Biolegend) prior to intracellular staining. Staining for cells expressing intracellular FoxP3 (259D, Biolegend) was performed according to the manufacturer's protocol using BD Biosciences' transcription factor buffer set. Analysis of phospho-ERK (6B8B69, Biolegend) and phospho-ZAP-70 (A16043E, Biolegend) was performed using True-Phos Perm buffer set (Biolegend).

Xenotransplantation analyses. Animal studies were performed in accordance with UW-Madison IACUC protocol M005199. Immunodeficient NOD/SCID/$gc^{-/-}$ (NSG) mice were purchased from Jackson Laboratories and bred and maintained in specific pathogen free facilities using aseptic housing. Male and female mice 6-12 weeks of age were used for experiments. Cord blood mononuclear cells (CBMCs) were exposed to 2,000 U of the M81 strain of EBV or mock treated in medium alone for 2 hours, then administered intraperitoneally at 1×10^7 cells per mouse as previously described (*39*). Splenocytes were harvested at the indicated time points, then stimulated using PMA/ionomycin in the presence of brefeldin A (Biolegend) for 4-6 hrs, stained for cell surface HLA (W6/32), human CD45 (HI30), CD3 (HIT3a), CD4 (OKT4), CD8 (RPA-T8), then fixed and permeabilized and stained for intracellular cytokines or isotype- matched controls. Human $CD4^+$ and $CD8^+$ T cell expansion was quantified by assessing the total number of each cell type in the spleen using counting beads.

Homeostatic differentiation in vitro. Cells were cultured at 37 ^{o}C and 5% CO_2 in medium consisting of RPMI 1640, 10% BCS (Hyclone), 5% fetal bovine serum (FBS) (Hyclone or Gibco), 3% pooled human AB serum (Gemini), 1% Penicillin/Streptomycin, 1% L-glutamine, 50 U/ml recombinant human IL-2 and 1 ng/ml recombinant human IL-7 (Peprotech). To generate MP cells and controls, $CD4^{+}$ cord T cells (5×10^{4}/well) were cultured in parallel in medium alone, or with autologous monocytes (2.5×10^{4}) in the presence or absence of 2 μg/ml purified Staphylococcal Enterotoxin C (SEC) superantigen (a generous gift of Dr. Wilmara Salgado- Pabon). For blocking experiments, 10 μg/ml anti-MHC class II (Tu39 from BD Biosciences, or L243 purified from hybridoma supernatant), anti-ICAM-1 (HCD54, Biolegend), or isotype-matched control mAbs (MOPC21 for IgG_1 from Biolegend and G155-17 for IgG_{2a} from BD Biosciences) were added at the start of the co-culture with autologous monocytes. Alternatively, to block ICAM-LFA interactions, a small molecule antagonist of LFA-1 called BI- 1950, or BI-9446, a chemically similar negative control compound (both from Boehringer- Ingelheim), were included in the co-cultures at a final concentration of 8 μg/ml.

Responses to secondary stimulation. LCLs generated from cord blood B cells were used to assess T cell responses to neoplastically transformed cells. LCLs were generated by incubating 1×10^{6} CD14- and CD4-depleted CBMCs with 2,000 U of the M81 lytic strain of EBV, and culturing the cells for 3-4 weeks in (RPMI 1640, 10% BCS, 1% Penicillin/Streptomycin and 1% L-glutamine) at 37 ^{o}C and 5% CO_2. T cells were mixed at a 1:1 ratio with autologous or allogeneic LCLs, or allogeneic LCLs in the presence of 2 μg/ml staphylococcus enterotoxin C, or incubated with titrated doses of human CD3/CD28 antibody complex (ImmunoCult^{TM}, Stemcell Technologies). After 24-48h stimulation, culture

supernatants were harvested and secreted IFN-g was quantitated by ELISA (Biolegend). Where indicated, T cell stimulation assays were performed in the presence of 10 mM 2-deoxy-D-glucose (2-DG) or 1 μM Oligomycin.

Metabolic Analyses. Assays were performed using a Seahorse XF Analyzer (Agilent). T cells were placed at 2.5×10^5 cells/well into Seahorse culture plates that were pre-coated with 50 μg/ml Poly-L-Lysine (Advanced biomatrix). Where indicated, 1 μM each of oligomycin and carbonyl cyanide p-trifluoromethoxy-phenylhydrazone (FCCP) were added. T cell intracellular ATP concentrations were measured using a colorimetric assay (Abcam).

Statistical Analyses. Two-tailed parametric paired t-tests were used to analyze datasets involving 4 or more independent cord samples, where cells from each sample were subjected in parallel to different treatment conditions. In cases involving less than 4 samples, data were analyzed using an unpaired t-test with Welch's correction. Mann-Whitney t-tests were used for comparisons between unrelated samples. Datasets involving analysis of the amount of antibody or drug blocking compared to a mock-treated control were analyzed using a one-sample t-test. * indicates $P < 0.05$; ** indicates $P < 0.01$; *** indicates $P < 0.001$.

Chapter II: ICAM stimulation drives differentiation of naïve CD4$^+$ T cells into stem-like Tcf1 positive effector cells

Nikhila S. Bharadwaj, Kelsey Smith, Akshat Sharma, Jenny E. Gumperz

ABSTRACT

T cells can be broadly divided into naïve (T_N), central memory (T_{CM}), effector memory (T_{EM}) and effector cells (T_{EFF}). Recently, a new subset has been identified called T memory stem cells (T_{SCM}), a subset of memory cells that are minimally differentiated and are involved in mediating both protective and pathological immune responses. We show that LFA-1 ligation by ICAM-1 promote naïve CD4 T cells to differentiate into effector cells that show increased responsiveness to autologous and allogeneic EBV transformed B cells and while remain BCL-2^{hi} and TCF-1$^+$, characteristics often associated with long term non-effector memory cells. These ICAM-1-exposed stem-like effector cells also showed increased rates of glycolysis and higher spare respiratory capacity. Preliminary analysis show that ICAM stimulated T cells show enhanced ability to carry out proliferation in low nutrient environment. This study identifies a novel role of ICAM-LFA stimulation in differentiation of stem like population from naïve CD4 T cells.

INTRODUCTION

The ability to fight cancer using adoptively transferred immune cells has been revolutionary in the field of cancer immunotherapy. Specifically, the use of T cells that can recognize tumor antigens has proven to be highly effective against wide variety of hematological malignancies. The process usually involves ex-vivo expansion and re-infusion of the expanded T cells that are either derived from tumor infiltrating lymphocytes or can be any T cell that is genetically engineered to express molecules such as chimeric antigen receptor

(CARs) that specifically recognize tumor antigen. However, these adoptively transferred T cells are prone to becoming exhausted or unresponsive due to activation of negative immunoregulatory pathways or being exposed to tumor derived immunosuppressive factors (1,2). Additionally, traditional protocol used to expand T cells often promote differentiation of effector T cells that appear terminally differentiated, which does not result in long lasting durable immune response (2,3).

Numerous strategies have been tested over the years to mitigate T cell exhaustion and to prolong the effects of T cells in the context of cancer therapy (4,5). This includes a popular therapy in use, checkpoint inhibitor antibodies. Another strategy is to use distinct T cell subsets, specifically T cells with a memory phenotype (6). Based on their differentiation status evaluated using phenotypic and functional properties, T cells can be grouped into four different categories, naïve (T_N), central memory (T_{CM}), effector memory (T_{EM}) and effector cells (T_{EFF}). T memory stem cell (T_{SCM}) is now another well-recognized T cell subset that is thought to resemble T_N in terms of their phenotype but functionally behave like memory T cells. Current research favors the use of T cells that are more memory like as they show better functional response but also are more resilient to getting exhausted. Mouse studies have shown that use of less differentiated T_{SCM} show superior anti-tumor activity and are more persistent compared to the T_{EFF} or T_{EM} subset (7). One caveat to this is that circulating T_{SCM}, are quite rare and strategies to efficiently expand small numbers ex-vivo has been an important area of research. Additionally, human clinical trials that followed T cell reconstitution post transplantation saw higher levels of T_{SCM} and memory phenotype cells in circulation (8,9).

In this study we investigated mechanistic pathways that can result in generation of stem like T cells. Using naïve CD4 T cells, we show that cells that undergo slow homeostatic

proliferation retain stem like characteristic. We also identified a novel role for ICAM mediated LFA-1 stimulation of T cells in inducing lasting metabolic changes. This increase in rates of glycolysis and higher levels of metabolic reserve in these ICAM exposed T cells potentiates their enhanced effector response to transformed cells. Preliminary results show that these ICAM primed cells show higher proliferative capacity in nutrient deprived environment.

RESULTS

Slow homeostatic proliferation is associated with stem-like properties.

Homeostatic proliferation (HP) can be categorized into slow and fast HP. We used isolated CD4 T cells and co-cultured them with autologous monocytes in presence of IL-2 and IL-7 and assessed cell division flow cytometrically. While T cell cultured in IL-2 and IL-7 alone (undifferentiated) underwent multiple rounds of proliferation with little to no accumulation of fast HP cells, two distinct types of proliferating cells, slow and fast HP cells were observed in T cells that were co-cultured with autologous monos (Fig. 1A). We next investigated if slow and fast HP cells within the IL-2+IL-7+monos condition showed phenotypic differences. Consistently across multiple cord samples, T cells that underwent fast HP had upregulated markers associated with memory cells like CD45RO and significantly lower levels of CD31, a surface marker that is highly expressed on naïve T cells that recently exit the thymus and gets downregulated as the cell divides. Additionally, fast HP cells also were able to exclusively produce IFN-g in response to PMA/ionomycin stimulation (Fig. 1B, filled circles). Interestingly, cells that underwent slow HP showed an undifferentiated status in terms of their memory phenotype (Fig 1B, unfilled circles), they also had expressed higher levels of BCL-2 (Fig 1C), a molecule associated with enhanced survival and transcription factor TCF1 (Fig 1D), which is thought to offer T cells stem like properties.

ICAM-LFA interaction impacts T cell proliferation and does not induce effector cell like phenotype.

We next investigated signals important in generating this heterogenous set of cells in the IL-2+IL-7+monos condition. We set up co-cultures where either MHC-II on monocytes was blocked using blocking antibodies or LFA-1 integrin signaling was inhibited using a small molecule inhibitor and appropriate negative controls in either condition. Cell division was assessed flow cytometrically. Blocking MHC-II had very little impact on cell division (Fig. 2A left panel). Surprisingly, blocking ICAM-LFA interaction using the LFA-1 antagonist had a substantial impact (Fig. 2A right panel). In our previous analysis (Fig. 4B from chapter I), we also show that both class II and interrupting LFA-ICAM interaction impacts acquisition of the ability to IFNg by these T cells. Therefore, to further investigate the role of LFA-1 interactions with ICAM-1, we used a system where freshly isolated $CD4^+$ cord T cells were cultured in medium containing IL-2 and IL-7 alone, or in the presence of plate-bound recombinant ICAM-1-Fc fusion protein. We also included conditions where isolated T cells were stimulated with anti-CD3 and anti-CD28 antibodies, or with anti-CD3/CD28 and ICAM-1-Fc, which results in very strong activation that mimics antigenic stimulation and promotes differentiation of Th1 like effector cells. Cells were harvested at end point and their functional and phenotypic changes were assessed. A large proportion of the T cells that were exposed to anti-CD3/CD28 acquired an experienced phenotype (loss of CD31, acquisition of CD45RO), and the frequency of cells showing these changes was significantly increased when CD3/CD28 stimulation occurred in the presence of plate-bound ICAM-1-Fc (Fig. 2B). In contrast, T cells exposed to plate-bound ICAM-1-Fc did not upregulate CD45RO (Fig. 2B). This was also accompanied by modest but significant increase in cell division and consequent downregulation of CD31 expression (Fig. 2B). Additionally, based on

proliferation analysis, significantly higher number of T cells entered cell division in presence of plate bound ICAM-Fc (Fig 2C, replication index panel) and these responding cells also underwent more rounds of cells division compared to T cells from IL-2+IL-7 condition (Fig. 2C Proliferation index panel). Exposure to anti-CD3/CD28 led to modest upregulation of IL-12 receptor but did not reproducibly result in T-bet expression, and T cells that were exposed to ICAM-1-Fc alone did not show any upregulation of these markers of T_{H1} differentiation (Fig. 3C). Results from this analysis point to an important role of ICAM-LFA stimulation in promoting cell division without causing upregulation of memory markers.

ICAM-1 exposure promotes subsequent IFN-g production in response to EBV transformed B cells.

We next tested if ICAM-1 exposure had any impact on their functional response. Freshly isolated $CD4^+$ cord T cells were cultured in medium containing IL-2 and IL-7 in the presence or absence of anti-CD3 and anti-CD28 stimulation, and in the presence or absence of plate-bound ICAM-1-Fc fusion protein. After 3-5 days, the T cells were removed from these stimulation conditions, and were rested for an additional 5-7 days in medium containing IL-2 and IL-7. ICAM-1 exposed T cells were able to make modest but significantly higher IFNg compared to T cells exposed to IL-2 and IL-7 only in response to PMA/ionomycin. As expected, exposure to anti-CD3/CD28 stimulation resulted in a significantly increased frequency of IFN-g producing T cells compared to the undifferentiated T cells (Fig. 3B). However, exposure to TCR stimulation in the presence of plate-bound ICAM-1-Fc led to a significant further increase in the frequency of IFN-g producing T cells (Fig. 3B).

We also tested the T cells ability to make effector cytokine in response to EBV transformed B cells. T cells were cultured as described and were then combined with autologous, allogeneic, or bacterial superantigen loaded allogeneic EBV transformed B cells and culture supernatants

were collected after 24-48h and tested for secreted IFN-g by ELISA. Remarkably, this analysis revealed that although exposure to ICAM alone did not produce an memory like phenotype (see Fig. 2B), T cells that had been pre-exposed to ICAM-1 showed elevated IFN-g secretion in response to autologous or allogeneic LCLs compared to T cells that were incubated in IL-2/IL-7 medium alone (Fig. 3A). Surprisingly, in contrast, T cells that were stimulated by anti-CD3/CD28 in the presence of ICAM-1-Fc showed reduced responses to autologous LCLs, and similar responses to allogeneic LCLs, compared to undifferentiated T cells (Fig. 3A). Exposure to allogeneic LCLs in the presence of bacterial superantigen typically elicited strong T cell cytokine production regardless of the pre-treatment condition (Fig. 3A). These results suggested that despite being insufficient to induce traditional memory T cell differentiation, exposure to ICAM nevertheless led to enhanced IFN-g production when naïve T cells were confronted with comparatively weak TCR stimulation.

To directly assess IFN-g production as a function of the level of TCR stimulation, we exposed T cells differentiated in the four culture conditions to titrated doses of anti-CD3/CD28 antibody complex. This analysis confirmed that T cells that were cultured in IL-2/IL-7 medium in the presence of plate-bound ICAM-1-Fc subsequently showed enhanced responses to low levels of TCR stimulation compared to T cells that were cultured in IL-2/IL-7 medium alone (Fig. 3C). T cells that were pre-exposed to anti-CD3/CD28 stimulation did not show elevated responses to weak TCR stimulation, and those that received anti-CD3/CD28 stimulation in the presence of plate-bound ICAM-1-Fc showed an intermediate phenotype (Fig. 3C). Importantly, in all of these experiments the T cells were “rested” for 5-7 days in the absence of plate-bound ICAM-1-Fc after their 3-5 day period of exposure, indicating that changes induced by prior exposure to ICAM-1 were durable in nature. Thus, together these results suggested that although exposure to ICAM-1 alone is not sufficient to

induce memory T cell differentiation, it nevertheless produces lasting changes in naïve T cells that lead to an enhanced ability to produce IFN-g effector responses against target cells that provide weak TCR stimulation.

Exposure to ICAM-1 induces lasting metabolic changes in naïve T cells that promote subsequent IFN-g responses.

Our results thus far showed that exposure to plate-bound ICAM-1-Fc alone did not result in transformation of naïve T cells into memory like population but promoted their ability to produce effector cytokine. This suggests that their elevated IFN-g secretion in response was not due to acquisition of a T_{H1} differentiation status that is seen with traditional effector memory T cells (Fig 2B and C). We therefore turned our attention to investigating alternative mechanisms that might account for enhanced effector cytokine production.

T cells that were cultured in IL-2/IL-7 medium in the presence or absence of plate-bound ICAM-1-Fc showed no significant difference in ZAP-70 or ERK phosphorylation following TCR stimulation using a sub-optimal dose of anti-CD3/CD28 antibody complex (Supplementary Fig. 1A and B). Since the ability to make IFN-g is closely linked to aerobic glycolysis in CD4 T cells (35, 36), we next investigated whether ICAM-1 exposure was associated with changes to the metabolic status of the T cells. T cells were exposed to plate-bound ICAM-1-Fc for 3-5 days, then cultured in IL-2/IL-7 medium alone for an additional 5-7 days, then tested for oxygen consumption rate (OCR) and extracellular acidification rate (ECAR) using a Seahorse Extracellular Flux Analyzer. ICAM-1-pre-exposed T cells displayed significantly increased basal and maximal rates for both OCR and ECAR compared to T cells that were cultured in parallel in IL-2/IL-7 medium alone (Fig. 4A and B). Since OCR is proportional to mitochondrial respiration and ECAR is proportional to glycolysis, these results suggested that aerobic glycolysis is elevated after exposure to ICAM-1. Thus,

ICAM-exposed T cells may mount stronger IFN-g responses as a result of increased rates of glycolysis.

Compared to undifferentiated T cells, T cells exposed to ICAM stained brighter for baseline intracellular ROS as well as in response to tert-butyl hyperoxide (THBP), a chemical that induces ROS production (Fig 4E). In addition to increased levels of aerobic glycolysis, ICAM exposed T cells showed greater mitochondrial activity. Based on imaging analysis, ICAM exposed T cells also displayed higher levels of active mitochondria when stained using a mitochondrial dye (Fig. 4F).

We next tested if oxidative and glycolytic metabolic pathways impact the ability of the T cells to produce IFN-g. T cells that were pre-exposed to plate-bound ICAM-1-Fc or kept in IL-2/IL-7 medium alone were stimulated with titrated doses of anti-CD3/CD28 complex in the presence or absence of 2-Deoxy-D-glucose (2-DG), a glucose analog that competitively inhibits glucose uptake and consequently abrogates glycolysis, or in the presence or absence of the ATP synthase inhibitor oligomycin A, which prevents the generation of ATP through oxidative phosphorylation. Addition of 2-DG completely abrogated IFN-g production by both ICAM-1 pre-exposed and undifferentiated T cells (Fig. 4E). Addition of oligomycin had little or no impact on IFN-g production by undifferentiated T cells, but the addition of this drug consistently resulted in elevated IFN-g release by ICAM-1-pre-exposed T cells (Fig. 4E). We also observed that T cells that were exposed to plate-bound ICAM-1-Fc showed significantly elevated levels of intracellular ATP compared to those that were kept in IL-2/IL-7 medium alone (Fig. 4D). Additionally, ICAM exposed T cells showed significantly higher spare respiratory capacity (SRC) (Fig. 4C). Interestingly, ICAM-1-Fc pre-exposed T cell enhanced IFN-g production in the presence of oligomycin was particularly apparent at low

doses of anti-CD3/CD28 stimulation and appeared to reach a plateau at a sub-optimal dose (~5 ml) of anti-CD3/CD28 multimer (Fig. 4E).

Together these results confirmed a key role for glycolysis in IFN-g production, and further suggested that ICAM-1-Fc exposure was associated with metabolic changes in the T cells.

DISCUSSION

Results from our current study uncovered a novel role for ICAM-LFA interaction in transforming naïve CD4 T cells into IFNγ positive effector cells while maintaining their naïve and stem-like phenotype. We also showed that exposure to ICAM promotes upregulation of aerobic glycolysis and enhances SRC and ATP reserve. These metabolic changes that accompany ICAM primed T cells allow them to mount an enhanced effector response against EBV transformed B cells and might potentially make these cells more resilient to nutrient low conditions.

Recent reports have highlighted a unique subset of memory T cells called T_{SCM} subset. These cells are often characterized by their enhanced proliferation potential and polyfunctionality and naïve phenotypic markers. In the periphery, human T_{SCM} subset can be identified by looking at surface markers like CD45RA, CD62L, CCR7, CD95 and IL-2Rβ^{+} (10). Although they appear naïve in terms of their phenotype, functionally they are thought to resemble experienced or memory T cells. Distinctive memory like characteristic of T_{SCM} subset includes having low levels of TRECs (10), and being able to respond with higher levels of IFNγ, IL-2 and TNFα compared to naïve subset (10,11).

Specific signals that promote differentiation of these stem like T cells are not very well explored. Prior work has suggested that cytokines like IL-15 can induce stem like program (12). One study also showed that IL-7 treatment can de-differentiate effector memory cells into naïve stem like cells (13). We have identified a naïve like population within the slow HP subset that expressed naïve markers but could mediate enhanced IFNγ response when challenged with transformed cells. We also showed that ligation of LFA-1 by ICAM in important in generation of such cells.

Although ICAM exposed T cells undergo more rounds of cell division and downregulate markers like CD31 (see Fig 2B and D), they maintain their BCL-2 expression compared to T cells that were stimulated with anti-CD3/CD28 with or without ICAM-Fc indicating enhanced cell survival (Fig. 5A). When compared to undifferentiated T cells and T cells that were expanded using anti-CD3/CD28, ICAM-Fc exposed T cells showed intermediate levels of transcription factor TCF1 staining (Fig. 5B). So far, our experiments have shown that ICAM exposed T cells upregulate their metabolic capacity and maintain stem like properties.

Based on these results, we wanted to conduct a preliminary test to see if ICAM exposed T cells would fare better in a nutrient deprived environment. In order to evaluate this, we set up culture conditions as described in prior sections. These cultured cells were then harvested and labelled with a cell permeable fluorescent dye to track cell division in response to anti-CD3/CD28 stimulation in hypoglycemic media (3.8mM/L) that contained IL-2 and IL-7. Proliferation analysis show that while undifferentiated T cells showed moderate amount of cell division and survival, ICAM treated cells tolerated the low nutrient environment better and showed higher levels of proliferated (Fig. 5C). In contrast, T cells that were expanded using anti-CD3/CD28 performed the worst with little to no surviving T cells (Fig. 5C).

While some of the results presented in this chapter are highly intriguing, they are preliminary. Once these results are confirmed and are shown to reproducible, T cells generated using this pathway can have important implications in generating T cells for adoptive cell therapy.

Author contributions:

Conceptualization: NSB, JEG

Data curation and formal analysis: NSB

Methodology: NSB, KS, AS, JEG

Investigation: NSB

Supervision: JEG

Visualization: NSB, JEG

Writing –NSB

FIGURES

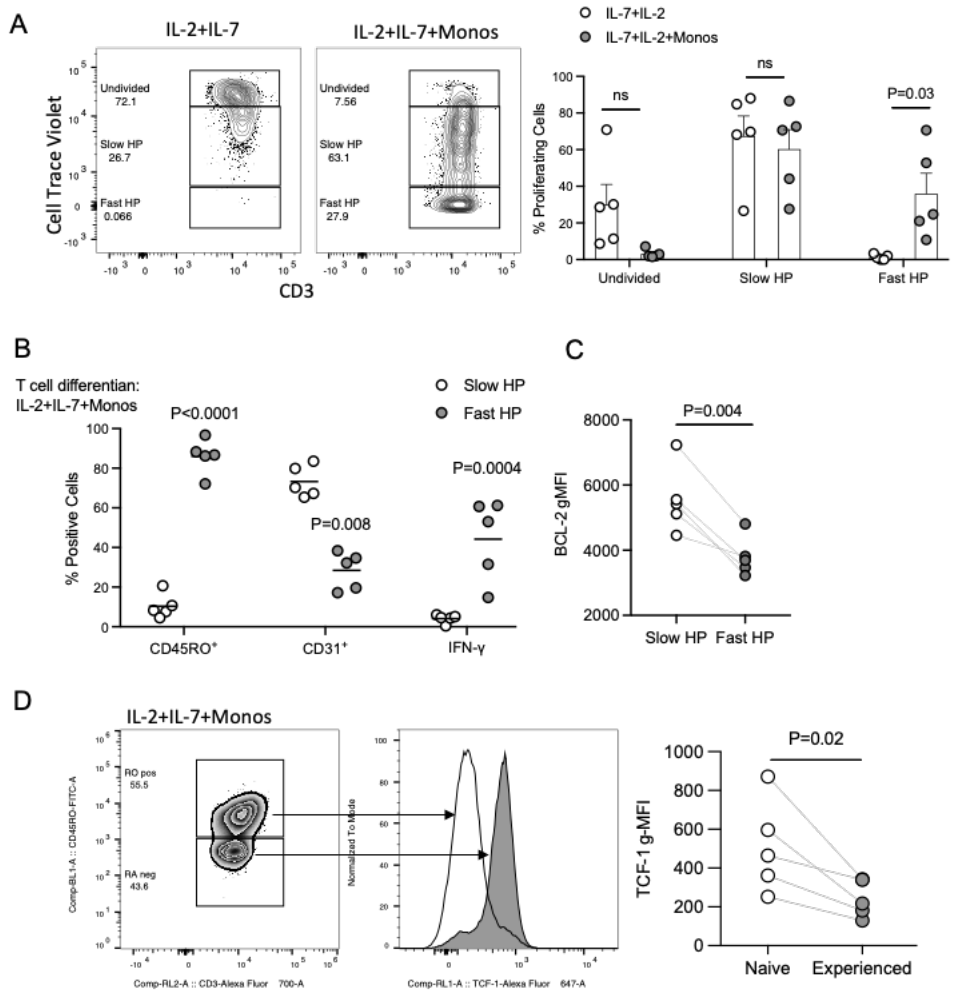

Figure 1. Slow homeostatic proliferation is associated with stem-like properties. Isolated CD4 T cells were labelled with cell trace violet (CTV) proliferation dye and were cultured in T cell media containing IL-2 and IL-7 alone or in presence of either autologous monocytes. Cell division and changes in cell phenotype was measured flow cytometrically on D10. (A) Representative flow plot (Left panel) and aggregated results (Right panel) showing proportion of undivided, slow and fast homeostatic proliferating (HP) cells. (B) Percent of CD45RO, CD31 positive cells and IFN-g positive cells in response to PMA/ionomycin stimulation in slow versus fast HP cells. (C) Level of BCL-2 expression in slow and fast HP cells. (D) Representative flow plot (Left panel) and aggregated results (Right panel) showing

TCF1 expression level in CD45RO positive and negative T cells found in the IL-2+IL-7+monos culture condition.

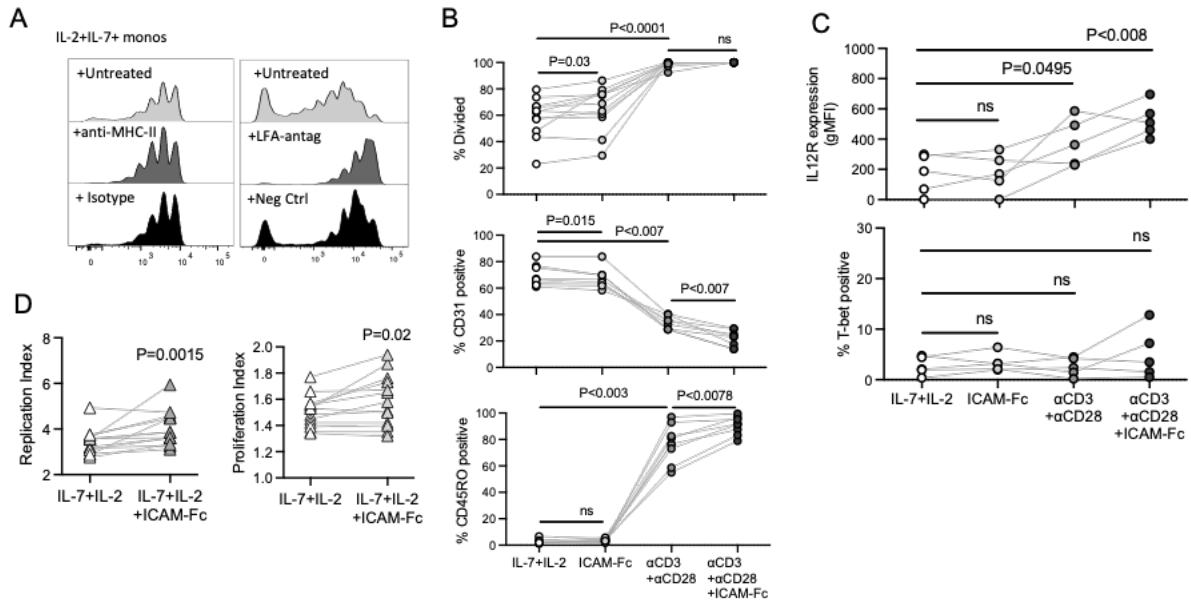

Figure 2. ICAM-LFA interaction impacts T cell proliferation and does not induce effector cell like phenotype. T cells were cultured with autologous monocytes alone or in presence of MHC II blocking antibodies and matched isotypes or LFA-1 antagonist and negative control. (A) After 10 days, cell proliferation was assessed flow cytometrically. Isolated T cells were cultured alone with IL-7 and IL-2 or with plate bound ICAM-Fc, plate bound anti-CD3/CD28 in presence or absence of plate bound ICAM-Fc. (B) Summary plot showing cell division as percent divided T cells and surface expression staining results for CD45RO, CD31. (C) Plot shows surface expression of IL12Rβ2 and upregulation of Tbet in response to PMA/ionomycin. (D) Cell proliferation of T cells cultured alone or in presence of plate bound ICAM-Fc was analyzed using a proliferation tool. Plot shows Replication and Proliferation index. P-values were calculated using paired non-parametric t test.

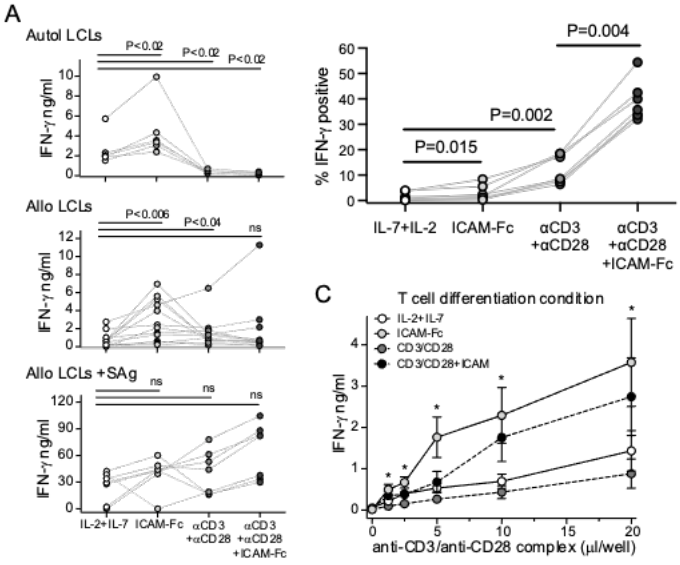

Figure 3. ICAM-1 exposure promotes subsequent IFN-g production in response to EBV transformed B cells. Isolated CD4 T cells were cultured for 10 days in culture media alone (IL-7+IL-2) or with plate bound ICAM-Fc, plate bound anti-CD3/CD28 in presence or absence of plate bound ICAM-Fc for 10 days. T cells were challenged with LCLs at 1:1 effector to target ratio, PMA/ionomycin or titrated amounts of anti-CD3/CD28 complex. Levels of IFN-g was measured either by ELISA in culture supernatants collected after 24-48 hrs or stained for intracellular IFN-g. (A) Levels of secreted IFNg in response to target LCLs (Each symbol represents an independent experiment). (B) Scatter plot showing percent positive cells. Statistical analysis was performed using paired non-parametric t test. (C) Levels of IFNg in response to titrated dose of TCR stimulation (Aggregated from 5 independent experiments). (A and C) P values were calculated a two-tailed parametric paired t-test.

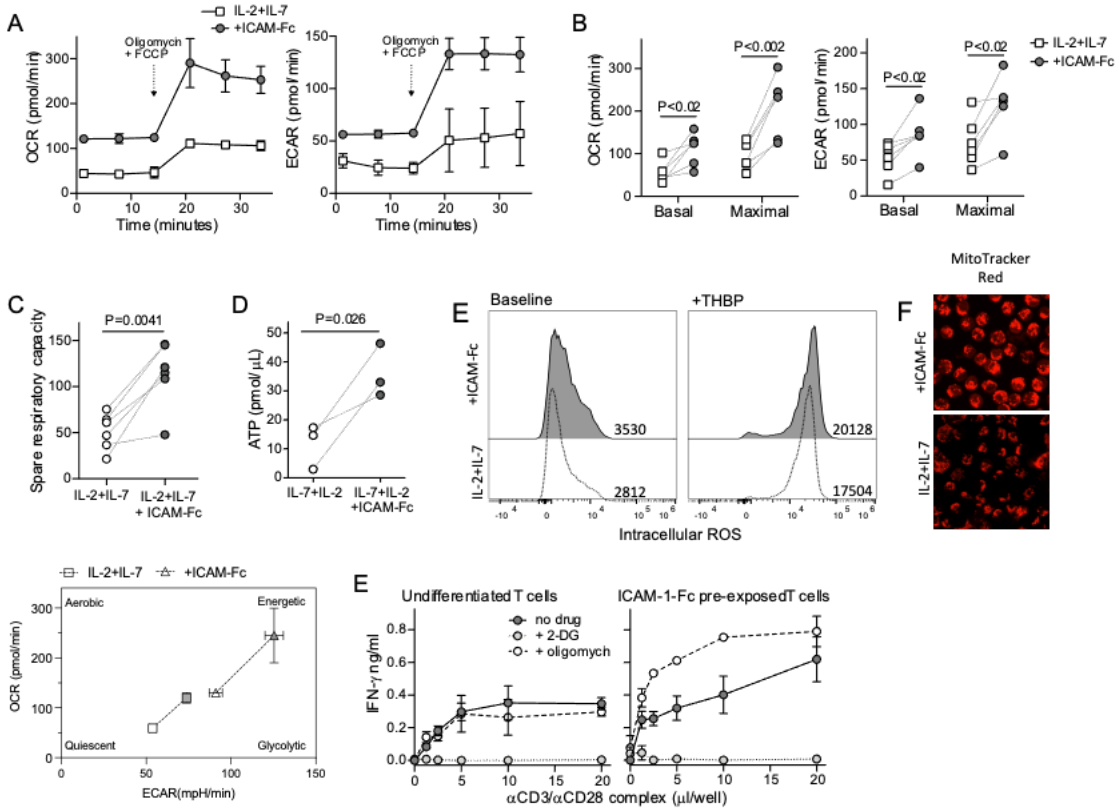

Figure 4. Exposure to ICAM-1 induces lasting metabolic changes in naïve T cells that promote subsequent IFN-g responses. T cells were cultured in T cell media with IL-7 and IL-2 or in presence of plate bound ICAM-Fc for 5 days and were rested in media containing IL-7 and IL-2 for 5 more days. A-B) On D10, the metabolic status of the cells was assessed using seahorse cell energy phenotype assay. (A) Representative plot showing Oxygen consumption rate (OCR) and Extracellular acidification rate (ECAR) of cultured T cells. (B) Scatter plot showing basal and maximal (readings taken after Oligomycin and FCCP injection) OCR and ECAR values. Aggregated data was put together by calculating the average basal and maximal OCR and ECAR values for each experiment. (**C**) T cell spare respiratory capacity calculated from OCR analysis. (D) T cells were cultured for 5 days in respective conditions and amount of intracellular ATP was quantified by ELISA. Unpaired t-

test was used to calculate statistical significance. (E) Day 10 T cells were harvested and stained with fluorogenic reagent that stains cellular reactive oxygen species (ROS) either in presence or absence of THBP, a ROS stimulating chemical. (F) Representative images showing mitochondrial staining using MitoTrackerRed dye. Similar results were observed in three independent cord samples. (G) Representative plot showing OCR (y axis) and ECAR (x axis) of T cells cultured alone in media or in presence of plate bound ICAM-Fc. (H) Cultured cells on D10 were stimulated with titrated amounts of anti-CD3/CD28 antibody complex alone or in presence of 2-Deoxy-D-glucose (2DG) that inhibits glycolysis or Oligomycin that inhibits oxidative phosphorylation. Graph shoes amount of IFNg in cell culture supernatant after 24 hrs determined by ELISA.

Preliminary results

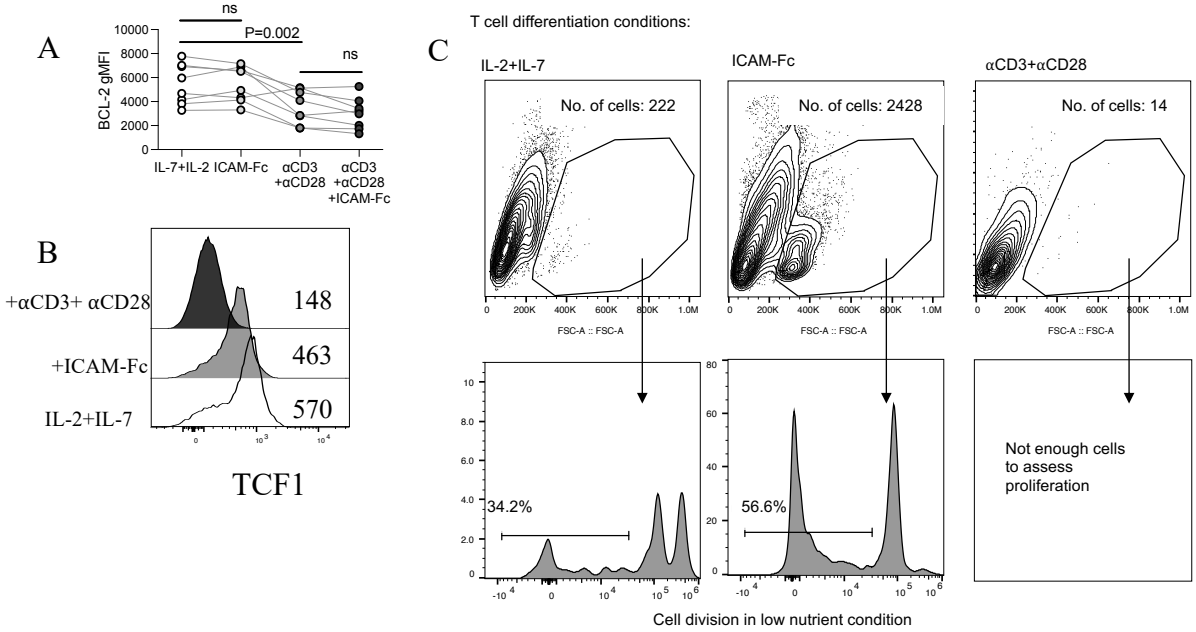

Figure 5. ICAM exposed T cells are stem like and show enhanced proliferation in nutrient deprived environment. T cells were cultured in specific conditions for 3-5 days and were rested in media with IL-2 and IL-7 until D10. (A) BCL-2 expression was measured

using intracellular staining. (B) Cells were stained for levels of TCF1 transcription factor. (C) T cells differentiated in respective conditions were harvested on D10, labelled with CFSE proliferation dye were stimulated with 5 µl anti-CD3/anti-CD28 antibody complex in low glucose media (3.8mM/L) with IL-2 and IL-7 for 7 additional days. Flow plots show cells within live gate (Top panel) and cell division of cells within the live gate (Bottom panel). P values were calculated using paired non-parametric t test.

Supplementary figure

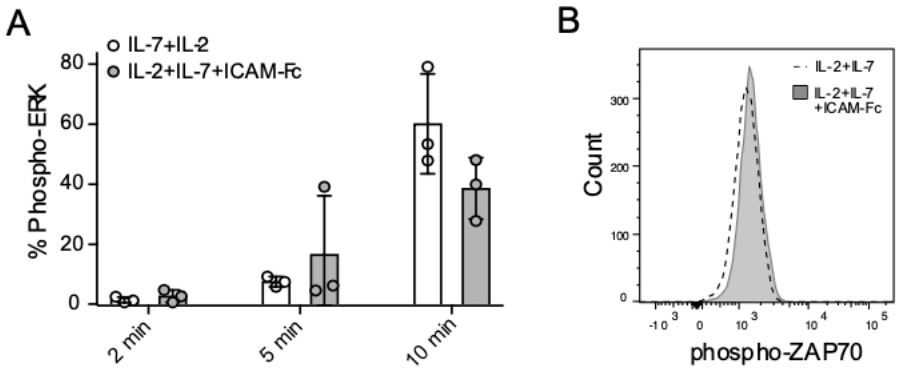

Fig. S1. Exposure to ICAM-1 alone does not lead to enhanced ERK or ZAP70 phosphorylation after TCR stimulation. (**A**) Undifferentiated or ICAM-exposed T cells were stimulated with 5 µl anti-CD3/anti-CD28 complex and tested for phospho-ERK. (**B**) Analysis of phospho-ZAP70 after 2 minutes of exposure to anti-CD3/anti-CD28 complex

MATERIALS AND METHODS

Biological samples, cell isolation and reagents. Cord blood (CB) were received from Obstetrics and Gynecology department at Meriter Hospital, Madison, WI or obtained from commercial cord blood banks. Mononuclear cells were isolated by density gradient centrifugation using Ficoll-plaque PLUS. If contaminating erythrocytes were observed, density gradient purification step was repeated to obtain a purer mononuclear cell fraction. $CD14^+$ monocytes from CBMCs were positively isolated using magnetic labelling (CD14 beads from Miltenyi Biotec). $CD4^+$ T cells were either positively selected (CD4 beads from Miltenyi Biotec) or were isolated using negative selection where unwanted cells were labelled and separated from $CD4^+$ T cells (CD4 T cells isolation kit by Miltenyi Biotec or EasySep CD4 T cell isolation kit by Stemcell technologies). To purify mononuclear cells from adult peripheral blood, fresh venous blood from heathy adult donors as per University of Wisconsin-Madison approved IRB protocol (2018-0304) and were collected and subsequently processed using density gradient centrifugation. Reagents: FACS buffer-PBS,5%BCS and 0.1% sodium azide; T cell media (TCM)-RPMI, 10% BCS, 5% FBS, 3% human serum, Pen/Strep and glutamine, 50 U/ml recombinant human IL-2 and 1ng/ml recombinant human IL-7 (Peprotech); Hypoglycemic media was prepared by using no glucose RPMI and glucose (Corning) was added at 3.8mM/L concentration with 10% heat inactivated dialyzed BCS with similar IL-2 and IL-7 concentration mentioned above.

In vitro culture system. To assess homeostatic proliferation- Isolated $CD4^+$ T cells were labelled with 5 μM Cell Trace Violet (CTV) proliferation dye (Thermo Fisher Scientific) following the manufacturer's protocol. In a 96 well plate, labeled T cells (5×10^4/well) were either cultured alone in T cell media (TCM) or with autologous monocytes (2.5×10^4). To assess impact of TCR and LFA stimulation - Isolated $CD4^+$T cells were also cultured either

in presence of 2 μg/ml plate bound human ICAM-1 Fc fusion protein (Acro Biosystems) alone or with 2 μg/ml plate bound anti-CD3 and 4 μg/ml soluble anti-CD28 antibodies (Biolegend), or with both anti-CD3/CD28 and ICAM-1-Fc. After 3-5 days, T cells from each culture condition were harvested and re-plated onto a new cell culture plate in fresh TCM for additional 7-5 days before using them for further analyses.

Flow cytometric analysis. Cells were resuspended in phosphate buffered saline (PBS) containing 5% bovine calf serum (BCS), 20% human AB serum and 0.1% sodium azide, then labeled with fluorescent antibodies for 20 min at 4°C. Cells were phenotyped using the following antibodies: CD3 (HIT3a, Biolegend), CD14 (63D3, Biolegend), CD45RO (UCHL1, Biolegend), CD45RA (HI100, Biolegend), CD31 (WM59, Biolegend), CD69 (FN50, Biolegend), IL-12Rβ2 (2B6/12beta2, BD Biosciences). For analysis of proliferation, T cells were labelled with 5 μM Cell Trace Violet (CTV) proliferation dye (ThermoFisher Scientific) prior to culture. For intracellular analysis of IFN-g (4S.B3; Biolegend), T-bet (04-46, BD Biosciences), BCL-2 (BCL/10C4, Biolegend) T cells were stimulated with PMA/ionomycin in the presence of brefeldin A for 4-6h, then fixed and permeabilized (Cyto-Fast Fix/Perm buffer set, Biolegend) prior to intracellular staining. Staining for cells expressing intracellular TCF1 (7F11A10, Biolegend) was performed according to the manufacturer's protocol using BD Biosciences' transcription factor buffer set. Analysis of phospho-ERK (6B8B69, Biolegend) and phospho-ZAP-70 (A16043E, Biolegend) was performed using True-Phos Perm buffer set (Biolegend).

Metabolic Assays. Seahorse cell energy phenotype test (Agilent) was performed to assess metabolic phenotype of the cells. T cells cultured for 10 days in respective conditions were harvested and plated on Poly-L-Lysine (50 μg/ml) (Advanced biomatrix) coated seahorse culture plates. Cell seeding concentration of 2.5×10^5 cells/well was used. Oligomycin and

FCCP stock solutions were prepared following the protocol provided by the manufacturer and were used at 1μM concentration per well. Intracellular ATP was measured using the colorimetric assay from Abcam. For experiments used to block glycolysis, cells were incubated with 10mM 2DG and to block oxidative phosphorylation Oligomycin was used at a concentration of 1μM

Chatper III: iNKT cells orchestrate a pro-hematopoietic switch that enables engraftment in non-conditioned hosts

Nicholas J Hess, Nikhila S Bharadwaj, Elizabeth A Bobeck, Courtney McDougal, Shidong Ma, John-Demian Sauer, Amy W Hudson, and Jenny E Gumperz

This is my co-first author manuscript that was published in Life science alliance in 2021. Text was co-written by Dr. Nicholas Hess and Dr. Jenny Gumperz. My contributions to this include designing and setting up experiments (excluding experiments shown in figures 1, 2, 3, 6A-C, 6E, S1, S2 and S5) and formal data analysis. Few in-vitro experiments (Fig 4B, 6B) were performed by Dr. Nicholas J Hess. Few in-vivo experiments shown in later figures were set up in collaboration with Dr. Nicholas J Hess.

Abstract

iNKT cells are a conserved population of innate T lymphocytes that interact with key antigen presenting cells to modulate adaptive T cell responses in ways that can either promote protective immunity, or limit pathological immune activation. Understanding the immunological networks engaged by iNKT cells to mediate these opposing functions is a key pre-requisite to effectively using iNKT cells for therapeutic applications. Using a human umbilical cord blood xenotransplantation model, we show here that co-transplanted allogeneic $CD4^+$ iNKT cells interact with monocytes and T cells in the graft to coordinate pro-hematopoietic and immunoregulatory pathways. The nexus of iNKT cells, monocytes, and cord blood T cells led to the release of cytokines (IL-3, GM-CSF) that enhance HSPC activity, and concurrently induced PGE_2-mediated suppression of T cell inflammatory responses that limit HSPC engraftment. This resulted in successful long-term hematopoietic engraftment without pre-transplant conditioning, including multi-lineage human chimerism and colonization of the spleen by antibody-producing human B cells. These results highlight the potential for using iNKT cellular immunotherapy to improve rates of hematopoietic engraftment independently of pre-transplant conditioning.

Introduction

Hematopoietic stem cell transplantation (HSCT) is used clinically to treat a variety of malignancies, as well as non-malignant hematologic diseases such as immunodeficiency disorders (Juric et al., 2016). Despite advances in pre-transplant conditioning regimens, which are used to reduce tumor burden and ablate host immune cells in order to facilitate engraftment of transplanted hematopoietic stem and progenitor cells (HSPCs), adverse outcomes including graft failure, graft-versus-host-disease (GVHD), and cancer relapse or progression remain highly problematic (Bishop et al., 2011; Chen et al., 2017; Tsai et al., 2016; Yang et al., 2017). Thus, there is an ongoing need for new approaches to improve engraftment success, while minimizing GVHD and maintaining graft-versus-tumor (GVT) activity.

Invariant natural killer T (iNKT) cells are innate T lymphocytes that appear to play a constitutive role in promoting hematopoietic activity, since iNKT cell deficient mice show impaired hematopoiesis (Kotsianidis et al., 2006). Additionally, iNKT cells may play important roles in regulating the outcome of immune reconstitution following human HSCT, since they are one of the earliest T cell subsets to reconstitute (Beziat et al., 2010; Dekker et al., 2020), and high frequencies of iNKT cells in graft tissue and at early times post-transplantation are associated with reduced GVHD (Chaidos et al., 2012; Haraguchi et al., 2004), as well as with lower rates of cancer relapse (Casorati et al., 2012; de Lalla et al., 2011). Prior studies have focused on the therapeutic potential of iNKT cells for preventing GVHD and promoting GVT following HSCT (Mavers et al., 2017; Negrin, 2019; Schneidawind et al., 2013). However, their therapeutic potential for promoting engraftment success remains poorly understood.

Importantly, iNKT cells are ideal candidates for use in allogeneic cellular immunotherapy applications such as HSCT. In contrast to MHC-restricted T cells that recognize foreign peptides, iNKT cells are restricted by CD1d molecules, which are highly conserved antigen presenting molecules that present lipids and glycolipids (Brigl and Brenner, 2004). Due to the limited polymorphism of human CD1d genes (Han et al., 1999), iNKT cells do not mediate allo-responses to antigen presenting cells (APCs) from unrelated individuals. Moreover, iNKT cells are activated by multiple endogenous pathways including recognition of self lipids presented by CD1d, TCR-independent cytokine exposure, and integrin-mediated signaling (Brigl et al., 2003; Brigl et al., 2011; Fox et al., 2009; Sharma et al., 2018). Thus, they can constitutively perform immunological functions following transplantation, without requiring pharmacological activation.

Here, we have used a model of human umbilical cord blood (UCB) transplantation into immunodeficient NOD/SCID/$g_c^{-/-}$ (NSG) mice to investigate how co-transplantation of allogeneic human $CD4^+$ iNKT cells affects engraftment outcomes. In clinical settings UCB transplantation is associated with low incidence of GVHD (Keating et al., 2019), but it is limited by high rates of graft failure (about 20% of transplant cases), and by longer median times to neutrophil and platelet recovery than bone marrow or G-CSF mobilized peripheral blood transplants (Lucchini et al., 2015; Tsai et al., 2016). A central component of the graft failure and delayed immune reconstitution in UCB transplantation is thought to be the comparatively low numbers of hematopoietic stem and progenitor cells (HSPCs) in UCB samples (Brown and Boussiotis, 2008). Additionally, inflammation, triggered by conditioning-associated damage to the host and/or by transplantation-associated activation of donor-derived immune cells, likely plays an important role in UCB graft failure (Luis et al., 2016; Ramadan and Paczesny, 2015). Using non-conditioned mice to minimize damage-

associated inflammation in the host, we observed that co-transplanted allogeneic human iNKT cells orchestrated a coordinated response involving the secretion of cytokines that promote hematopoietic activity, while concurrently regulating the production of inflammatory cytokines that adversely affect engraftment.

Results

Human hematopoietic engraftment in non-conditioned hosts.

Pre-transplant conditioning is typically required for successful engraftment of purified human HSPCs transplanted into immunodeficient murine hosts (McIntosh et al., 2015; Sippel et al., 2019; Waskow et al., 2009). However, prior studies have established that immunodeficient mice with mutations that lead to reduced functioning of *c-kit* (the receptor for stem cell factor) support robust human hematopoietic engraftment without requiring pre-transplant conditioning (Cosgun et al., 2014; Czechowicz et al., 2019; Hess et al., 2020b; McIntosh et al., 2015; Yurino et al., 2016), presumably because the transplanted human cells (which have normal *c-kit* activity) have a competitive advantage over the endogenous murine hematopoietic cells. Therefore, we used NBSGW mice, which bear a hypomorphic W^{41J} *c-kit* mutation as a positive control to generate successful human hematopoietic engraftment in a non-conditioned host. Three months after transplanting NBSGW mice with purified human $CD34^+$ HSPCs, a sizeable population of human immune cells was present in the murine bone marrow (Fig. 1A, top row, left panel). The human immune compartment contained a $CD34^+$ subset comprising multiple sub-populations, including multi-potent progenitors ($CD38^-$ $CD45RA^-$), committed progenitors ($CD38^+CD45RA^+$), myeloid progenitors ($CD33^+$ or $CD123^+$), and early B lymphocytic lineage cells ($CD19^+$) (Fig 1A, top row, middle and right panels). These results indicated that, consistent with prior analyses (Cosgun et al., 2014; Czechowicz et al., 2019; Hess et al., 2020b; McIntosh et al., 2015; Yurino et al., 2016),

transplanting human cord blood HSPCs into non-conditioned NBSGW mice resulted in successful hematopoietic engraftment that was sustained for at least three months.

We next investigated transplantation of total human umbilical cord blood mononuclear cells (CBMCs) into non-conditioned NSG mice (a strain that is similarly immunodeficient as NBSGW, but is wild-type for *c-kit*). When we transplanted CBMCs alone ($5x10^6$ cells per mouse), there was typically only a small population of human cells detected in the bone marrow after 3 months (Fig 1A, middle row). The human population found in these mice showed little or no positive staining for CD34 (Fig 1A, middle row), and instead the human population was comprised almost exclusively of T cells (Figure 2C, middle panel), indicating hematopoietic failure had occurred. In contrast, when we co-transplanted CBMCs ($5x10^6$ cells) along with allogeneic $CD4^+$ iNKT cells ($1x10^6$ cells) into non-conditioned NSG mice we observed abundant human cells in the murine bone marrow after 3 months (Fig 1A, bottom row). Similar to what we had observed in HSPC-transplanted NBSGW mice, the human compartment in the bone marrow of NSG mice co-transplanted with human CBMCs + iNKT cells contained a $CD34^+$ subset made up of multiple progenitor sub-populations (Fig 1A, bottom row). Quantitative flow cytometric analysis confirmed that mice that received CBMCs + iNKT cells had significantly higher numbers of human $CD34^+$ cells in the murine bone marrow than mice that received CBMCs alone (Fig 1B), suggesting that co-transplantation of iNKT cells promoted human cord blood hematopoietic engraftment.

Since most of the human cells in the murine bone marrow at three months post-transplantation were negative for CD34 (Fig 1A), we performed flow cytometric analyses to identify types of differentiated cells. As expected, based on prior reports indicating that myelopoiesis is comparatively efficient in Kit-mutant mice (Cosgun et al., 2014; Hess et al., 2020b; McIntosh et al., 2015), we observed populations of CD34-negative human cells

expressing the myeloid lineage markers CD33 or CD123 in NBSGW mice transplanted with purified cord blood HSPCs (Fig 2A, left panel). Similar $CD33^+$ or $CD123^+$ populations were also observed in the bone marrow of NSG mice transplanted with CBMCs + iNKT cells (Fig 2A, right panel), whereas these cells were absent in the bone marrow of NSG mice transplanted with CBMCs alone (Fig 2A, middle). Human cells expressing B-lineage markers (CD19, CD38) were also present in both the HSPC-transplanted NBSGW mice and CBMC + iNKT-transplanted NSG mice, but were rare or absent in NSG mice that received CBMCs alone (Fig 2B). Staining for T lymphocytes and NK cells revealed that nearly all the human cells in the bone marrow of NSG mice that received CBMCs alone were T cells (Fig 2C, middle), whereas the bone marrow of HSPC-transplanted NBSGW mice and CBMC + iNKT-transplanted NSG mice contained few T cells (Fig 2C, left and right panels). Phenotypic analysis of the T cells present in the bone marrow of mice transplanted with CBMCs alone compared to CBMCs + iNKT cells showed that they did not differ significantly in their frequencies of $CD4^+$ or $CD8^+$ T cells, but the T cells of mice that received CBMCs alone appeared strongly biased towards an activated effector phenotype, with significantly higher frequencies of $CD45RO^+$ cells and lower frequencies of $CD45RA^+$ and a higher proportion of T cells showing a blasting phenotype (Fig 2D). Since we have previously established that human $CD3^+$ T cells do not arise from HSPCs under the experimental conditions used here (Hess et al., 2020a; Hess et al., 2020b), these results suggest that in mice that received CBMCs alone, T cells that were present in the starting graft tissue became activated into an effector status and this was associated with a failure of multi-lineage immune reconstitution. In contrast, in mice that received CBMCs + iNKT cells, T cell activation was more limited and there was successful immune reconstitution of myeloid and B lineage cells at three months post-transplant.

Productive B cell engraftment.

We noted that human B cell chimerism appeared more robust in the bone marrow of NSG mice transplanted with CBMCs + iNKT cells compared to NBSGW mice transplanted with purified umbilical cord blood HSPCs (Fig 3A). We therefore delved further into the characteristics of human B cell reconstitution in NSG mice transplanted with CBMCs + iNKT cells. There was little or no evidence of human B cells in the murine bone marrow for the first 4-5 weeks following transplantation, and a population of human cells staining brightly for CD38 and co-expressing CD19 emerged after approximately 6 weeks (Fig. 3B). Notably, this is similar to the timing observed for the emergence of B cells following hematopoietic transplantation in humans (van der Maas et al., 2019).

Human B cell chimerism was maintained in the NSG bone marrow and spleen for at least 9 months following transplantation of CBMCs + iNKT cells (Fig. 3C). The human compartment in the spleens of mice transplanted with CBMCs + iNKT cells appeared dominated by B cells, but we also detected human monocytic cells ($CD14^+$) and human T cells ($CD3^+$) that remained for at least 6 months following transplantation (Fig 3D). We also performed histological analyses of spleen tissue from NSG mice transplanted with CBMCs + iNKT cells at 10-months post-transplantation. Immunohistochemical staining revealed large aggregates of $CD20^+$ cells (a marker of mature B cells), and within these areas were isolated cells staining positively for Bcl-6, which is a marker of germinal centers (Fig. 3E, left panel). Additionally, isolated cells staining strongly for human IgM or human IgG were visible in these areas (Fig. 3E, middle and right panels), suggesting the presence of B cells expressing successfully rearranged surface immunoglobulin. Plasma samples taken at 5-9 months post-transplantation typically contained clearly detectable levels of human immunoglobulin, confirming the presence of immunoglobulin-producing human B cells (Fig. 3F). Thus, non-

conditioned NSG mice given CBMCs + iNKT cells developed a durable and productive human B cell compartment.

To confirm that the enhanced human immune reconstitution observed in NSG mice given CBMCs + iNKT cells was selectively associated with iNKT cells and not simply due to co-transplantation of cultured human T cells, we tested mice that were given CBMCs combined with allogeneic polyclonal $CD4^+$ T cells that were expanded in vitro under the same conditions as those used for the iNKT cells. These mice had too few human cells in the bone marrow for reliable analysis at 12 weeks post-transplantation (data not shown), and at 10 weeks post-transplantation they contained only a small human cell population that lacked B cells (Fig. S1). We also found that human iNKT cells transplanted into non-conditioned NSG mice were detectable in the murine bone marrow within two days following transplantation and remained detectable there for at least 3 weeks (Fig. S2A). Flow cytometric analysis of mice transplanted with a 1:1 ratio of iNKT cells and CMBCs revealed that by five weeks after transplantation the iNKT cells comprised less than 1% of the human cells in bone marrow (Fig. S2B), suggesting that the iNKT cells expanded less efficiently than the cord blood T cells in the weeks following transplantation. Together, these results confirmed that iNKT cells promote immune reconstitution by allogeneic CBMC-derived cells.

Role of accessory cells.

We next investigated whether the impact of iNKT cells was due to direct interactions with HSPCs. Co-transplanting iNKT cells with purified HSPCs was not sufficient to promote successful engraftment (Fig. 4A), suggesting other cell types present in CBMC grafts were required. Using a live cell in vitro imaging system, we investigated the amount of cell-cell interaction between fluorescently labeled allogeneic iNKT cells and each of the three most abundant immune populations present in the CBMC grafts (T cells, monocytes, and B cells).

We observed the highest amount of fluorescence signal overlap between iNKT cells and monocytes, and the lowest amount between iNKT cells and B cells, with slightly elevated overlap signal for iNKT cells and cord T cells (Fig. 4B). Notably, while CD1d staining appeared uniformly positive on cord blood monocytes, CD1d appeared only to be expressed at low levels on a fraction of cord T cells (Fig. 4C).

Since these results suggested a potential role for the monocytes and/or T cells that are present in CBMC samples, we tested the impact of these cell types on HSPC engraftment in vivo. Purified HSPCs were co-transplanted with purified autologous monocytes, or purified autologous monocytes and purified autologous T cells, in the presence or absence of allogeneic iNKT cells. Co-transplantation of HSPCs with monocytes and iNKT cells resulted in significantly higher numbers of human $CD34^+$ cells in the murine bone marrow after 3 months compared to HSPCs transplanted only with autologous monocytes (Fig. 4D, left plot). Similarly, significantly higher numbers of total differentiated cells (all human $lineage^+$ cell types, excluding T cells) were detected in mice that received HSPCs + monocytes + iNKT cells (Fig. 4D, right plot). This suggested that interactions between iNKT cells monocytes have pro-hematopoietic effects that promote HSPC engraftment and immune reconstitution in non-conditioned hosts.

In contrast, inclusion of autologous T cells with the HSPCs + monocytes resulted in significantly reduced numbers of $CD34^+$ and $lineage^+$ cells compared to mice that received only HSPCs + monocytes (Fig. 4D), indicating that the presence of autologous T cells had an adverse impact on human HSPC engraftment. However, when allogeneic iNKT cells were co-transplanted with the monocytes and T cells, the engraftment of $CD34^+$ cells was increased and enhanced reconstitution of non-T cell $lineage^+$ cells was observed (Fig. 4D).

Thus, the co-transplanted iNKT cells appeared to counteract the adverse effects of cord T cells on HSPC engraftment and immune reconstitution.

Pro-hematopoietic activity of iNKT cells.

To further investigate the pro-hematopoietic effects of co-transplanted iNKT cells, we assessed the ability of our iNKT cells to produce factors that promote hematopoietic expansion. Purified $CD34^+$ cells were cultured in serum-free medium containing a cytokine cocktail (SCF, TPO, Flt-3L, IL-7) with concentrations adjusted to support HSPC differentiation at a somewhat sub-optimal level. In parallel, $CD34^+$ cells were cultured in the presence of transwell inserts containing iNKT cells alone or iNKT cells and anti-CD3/anti-CD28 coated beads. After 10 days in culture, the number of cells in the lower transwell expressing lineage markers (CD33, CD38, CD45RA) was quantitated. While the presence of iNKT cells alone in the upper transwell had no detectable impact, the differentiation of HSPCs in the lower well was markedly increased when CD3/CD28-activated iNKT cells were present in the upper transwell (Fig. 5A). Thus, this analysis indicated that activated but not resting iNKT cells secreted factors that promote the hematopoietic activity of $CD34^+$ HSPCs.

In prior studies we have observed that even weak TCR agonism resulting from exposure to CD1d molecules presenting cellular antigens was sufficient to activate human $CD4^+$ iNKT cells to produce GM-CSF (Wang et al., 2008). We also found that the *IL3* locus of resting human $CD4^+$ iNKT cells resembled that of *CSF2* (GM-CSF) in showing a histone acetylation pattern associated with active chromatin (Wang et al., 2012). Thus, we hypothesized that human $CD4^+$ iNKT cells may also be able to produce IL-3 in response to comparatively low levels of TCR stimulation. To test this, we assessed secretion of IL-3 versus GM-CSF by our iNKT cells in response to recombinant CD1d molecules loaded with titrated doses of the

synthetic antigen a-GalCer. Compared to GM-CSF, half maximal production of IL-3 required approximately 2-fold lower doses of a-GalCer (Fig. 5B), indicating that iNKT cells produce IL-3 even more readily than GM-CSF in response to TCR stimulation.

Since these results suggested that exposure to $CD1d^+$ cells might be sufficient to activate iNKT cell secretion of both GM-CSF and IL-3, we assessed the levels of these cytokines in culture supernatants of iNKT cells with cord monocytes and T cells. Co-cultures of all three cell types consistently showed elevated levels of both GM-CSF and IL-3 (Fig. 5C). Co-cultures of iNKT cells + monocytes or iNKT cells + T cells sometimes contained elevated levels of GM-CSF or IL-3, but overall did not reproducibly differ from iNKT cells alone, suggesting that the nexus of iNKT cells and cord monocytes with autologous T cells was key for inducing release of GM-CSF and IL-3 (Fig. 5C). To confirm the presence of this iNKT cell-dependent cytokine pathway in vivo, we transplanted NSG mice with CBMCs alone or CBMCs + iNKTs then harvested bone marrow and blood plasma after 72 hours and analyzed human GM-CSF and IL-3 by ELISA. Significantly elevated levels of GM-CSF and IL-3 were detected in bone marrow of mice that received CBMCs + iNKT cells compared to those that got only CBMCs, and these cytokines also appeared modestly elevated in the blood (Fig. 5D).

We next investigated whether factors secreted during co-cultures of iNKT cells with cord monocytes and autologous T cells were sufficient to promote the hematopoietic activity of cord blood HSPCs. Culturing purified $CD34^+$ HSPCs in the presence of transwell inserts containing a combination of iNKT cells + monocytes + autologous T cells led to significantly enhanced hematopoietic activity, whereas exposure to transwells containing any of these cells alone or in pairs did not increase the output of differentiated cells (Fig. 5E). Together, these

results demonstrate a pro-hematopoietic nexus consisting of iNKT cells, cord monocytes, and autologous T cells.

Adverse effects of cord T cells.

The observation that hematopoietic engraftment fared significantly worse in mice co-transplanted with purified $CD34^+$ HSPCs + autologous monocytes + T cells compared to mice that received HSPCs + autologous monocytes alone (Fig. 4D) suggested that cord T cells promote graft failure in this model. Consistent with this, we found that NSG mice given T-depleted CBMCs showed significantly greater numbers of $CD34^+$ and $lineage^+$ cells (excluding T cells) in the murine bone marrow after three months compared to those given total CBMCs (Fig. 6A). Additionally, we found that the in vitro expansion of HSPC-derived cells was significantly limited when they were co-cultured with CBMCs in the presence of anti-CD3 antibody stimulation, but expansion recovered when a blocking antibody against either IFN-g or TNF-a was included (Fig. 6B). Analysis of blood plasma samples taken at regular intervals during the first 3 months post-transplantation revealed that mice transplanted with CBMCs alone showed clearly detectable human IFN-g in the blood that peaked at 6 weeks following transplantation (Fig. 6C), suggesting that the cord T cells become activated following transplantation in this model. Mice given CBMCs + iNKT cells showed significantly lower plasma IFN-g concentrations at 3 weeks post-transplantation ($P=0.0033$, $n=13$), and also showed a trend towards reduced levels at later time points (Fig. 6C). Thus, co-transplantation of iNKT cells was associated with reduced inflammatory activation following CBMC transplantation.

We have previously shown that human $CD4^+$ iNKT cells induce monocytes from adult peripheral blood to differentiate into cells that potently suppress adult T cell IFN-g production (Hegde et al., 2009; Hegde et al., 2011). We therefore hypothesized that iNKT

cells might interact with monocytes from cord blood to silence the activation of cord T cells. Using an in vitro co-culture system, we found that cord T cells cultured with autologous monocytes and iNKT cells showed significantly reduced proliferation and produced significantly less TNF-a and IFN-g after PMA and ionomycin stimulation compared to cord T cells cultured only with autologous monocytes (Fig. 6D). Additionally, we confirmed that transplanting purified cord T cells with autologous monocytes was sufficient to produce detectable levels of human IFN-g in the plasma that peaked at 6 weeks after transplantation into NSG mice, and co-transplantation of iNKT cells led to reduced circulating IFN-g (Fig. 6E). Taken together, these results suggested that iNKT cells interact with cord monocytes to suppress the responses of cord T cells.

Cord T cell suppression mediated via eicosanoid production.

In prior analyses, we observed that $CD4^+$ iNKT cells activated multiple inhibitory pathways in human monocytes from adult peripheral blood, including ones that were mediated via cell contact (e.g. up-regulation of PD-L1 and PD-L2) as well as ones mediated by secreted factors (e.g. IL-10 production) (Hegde et al., 2009; Hegde et al., 2011). We therefore tested whether contact with the iNKT cells and monocytes was required for the inhibition of cord T cell IFN-g production, or whether secreted factors were sufficient. Purified cord T cells were placed in wells coated with anti-CD3 and anti-CD28 antibodies in the presence or absence of transwell inserts containing autologous monocytes and allogeneic iNKT cells for 3-7 days. Intracellular cytokine staining after PMA and ionomycin stimulation of the cord T cells revealed a significant reduction in the percent that produced IFN-g in cultures that were exposed to transwells containing iNKT cells and monocytes (Fig. 7A). These results demonstrated that soluble factors produced during iNKT-monocyte interactions were

sufficient to inhibit cord T cells from acquiring IFN-g effector function in response to TCR-stimulation.

We next sought to determine the nature of the inhibitory factor. Because experiments to block the release of proteins through the secretory pathway using brefeldin A pre-treatment of the monocytes did not prevent the inhibitory effect (Fig. S3), we investigated whether the relevant soluble factor might be an eicosanoid, such as prostaglandin E_2 (PGE_2). A prior study found that human cord blood T cells mainly express the EP4 receptor, which is a G-protein coupled receptor that binds PGE_2 with high affinity and leads to cyclic AMP production (Li et al., 2014). Since the accumulation of cyclic AMP in T cells is suppressive (Arumugham and Baldari, 2017), this finding suggested that exposure to PGE_2 might inhibit cord T cells. Flow cytometric analysis for the two high affinity PGE_2 receptor subtypes, EP3 and EP4, demonstrated positive staining only for EP4 on our cord T cells (Fig. 7B). Using an enzyme assay to test supernatants from iNKT-monocyte co-cultures for the presence of PGE_2, we consistently observed detectable levels of PGE_2 (Fig. 7C). Mass spectrometric analysis of supernatants from iNKT-monocyte co-cultures also revealed the presence of PGE_2 and associated products from its biosynthetic pathway (Fig. S4). Moreover, addition of synthetic PGE_2 to cord $CD4^+$ T cells resulted in a significant reduction in their ability to produce IFN-g after CD3/CD28 stimulation (Fig. 7D). Thus, PGE_2 is released during iNKT-monocyte interactions, and exposure to PGE_2 inhibits the ability of cord T cells to produce IFN-g in response to TCR-stimulation.

We next investigated whether interrupting the PGE_2 pathway prevented the iNKT-monocyte inhibitory effects on cord T cells. Purified cord $CD4^+$ T cells were stimulated by anti-CD3 and anti-CD28 in the presence of transwell inserts containing iNKT cells and monocytes, with the monocytes pre-treated with dexamethasone, or a selective cyclooxygenase-2 (Cox-2)

inhibitor, or with vehicle. Similar to what we observed previously (Fig. 7A), cord T cell production of IFN-g in response to anti-CD3/CD28 was inhibited when iNKT cells and vehicle-treated monocytes were present in the upper transwell (Fig. 7E). However, cord T cell IFN-g production was nearly completely recovered when the monocytes in the upper well were pre-treated with dexamethasone or Cox-2 inhibitor (Fig. 7E). Moreover, pre-treating the cord T cells with a selective inhibitor of the EP4 receptor also led to marked recovery of their IFN-g production (Fig. 7E). Thus, blocking eicosanoid production by the monocytes, or blocking the main receptor for PGE_2 on cord T cells, prevented the inhibition mediated by iNKT-monocyte soluble factors.

To confirm that similar iNKT-monocyte interactions are important for the suppression of cord T cell responses in vivo, we tested the impact of pre-treating monocytes with dexamethasone in vivo. Non-conditioned NSG mice were co-transplanted with iNKT cells and unmanipulated CBMCs, or with iNKT cells and CBMCs where the monocytes were first removed and pre-treated with dexamethasone and then added back to the mixture prior to transplantation. Mice that received iNKT cells and CBMCs with dexamethasone pre-treated monocytes showed a trend towards higher plasma IFN-g levels than those that received iNKT cells and untreated CBMCs (Fig. 7F), indicating that the inhibition of T cell IFN-g associated with co-transplantation of iNKT cells requires intact eicosanoid production by cord monocytes. Thus, in addition to production of the pro-hematopoietic cytokines IL-3 and GM-CSF, the nexus of iNKT cells, cord monocytes, and cord T cells was concomitantly associated with reduced T cell secretion of inflammatory cytokines that adversely affect cord HSPC function.

Discussion

The results presented here identify a powerful functionality of human iNKT cells that enables successful human hematopoietic engraftment in non-conditioned NSG mice. Prior studies have shown that NSG mice can serve as excellent hosts for human hematopoietic transplantation because they are deficient in immune cell types that ordinarily reject xenogeneic transplants (Shultz et al., 2005; Shultz et al., 1995). However, conditioning was thought to be required in order to eliminate endogenous murine hematopoietic cells that would otherwise compete with transplanted human HSPCs for critical hematopoietic factors. In contrast, successful engraftment by human HSPCs can be achieved without conditioning in mouse strains that carry hypomorphic variants of the *c-kit* gene or in wild-type mice that have been pre-treated with antibodies to block the KIT receptor (CD117) (Cosgun et al., 2014; Czechowicz et al., 2019; McIntosh et al., 2015). Thus, eradication of $CD117^{+}$ host cells or their genetic impairment is known to create a murine environment that is permissive for engraftment of human HSPCs without conditioning. However, it is a highly surprising observation that co-transplanting human iNKT cells with CBMCs appears to phenocopy this situation in NSG mice, a KIT-sufficient strain.

A key mechanism underlying this effect of the co-transplanted iNKT cells is probably that they supply critical hematopoietic factors that promote the engraftment of human HSPCs. It has previously been observed that iNKT cell deficient mice show impaired hematopoiesis, suggesting iNKT cells play a constitutive role in promoting hematopoietic activity in vivo (Kotsianidis et al., 2006). Moreover, prior studies have established that after administration of the highly potent synthetic antigen a-GalCer murine iNKT cells produce GM-CSF and IL-3 in vivo, which leads to markedly enhanced colony-forming activity (Kotsianidis et al., 2006; Leite-de-Moraes et al., 2002). Consistent with this, we found that our human iNKT

cells efficiently produced IL-3 and GM-CSF in response to CD1d-mediated presentation of a-GalCer, and they also produced these cytokines during interactions with cord blood monocytes and autologous T cells. Thus, it is likely that the co-transplanted iNKT cells promote cord blood HSPC activity in this model at least in part through secretion of GM-CSF and IL-3. In this way they may produce a milieu in the host similar to that of knock-in mouse strains expressing human GM-CSF and IL-3, which have been shown to support improved multi-lineage human engraftment (Jangalwe et al., 2016; Rongvaux et al., 2014; Willinger et al., 2011).

However, pre-transplant conditioning is still required for efficient engraftment of human HSPCs in human cytokine knock-in mouse strains, suggesting that the presence of human hematopoietic cytokines is not sufficient to allow transplanted human HSPCs to compete successfully with endogenous murine hematopoietic cells. Therefore, production of human GM-CSF and IL-3 probably does not fully explain the effects of co-transplanting iNKT cells and CBMCs in this model. Interestingly, we found that even without co-transplanted iNKT cells, transplanting purified cord blood HSPCs with autologous monocytes resulted in 1-2 orders of magnitude greater engraftment than transplanting purified HSPCs alone (compare Fig. 4A and 4D). This suggests that cord blood monocytes support the engraftment of human HSPCs in non-conditioned NSG mice. We speculate that co-transplanting iNKT cells enhances this basal pro-hematopoietic effect of the cord blood monocytes. Specifically, given that PGE_2 has been identified as a powerful regulator of HSPC homing and survival that markedly enhances engraftment (Durand and Zon, 2010; North et al., 2007), we hypothesize that the ability of iNKT cells to induce PGE_2 secretion by cord monocytes (Fig. 7C and S4) is a key component of their engraftment promoting effects. Since eicosanoids such as PGE_2 are rapidly degraded in extracellular environments, this pathway would likely

require co-localization of transplanted iNKT cells, monocytes, and HSPCs. It will thus be important to determine where and when such exposure might occur following transplantation.

Our analysis shows that PGE_2 is produced during interactions between iNKT cells and cord blood monocytes, without a requirement for added antigens. This is consistent with prior studies demonstrating that human iNKT cells recognize cellular lipids presented by CD1d molecules, including lyso-phosphatidylcholine (LPC) (Chang et al., 2008; Fox et al., 2009; Lopez-Sagaseta et al., 2012), which is constitutively expressed at low levels by many cell types and is also produced at high levels during eicosanoid biosynthesis (Exton, 1994; Funk, 2001). We show here that PGE_2 produced during iNKT interactions with cord monocytes inhibits cord T cells through the EP4 receptor, and that this pathway is active in vivo, since pre-treating the monocytes with dexamethasone resulted in increased circulating human IFN-g in vivo following transplantation (Fig. 7). This pathway likely also promotes HSPC engraftment, since we observed that co-transplanting purified HSPCs with autologous monocytes and T cells resulted in engraftment failure, and this was mitigated when iNKT cells were also co-transplanted (Fig. 4D). Thus, we hypothesize that following transplantation cord blood T cells are activated to produce inflammatory cytokines and this response adversely affects autologous HSPCs, similar to effects observed previously in a model where total human umbilical cord blood was transplanted into pre-conditioned NSG mice (Wang et al., 2017). Since exposure to iNKT cells and monocytes limited cord blood T cell proliferation and TNF-a production in vitro (Fig. 6D), and nearly completely abrogated their IFN-g production (Fig. 6D and E), it seems likely that the iNKT-monocyte regulatory axis promotes HSPC engraftment by limiting the adverse impact of cord T cell inflammatory responses. However, in an unexpected and paradoxical twist, we also observed that secretion of factors that enhance HSPC activation was elevated when iNKT cells were co-incubated

with both monocytes and T cells compared to co-incubation with either cell type alone (Fig. 5C and E). Thus, our results point to a unique interrelationship, where iNKT cells and monocytes interact to limit the activation of cord T cells yet the presence of the T cells also enhances the release of pro-hematopoietic factors.

Interestingly, we observed little evidence of GVHD during these studies. About 5% of all the mice included in our analysis showed one or more signs of GVHD (weight loss, ruffled fur, jaundice, eye irritation), and only one of these was a mouse that received iNKT cells. This lack of GVHD is consistent with observations that umbilical cord blood transplantation in clinical settings is associated with comparatively low incidence of GVHD (Ballen et al., 2013; Keating et al., 2019), but contrasts with prior studies that have observed marked GVHD responses following transplantation of human cord blood cells into irradiated NSG mice (Wang et al., 2017). The relative lack of GVHD in our analysis likely results from minimizing the introduction of molecular patterns (e.g. conditioning-associated damage ligands, human red blood cell glycans) that have been shown to play a key role in the initiation of GVHD responses and xenograft rejection (Navarro-Alvarez and Yang, 2011; Ramadan and Paczesny, 2015; Toubai et al., 2016), but may also be due to tolerogenic effects of the iNKT cells, since prior studies in murine models have shown that iNKT cells protect against GVHD by interacting with myeloid-derived suppressor cells (MDSCs) to expand donor-derived regulatory T cells (Du et al., 2017; Schneidawind et al., 2015; Schneidawind et al., 2014). Consistent with this, we observed that nearly half of the small population of human T cells present in the bone marrow of mice that received CBMCs + iNKT cells retained a naive phenotype ($CD45RA^{+)}$, whereas the T cells from mice that received CBMCs alone were nearly all $CD45RO^{+}$ (Fig. 2D).

It is not clear whether co-transplantation of iNKT cells specifically promotes the establishment of the human B cell compartment in our model. Murine iNKT cells have been shown to induce the formation of early germinal centers in a Bcl-6 dependent manner (Chang et al., 2011), and therefore it is possible that the presence of co-transplanted iNKT cells may contribute to the durable and productive B cell compartment we observed in engrafted mice (Fig. 3C-F). However, while we also noted that NSG mice transplanted with CBMCs and iNKT cells had a higher B:myeloid ratio compared to NBSGW mice transplanted with purified HSPCs (Fig. 3A), it is possible that the KIT-sufficient status of the NSG host strain results in less efficient human myeloid differentiation in this strain.

Together, these findings support the potential utility of adult allogeneic iNKT cells as a cellular immunotherapy to improve outcomes of allogeneic human UCB transplantation. UCB transplantation in clinical settings is limited by high rates of graft failure and by longer times to neutrophil and platelet recovery compared to bone marrow and G-CSF mobilized peripheral blood transplants (Brown and Boussiotis, 2008; Lucchini et al., 2015). Our results suggest that iNKT-mediated production of hematopoietic factors and silencing of T cell inflammation produces an environment that is favorable for cord blood HSPC engraftment, and thus might significantly improve these limitations. However, further studies will be needed to determine the impact of co-transplanted iNKT cells on anti-microbial immunity and GVT activity following transplantation, since it is possible that the iNKT-monocyte axis described here may suppress immune responses that provide protection against infections and cancer relapse. In this regard it is important that we have previously found that eicosanoid-producing interactions between human iNKT cells and monocyte-derived DCs actually led to enhanced neutrophil-mediated control of cutaneously administered Candida albicans (Xu et al., 2016). Moreover, increased iNKT cell frequency following human haplo-identical

hematopoietic transplantation is associated with lower cancer relapse rates (Casorati et al., 2012; de Lalla et al., 2011), and human iNKT cells expanded from blood or donor lymphocyte infusions have been shown to directly lyse primary human leukemic blasts in vitro (Jahnke et al., 2019; Schmid et al., 2018). Thus, there is reason for optimism that iNKT cell immunotherapy may actually promote key aspects of immune function following hematopoietic transplantation, while also limiting the inflammatory activation of cord T cells and promoting HSPC engraftment

Figures

Figure 1

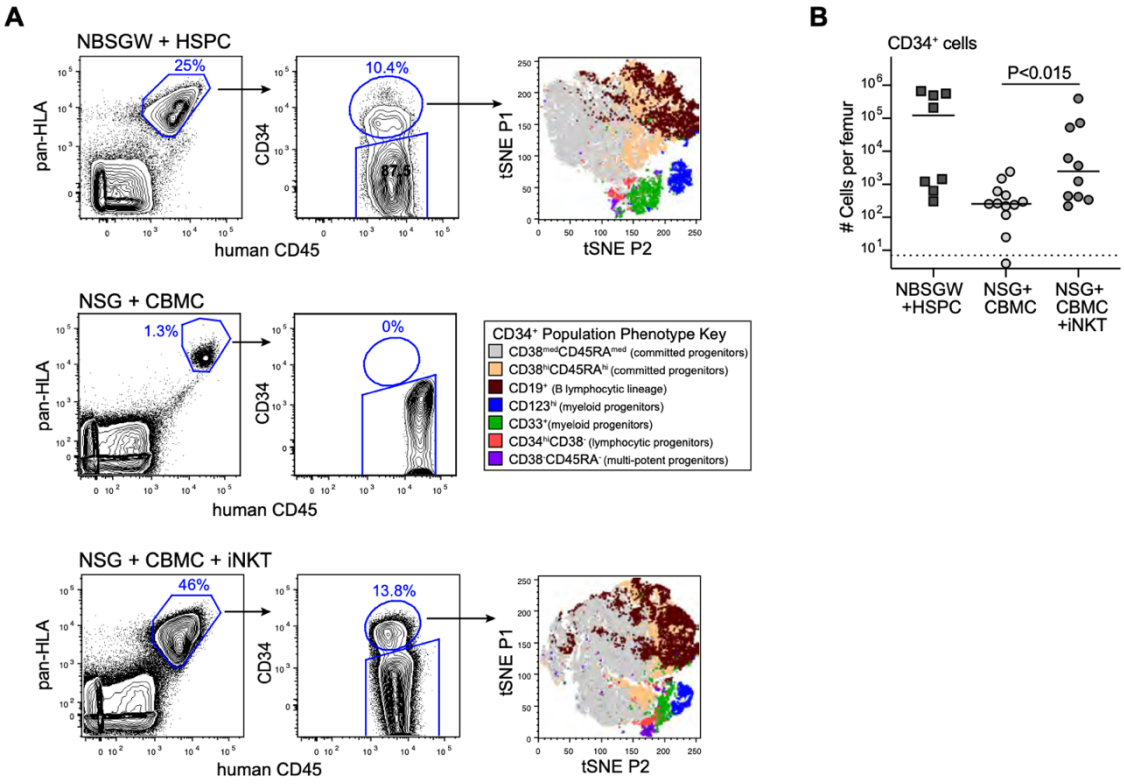

Co-transplanting nonconditioned NSG mice with cord blood mononuclear cells (CBMCs) and invariant natural killer T cells phenocopies HSPC engraftment observed in a KIT-deficient mouse strain. (A) Flow cytometric analysis to detect human cells expressing CD34 in murine bone marrow at 3 mo post transplantation. Top row shows results from an NBSGW (KIT deficient) mouse transplanted with 5×10^5 purified human cord blood $CD34^+$ HSPCs; (t-SNE) t-distributed stochastic neighbor embedding plot was generated from a concatenation of the human $CD34^+$ subsets of four similarly transplanted NBSGW mice (see color-coded key for populations in middle row). Middle row shows results from an NSG mouse transplanted with 5×10^6 human CBMCs. Bottom row shows results from an NSG mouse transplanted with 5×10^6 human CBMCs and 0.5×10^6 allogeneic $CD4^+$ invariant natural killer T cells; tSNE plot was generated from a concatenation of the human $CD34^+$ subsets of

three similarly transplanted NSG mice. (B) Aggregated data showing numbers of human $CD34^+$ cells detected in bone marrow at 3 mo post transplantation. Each symbol shows the result from one femur bone of an individual mouse, with bars showing the median; symbol below dotted line indicates specifically stained cells were not detected. Data are aggregated from six independent experiments; *P*-value calculated using a tailed Mann–Whitney test

Figure 2

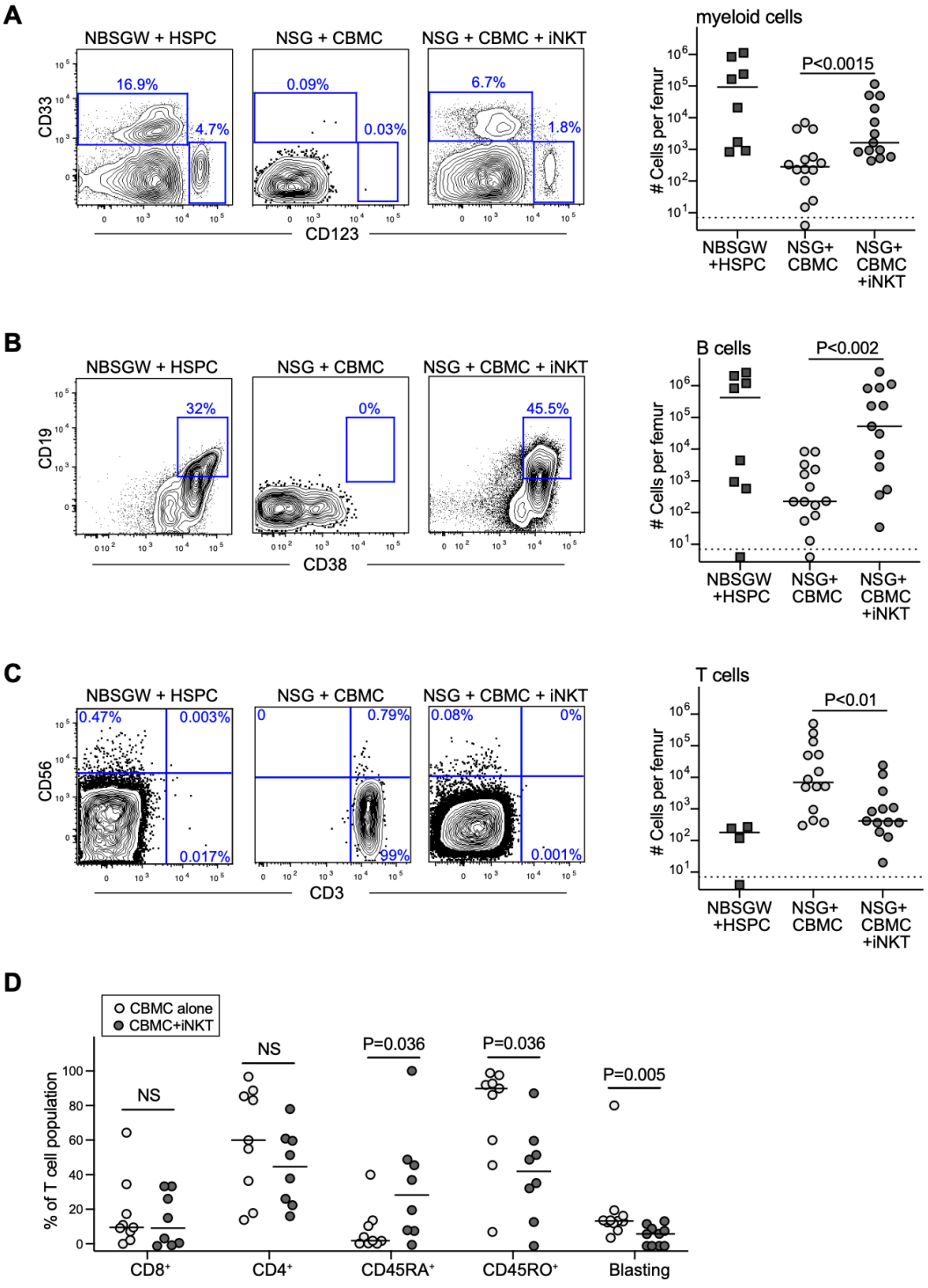

Figure 2. Establishment of multi-lineage immune engraftment.

(A) Flow cytometric analysis of murine bone marrow samples collected at 3 mo post transplantation showing staining of the CD34-negative human population for myeloid lineage markers (CD33 and CD123). Plot on right shows numbers of human myeloid cells detected in one femur bone of mice in the indicated treatment groups, with bars showing the median for each group (symbol below dotted line indicates no specifically detectable cells). Results aggregated from nine independent experiments; *P*-values calculated using a two-tailed Mann–Whitney test. **(B)** Staining for B-lineage cells, and aggregated data for numbers of B cells in bone marrow. **(C)** Staining for T cells and NK cells, and aggregated data for numbers of T cells in bone marrow. **(D)** Aggregated data for phenotypic analysis of T cells detected in bone marrow of mice that received cord blood mononuclear cells alone (light symbols) compared with cord blood mononuclear cells + invariant natural killer T cells (dark symbols).

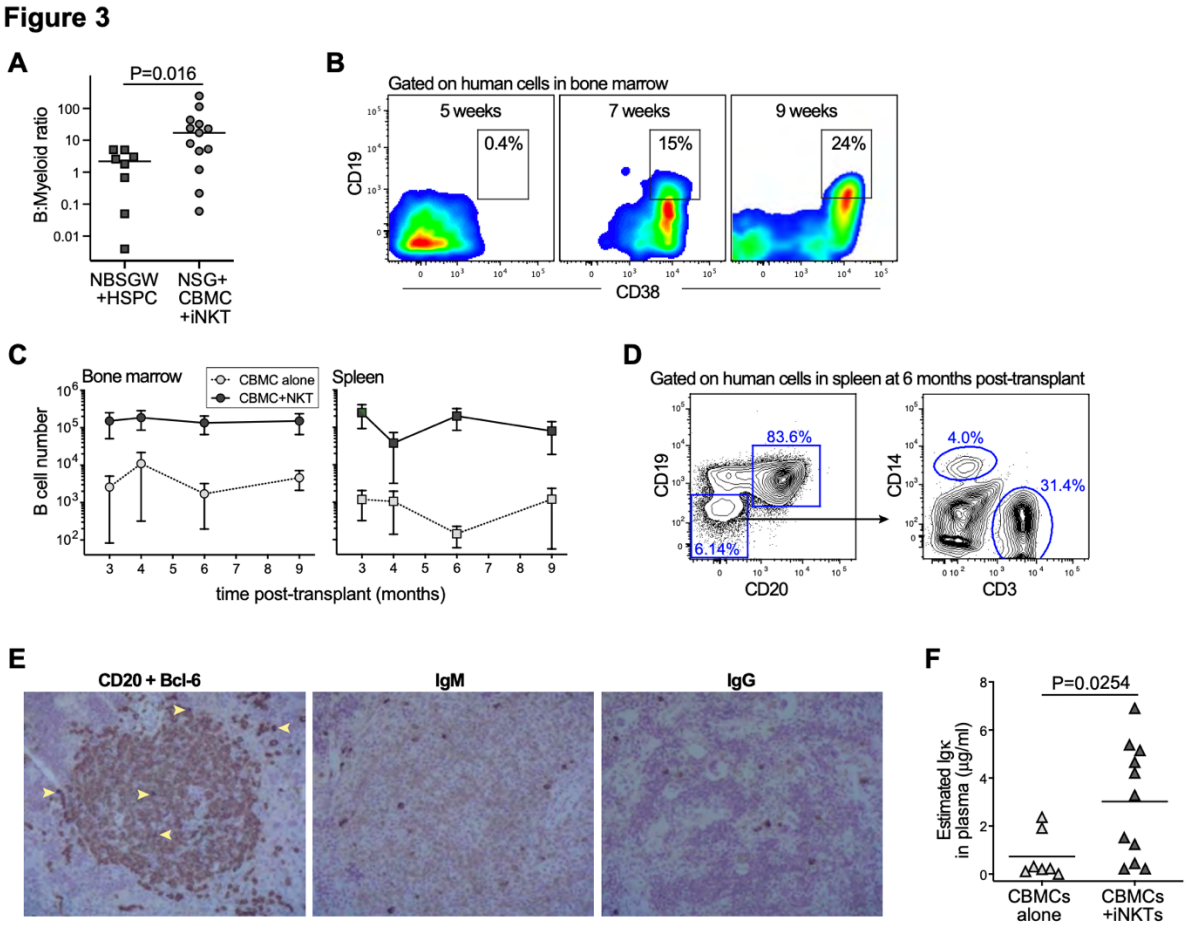

Figure 3. Establishment of a productive human B-cell compartment in NSG mice given cord blood mononuclear cells (CBMCs) and invariant natural killer T (iNKT) cells.

(A) Human compartment in bone marrow of NSG mice transplanted with CBMCs and iNKT cells show significantly greater ratio of B cells to myeloid lineage cells than in NBSGW mice transplanted with purified $CD34^{+}$ HSPCs. **(B)** Flow cytometric analysis of human cells in bone marrow at the indicated time points post transplantation showing the emergence of B-lineage cells. **(C)** Mean (±SEM) numbers of human B cells detected in murine bone marrow (left plot) or spleen (right plot) at the indicated times post engraftment. Data are aggregated from six independent experiments; with each symbol representing the average of three to

eight mice. **(D)** Flow cytometric analysis of human cells in spleen of an NSG mouse given CBMCs and iNKTs at 6 mo post transplantation. **(E)** Immunohistochemical analysis of serial tissue sections from the spleen of a mouse transplanted 10 mo earlier with human CBMCs and iNKT cells. Left panel shows co-staining for human CD20 (brown color) and Bcl-6 (dark purple color; examples of Bcl-6^+ cells indicated by yellow arrows). Middle panel shows staining for human IgM (μ chain). Right panel shows staining for human IgG (γ chain). Images from light microscopic analysis at 10× magnification. **(F)** Plasma samples were collected at 5–9 mo post transplantation, and tested using an ELISA specific for human Igκ light chain. Total amounts of Igκ were estimated by comparing plasma sample titers to a pooled human AB serum standard, and multiplying by previously determined values for human immunoglobulin (Cassidy & Nordby, 1975). Each symbol represents the mean of three replicate analyses of a plasma sample from an individual mouse. Data aggregated from three independent experiments; *P*-value calculated by two-tailed Mann–Whitney test.

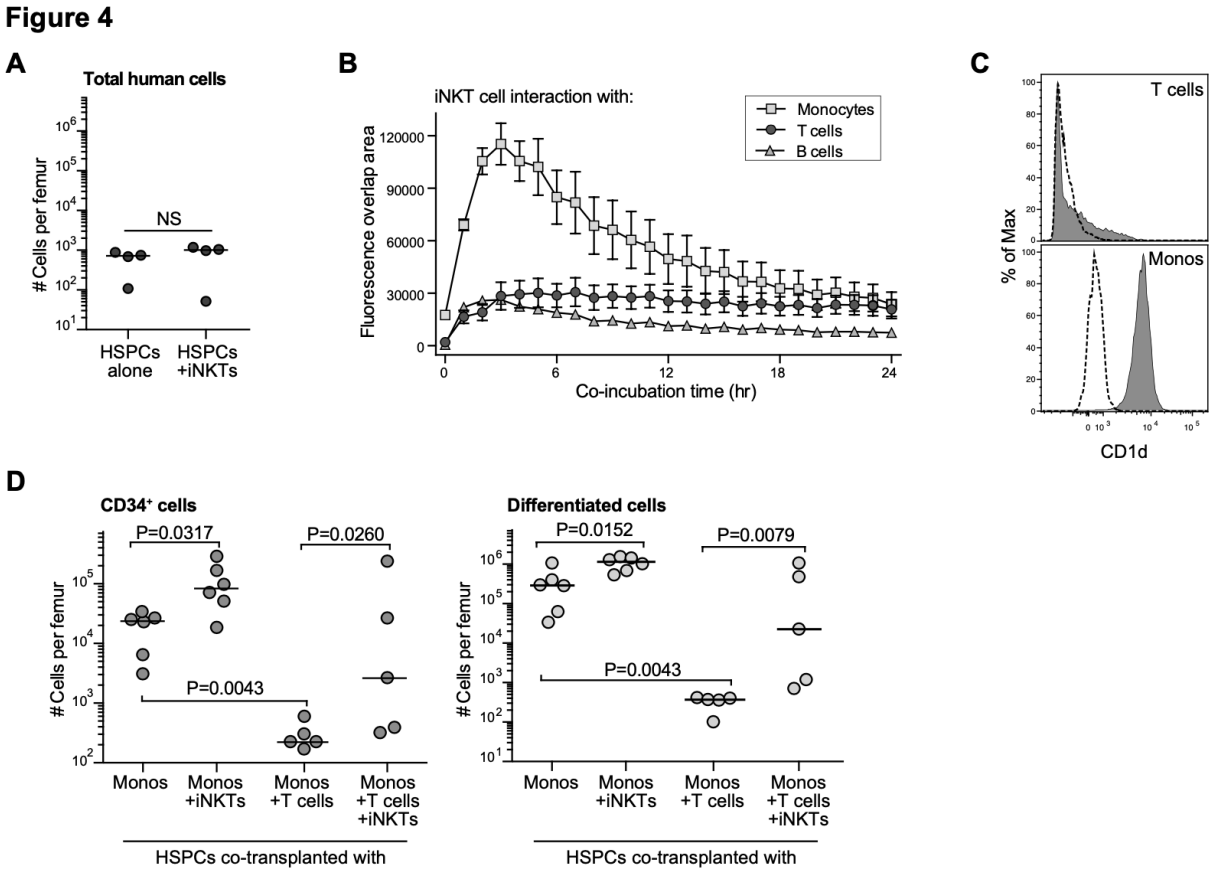

Figure 4. Invariant natural killer T (iNKT) cells interact with cord monocytes to promote HSPC engraftment.

(A) Analysis of the number of total human cells detected in one femur of NSG mice transplanted with 0.5–1 × 10^5 purified $CD34^+$ cells alone or in combination with 1 × 10^6 allogeneic $CD4^+$ iNKT cells. **(B)** Analysis of the amount of cell–cell interaction between iNKT cells and the three most abundant cell types found in cord blood. iNKT cells were labeled with a red dye and placed into tissue culture wells with equivalent numbers of purified cord blood monocytes, T cells, or B cells that had been labeled with a green dye. Fluorescence microscopic images were taken at 20× magnification every 60 min using an IncuCyte Live Cell imaging system. The plot shows the mean ± SEM area of fluorescence

overlap calculated from three replicate wells for each co-culture condition. **(C)** Flow cytometric staining of CD1d (filled histograms) compared with isotype (dotted lines) on cord blood T cells (upper panel) or monocytes (lower panel). **(D)** NSG mice were transplanted with 0.5–1 × 10^5 purified $CD34^+$ cells in combination with the indicated cell types. Left plot shows number of human $CD34^+$ cells per femur, and right plot shows number of $lineage^+$ human cells (excluding T cells) per femur at 3 mo post transplantation. Results aggregated from three independent experiments; *P*-values calculated using a two-tailed Mann–Whitney test.

Figure 5

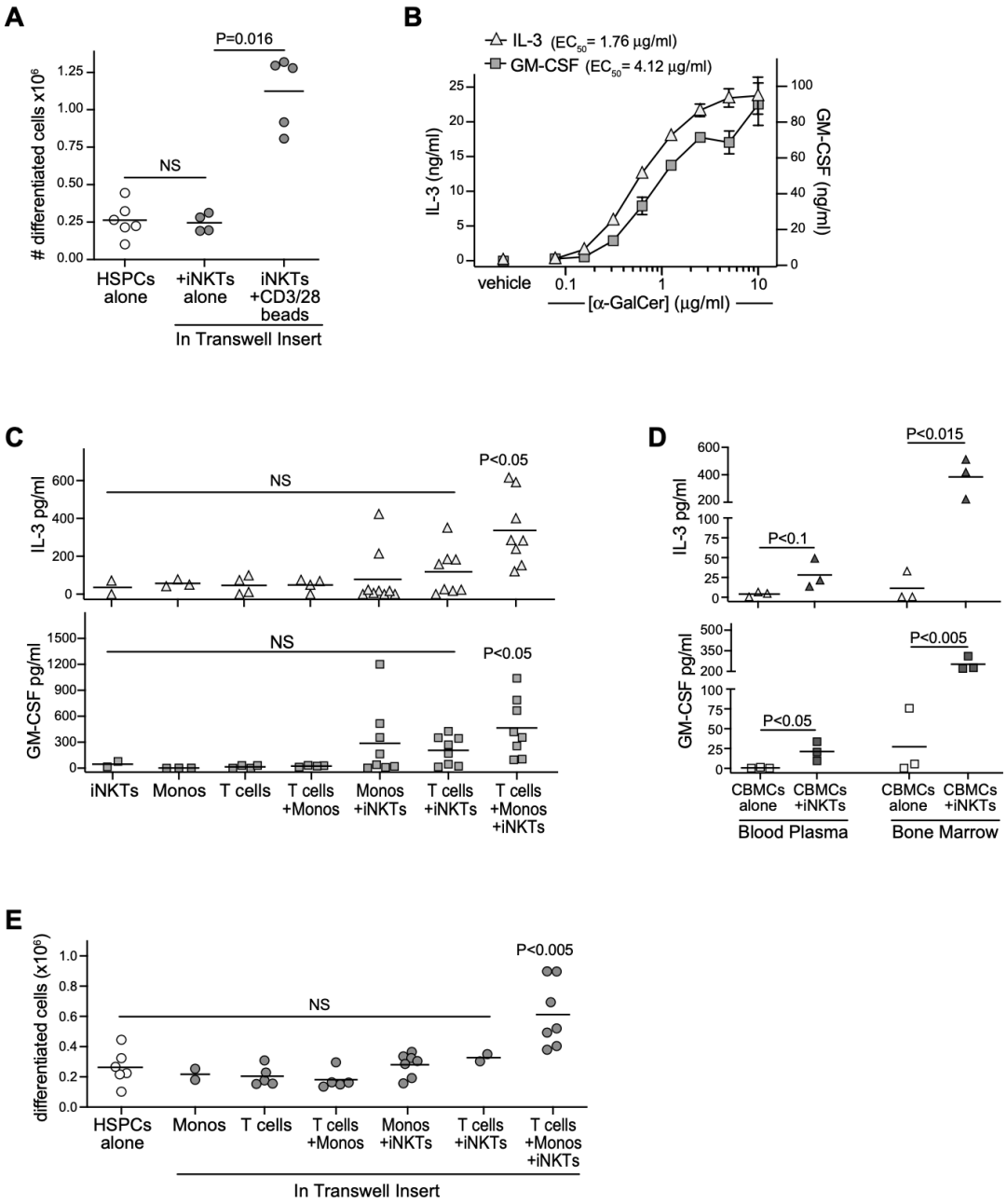

Figure 5. Invariant natural killer T (iNKT) cells show pro-hematopoietic activity that is activated by exposure to cord T cells and monocytes.

(A) Purified $CD34^+$ HSPCs were seeded at 2.5×10^4 cells/well and cultured in the lower wells of transwell plates in medium containing a hematopoietic cytokine cocktail. Where indicated, iNKT cells were added to the transwell inserts alone or in combination with CD3/CD28 Dynabeads. After 10 d, the number of $lineage^+$ cells in the lower transwell was quantitated. Plot shows aggregated results from six independent experiments with bars at the means and *P*-values calculated by a two-tailed Mann–Whitney test. **(B)** $CD4^+$ iNKT cells were exposed to plate-bound recombinant CD1d–Fc fusion protein that had been pretreated with the indicated concentrations of α-GalCer lipid antigen or with vehicle alone. Plot shows amounts of IL-3 (left axis) or GM-CSF (right axis) detected in the culture supernatant after 24 h. Symbols show means of three replicate wells, with error bars showing standard deviations (not always large enough to be visible). **(C)** iNKT cells, isolated cord T cells, and/or autologous cord monocytes were cultured alone or in the indicated combinations for 48 h, and amounts of GM-CSF and IL-3 in the culture supernatants were quantitated. Each symbol represents the mean amount of cytokine detected from two to three replicate wells of an independent analysis, with bars showing means of aggregated results. *P*-values were calculated using a two-tailed Mann–Whitney test for each condition in comparison to iNKT cells alone. **(D)** Analysis of human GM-CSF and IL-3 levels in bone marrow or blood plasma of NSG mice transplanted with cord blood mononuclear cells alone or cord blood mononuclear cells + iNKTs. Each symbol represents the mean amount of cytokine detected from an individual mouse; *P*-values calculated using a two-tailed unpaired *t* test. **(E)** Purified $CD34^+$ HSPCs were seeded at 2.5×10^4 cells/well and cultured in the lower wells of transwell plates in medium containing a hematopoietic cytokine cocktail. Where indicated, iNKT cells, cord monocytes, and/or autologous cord T cells were added to the transwell inserts. After 10 d, the number of $lineage^+$ cells in the lower transwell was quantitated. Plot shows aggregated results from five independent experiments with bars at the means. *P*-values

were calculated using a two-tailed Mann–Whitney test for each transwell culture condition in comparison to HSPCs cultured alone.

Figure 6

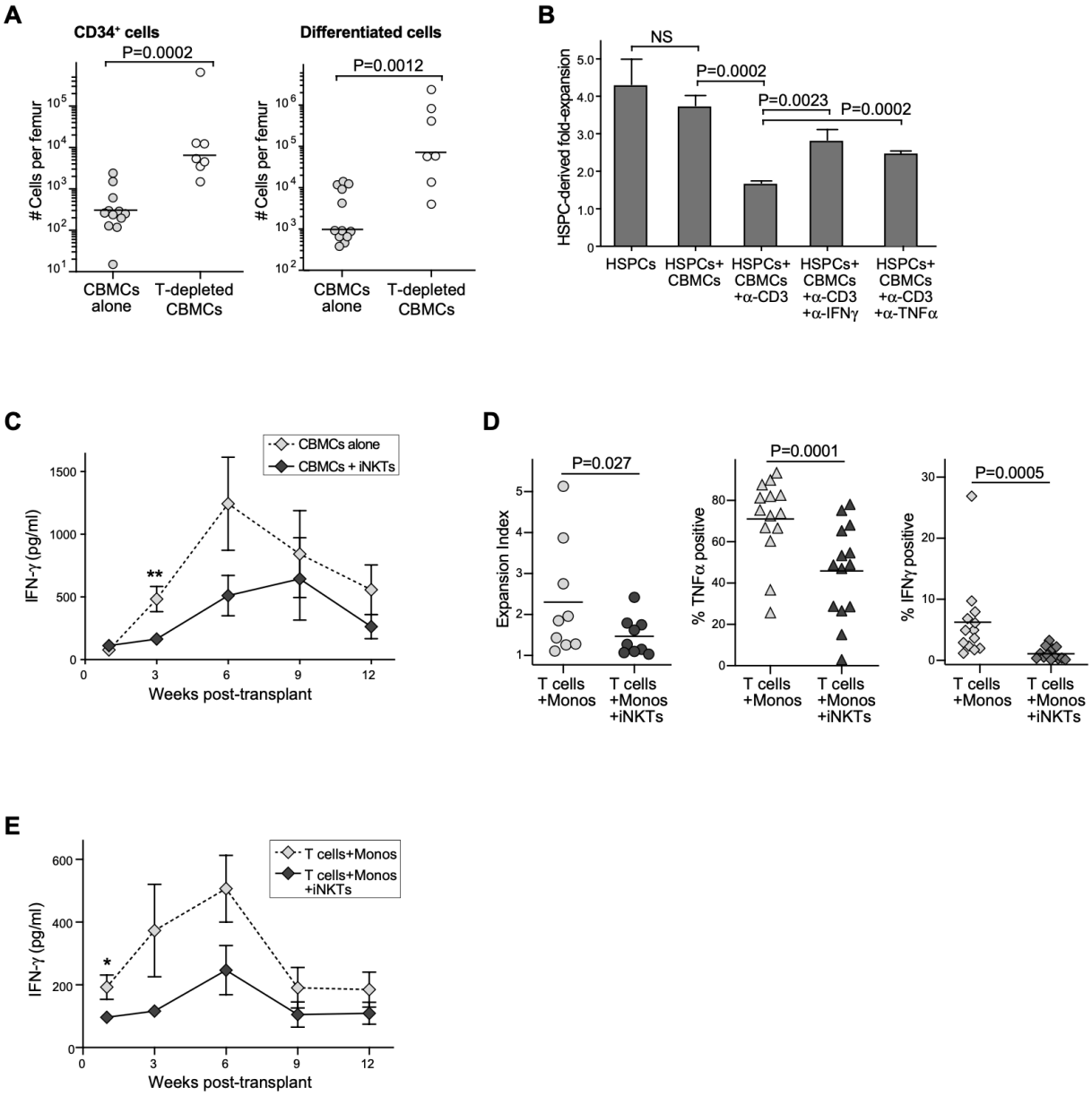

Figure 6. Invariant natural killer T (iNKT)–monocyte interactions inhibit cord T-cell responses.

(A) NSG mice were transplanted with 5×10^6 total cord blood mononuclear cells (CBMCs) or 3×10^6 T-cell–depleted CBMCs. Left plot shows number of $CD34^+$ human cells and right plot shows number of $lineage^+$ human cells (excluding T cells) in one femur at 3 mo post transplantation. Results aggregated from seven independent experiments; *P*-values calculated by two-tailed Mann–Whitney test. **(B)** Purified HLA-$A2^+$ $CD34^+$ HSPCs were cultured alone or in the presence of CD34-depleted HLA-$A2^-$ CBMCs in medium containing a hematopoietic cytokine cocktail. Where indicated, anti-CD3, and anti-CD28 antibodies were added to activate the cord T cells, and anti-IFN-γ or anti–TNF-α–blocking antibodies were added. Plot shows the fold expansion of HLA-$A2^+$ cells after 7 d (mean ± SD of three replicate cultures), with *P*-values calculated using a two-tailed unpaired *t* test. **(C)** Samples of blood plasma were collected at the indicated times from mice transplanted with CBMCs alone or with iNKT cells and analyzed for human IFN-γ by ELISA. Symbols represent mean ± SEM from 8–14 individual mice; data aggregated from four independent experiments. **Indicates $P = 0.0033$ as determined by two-tailed Mann–Whitney test. **(D)** Cord blood T cells were labeled with CTV dye and co-cultured with autologous monocytes alone, or with monocytes and iNKT cells, in medium containing IL-7 and IL-2 to drive T-cell expansion. Left plot shows expansion index of the cord T cells after 3–7 d, as determined by flow cytometric analysis of CTV staining. Middle and right plots show percentage of cord T cells staining positively for TNF-α (middle) or IFN-γ (right) after PMA and ionomycin stimulation. *P*-values calculated by two-tailed nonparametric paired *t* test. **(E)** NSG mice were transplanted with isolated cord T cells and autologous monocytes in the presence or absence of allogeneic iNKT cells. Samples of blood plasma were collected at the indicated

times post transplantation and analyzed for human IFN-γ by ELISA; symbols represent mean ± SEM from 5 mice tested in parallel.

Figure 7

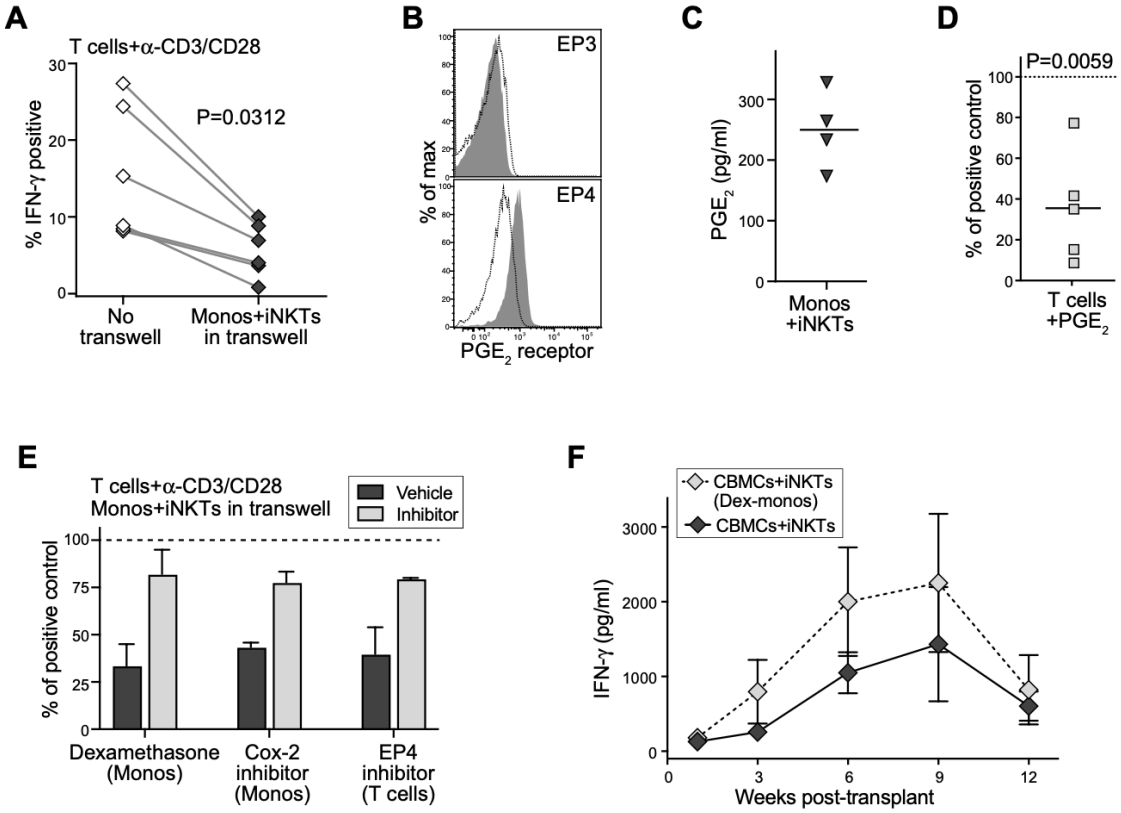

Figure 7. Eicosanoids produced during invariant natural killer T (iNKT)–monocyte interactions suppress cord T cells.

(A) Isolated $CD4^+$ cord blood T cells were cultured for 3–5 d with anti-CD3 and anti-CD28 antibodies in the presence or absence of transwell inserts containing iNKT cells and cord blood monocytes. Plot shows percentage of T cells staining positively for intracellular IFN-γ after PMA/ionomycin stimulation; paired symbols show results from independent experiments. *P*-value calculated by two-tailed nonparametric paired *t* test. **(B)** Flow cytometric staining of cord T cells for PGE_2 receptors EP3 and EP4. Filled histograms show staining by specific antibodies; dotted line shows isotype control antibody. **(C)** iNKT cells and cord blood monocytes were co-cultured for 24 h and PGE_2 in the supernatant was quantitated using an enzyme assay. Symbols represent means from independent experiments. **(D)** Cord blood T cells were cultured for 3–4 d with anti-CD3 and anti-CD28 antibodies in medium containing 500 pg/ml PGE_2, then stimulated with PMA/ionomycin. Plot shows the IFN-γ^+ T cells as a percent of the response by parallel cultures of cord T cells that were not exposed to PGE_2. Symbols show results from independent experiments. *P*-value calculated by two-tailed one sample *t* test. **(E)** Cord blood T cells were cultured for 3–5 d with anti-CD3 and anti-CD28 antibodies in the presence of transwell inserts containing iNKT cells and cord blood monocytes, then stimulated with PMA/ionomycin. Before co-culture, the monocytes were pretreated with dexamethasone (500 ng/ml) or Cox-2 inhibitor (NS-398, 10 μM), or the cord T cells were pretreated with an inhibitor of EP4 (L-161,982, 10 μM). Plot shows IFN-γ production from the transwell co-cultures as a percent of the response by positive control T cells that were cultured with anti-CD3/CD28 alone (dashed line). Bars represent mean ± SEM of two to three independent experiments. **(F)** NSG mice were transplanted with cord blood mononuclear cells and iNKT cells and blood samples were removed at the indicated times and tested for human IFN-γ by ELISA. Where indicated, the monocytes were isolated and

treated with 500 pg/ml dexamethasone, then washed and added back to the cord blood mononuclear cells before injection. Symbols represent mean ± SEM from five mice tested in parallel.

Figure S1

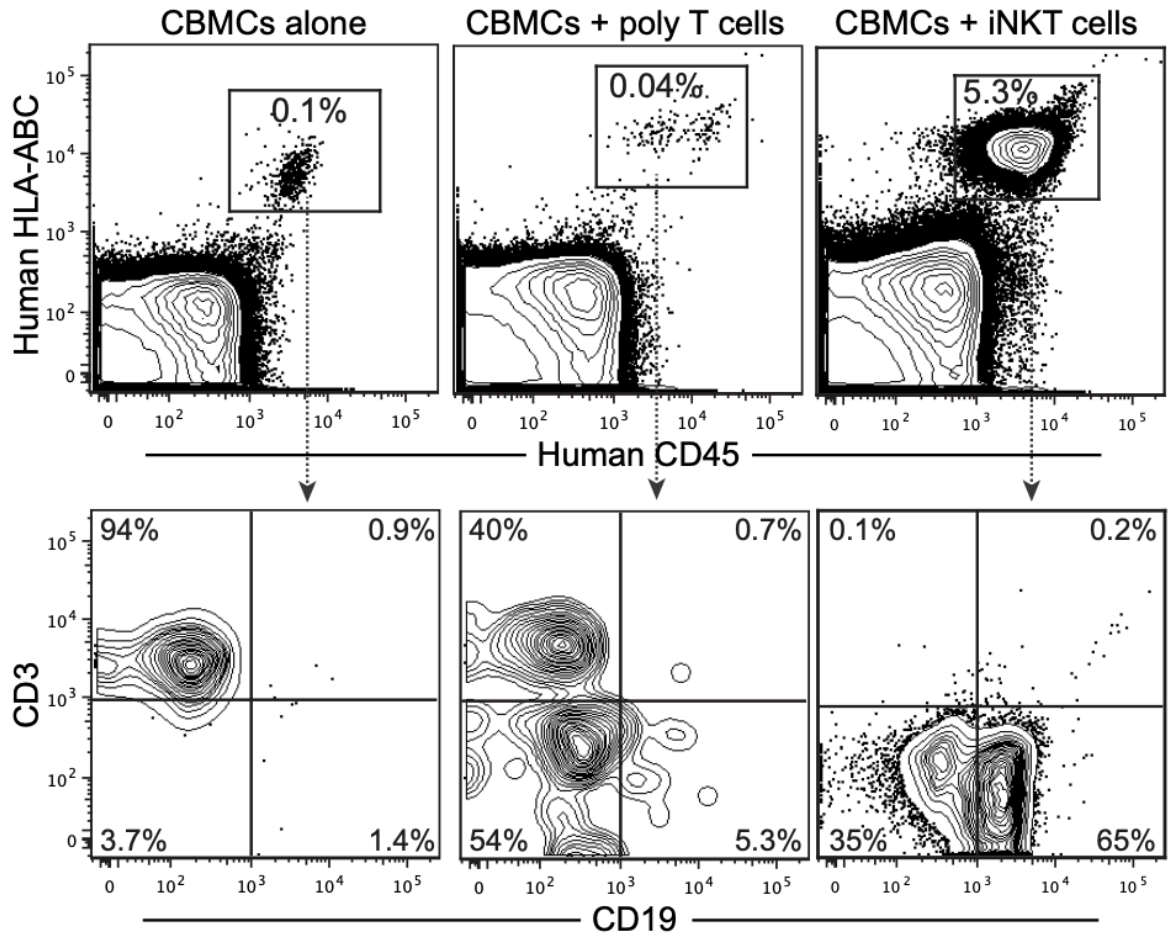

Figure S1. Co-transplanting allogeneic polyclonal $CD4^+$ T cells does not promote human chimerism.

NSG mice were transplanted with 5×10^6 cord blood mononuclear cells (CBMCs) alone, or CBMCs with 5×10^6 allogeneic polyclonal $CD4^+$ T cells or 5×10^6 allogeneic $CD4^+$ invariant natural killer T cells. Bone marrow was analyzed by flow cytometry at 10 wk post transplantation. By 12 wk post transplantation, the number of human cells in bone marrow or mice given CBMCs with polyclonal T cells was too low for reliable analysis.

Figure S2

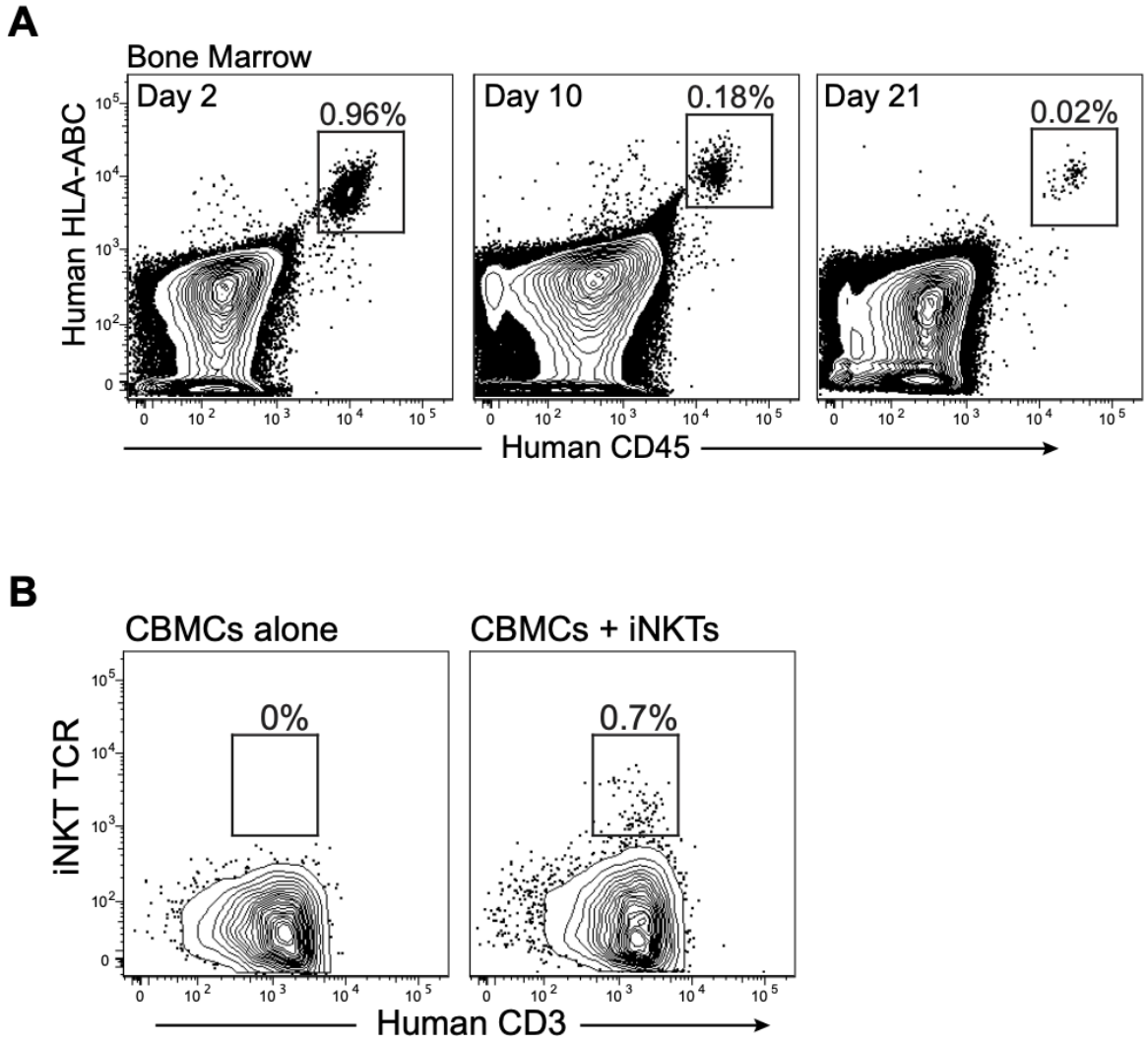

Figure S2. Detection of invariant natural killer T (iNKT) cells after transplantation into NSG mice.

(A) NSG mice were injected with purified human iNKT cells (5×10^6 cells per mouse), and bone marrow was analyzed by flow cytometry at the indicated time points. Similar results were observed using five different iNKT cell lines. **(B)** NSG mice were injected with 5×10^6 cord blood mononuclear cells alone or with 5×10^6 iNKT cells and bone marrow was

analyzed by flow cytometry at 5 wk posttransplantation. Plots are gated on human cells, and show staining for human CD3 and iNKT TCR (6B11 mAb).

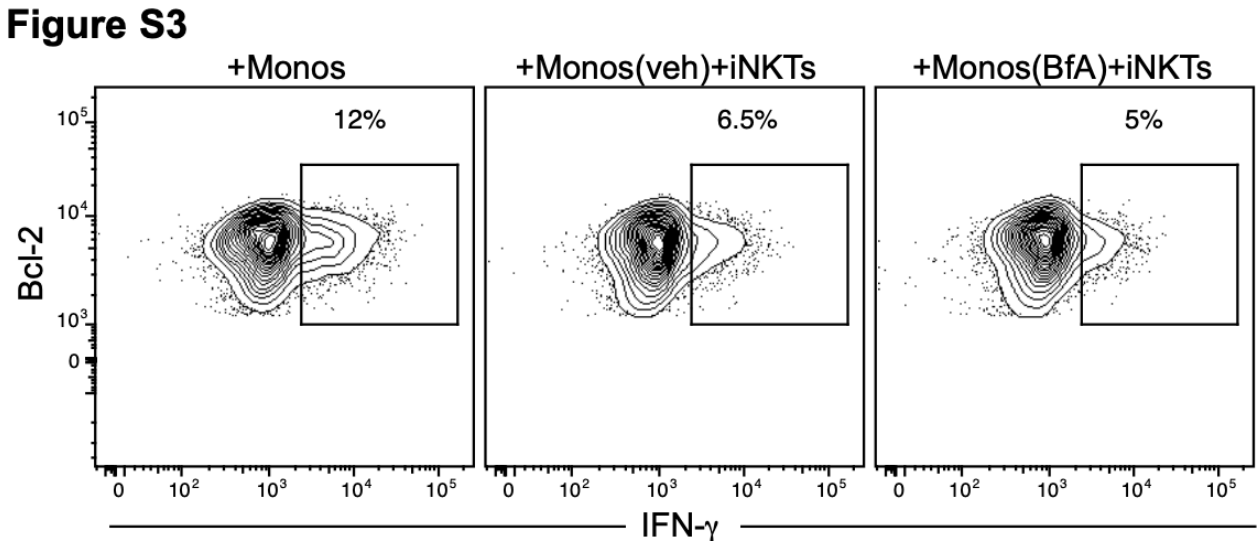

Figure S3. Brefeldin A treatment does not prevent suppression of cord T-cell cytokine production resulting from exposure to invariant natural killer T cells and monocytes.

Isolated $CD4^+$ cord blood T cells were cultured for 5 d with autologous monocytes alone, or with autologous monocytes and invariant natural killer T cells. Where indicated, the monocytes were pretreated with brefeldin A (BfA) or vehicle (veh) before being added to the co-cultures.

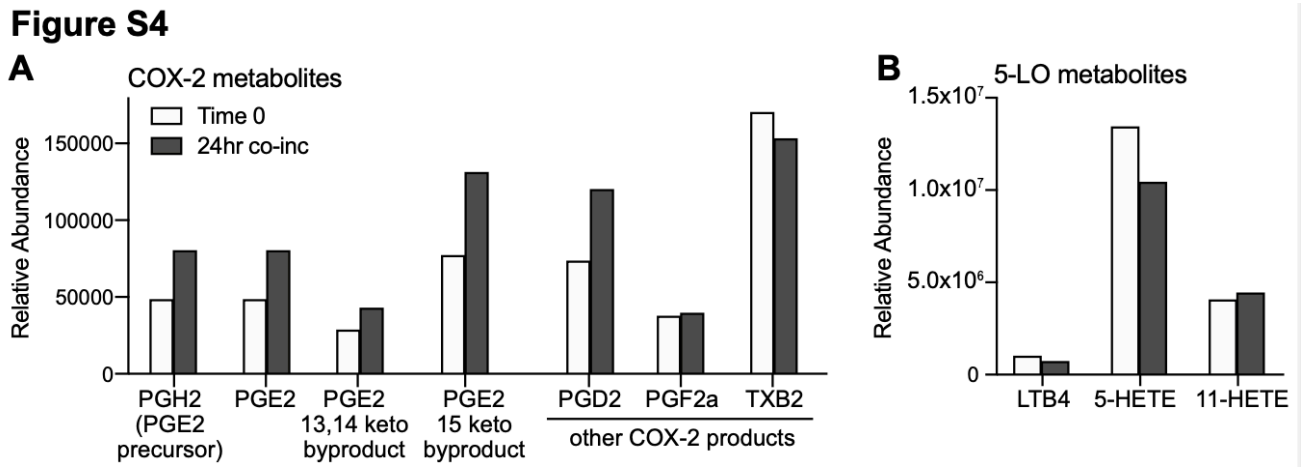

Figure S4. Mass spectrometric analysis of eicosanoids in invariant natural killer T–monocyte culture supernatants.

Cell-free supernatants were collected from invariant natural killer T–monocyte co-cultures immediately after mixing the cells ("Time 0") and after 24 h together in culture ("24 h co-inc"). Samples were spiked with a known concentration of deuterated internal control (d4-PGE_2), and eicosanoid-containing fractions were prepared by organic extraction then subjected to mass spectrometric analysis. **(A)** Relative abundance of PGE_2 and related metabolic products produced by the COX-2 pathway in the starting sample (light bars) compared with the 24 h co-culture (dark bars). **(B)** Results from the same samples for products of the 5-lipoxygenase pathway.

Figure S5

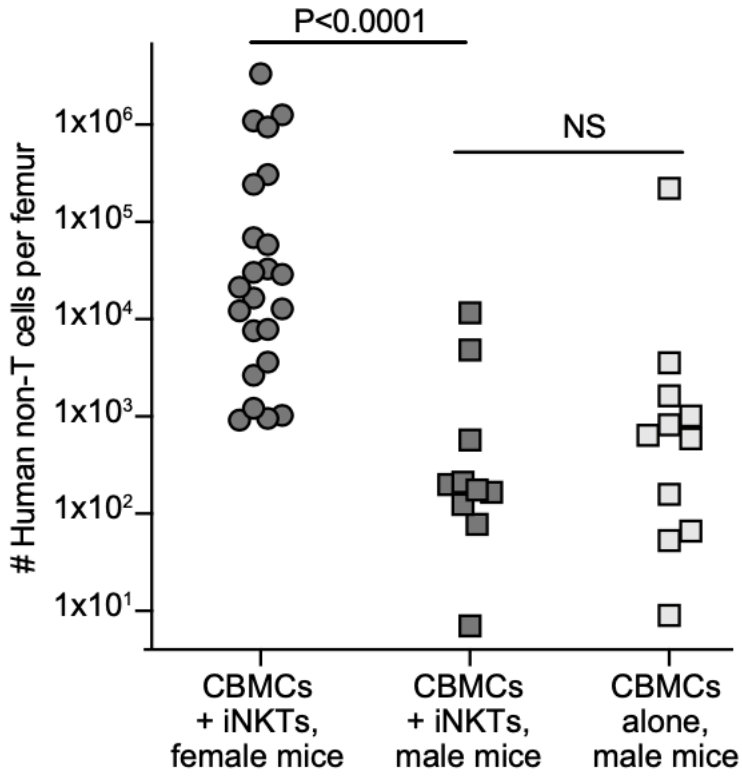

Figure S5. Sex of NSG mice impacts transplantation outcome.

Nonconditioned male or female NSG mice were transplanted with human cord blood mononuclear cells alone or in combination with allogeneic invariant natural killer T cells. Plot shows total number of human cells (excluding T cells) in one femur at 3 mo posttransplantation according to the treatment group and sex of recipient mic

Materials and Methods

Cord blood. De-identified human umbilical cord blood samples were acquired from University of Colorado's ClinImmune Labs cord blood bank, or from the Medical College of Wisconsin's tissue bank, or from the OB/Gyn department at Meriter Hospital in Madison, WI. Blood samples were diluted with a 1:1 volume of leukocyte isolation buffer (PBS containing 2% bovine calf serum and 1mM EDTA), and mononuclear cells were isolated by density gradient centrifugation using Ficoll-paque PLUS (GE Healthcare). If red blood cell contamination was apparent, the isolated cells were resuspended in leukocyte isolation buffer and the density gradient purification was repeated. For some experiments CBMCs were specifically depleted of T cells, or cells populations of interest (e.g. cord T cells or monocytes) were isolated using RosetteSep reagents from StemCell Technologies, or by magnetic sorting using reagents from Miltenyi Corp.

iNKT cells. Human blood samples were collected and used in accordance with UW-Madison IRB protocol 2018-0304. Human $CD4^+$ iNKT cells were sorted from peripheral blood of healthy adult volunteer donors using human CD1d tetramers loaded with synthetic lipid antigen, and expanded in vitro using irradiated PBMC feeder cells, phytohemagglutinen, and recombinant human IL-2. iNKT cells used in these analyses included $CD4^+$ clonal lines that we have previously established (Brigl et al., 2006; Chen et al., 2007; Fox et al., 2009), and short-term polyclonal cultures of $CD4^+$ iNKT cells sorted using a-GalCer loaded CD1d tetramer provided by the NIH tetramer facility at Emory University (Sharma et al., 2018). Clonal and polyclonal iNKT cell cultures were maintained in culture medium ("T cell medium") comprised of RPMI 1640 medium diluted with 10% heat-inactivated fetal bovine serum (GeminiBio), 5% heat-inactivated defined/supplemented bovine calf serum (Hyclone), 3% pooled human AB serum (Atlanta Biologicals), 1% L-glutamine (2 mM final

concentration), 1% Penicillin/Streptomycin (100 IU/ml and 100 μg/ml final concentration, respectively), 200 U/ml recombinant human IL-2 (Peprotech). All iNKT cultures used for experiments were of 98-100% purity as assessed by flow cytometric analysis with a-GalCer loaded CD1d tetramers.

Transplantation of human cells into mice. Animal studies were performed in accordance with UW-Madison IACUC protocol M005199. Mice were maintained using autoclaved cages, bedding, and food. Because preliminary studies revealed that male NSG mice did not support successful engraftment (see Fig. S5), only female NSG mice were included in this study. Human cells were resuspended in 150-200 mL sterile PBS per mouse and injected intravenously (retro-orbital route) under isoflurane anesthesia. NSG mice received $5x10^6$ CBMCs alone, or in combination with $0.5\text{-}1x10^6$ allogeneic iNKT cells. Alternatively, where indicated NSG mice were transplanted with $0.5\text{-}1x10^5$ purified $CD34^+$ cells alone or in combination with one or more of the following: $0.5\text{-}1x10^5$ purified autologous monocytes, $2x10^6$ purified autologous T cells, $0.5x10^6$ allogeneic iNKT cells. Mice were randomly assigned to treatment groups, ear-tagged, and co-housed in cages with mice from other treatment groups. Mice were weighed and monitored for signs of GVHD (ruffled fur, hunching, squinting, lethargy) weekly, and those showing signs of GVHD were excluded from the analysis. Mice were euthanized by CO_2 for analysis of tissues at prospectively determined time points (day 100 post-transplant, unless otherwise indicated).

Flow cytometric analysis. Bone marrow was collected from one femur of each mouse by removing one end of the bone and centrifuging at 8000xg for 60 seconds. Spleen cells were prepared by gently homogenizing the tissue using a blunt plastic syringe. Cell samples were resuspended in flow cytometry buffer (PBS containing 10% pooled human AB serum) and filtered through a 40 μM nylon mesh. prior to staining with fluorescently conjugated

antibodies. Monoclonal antibodies used for staining were purchased from Biolegend and included the following antibody clones: CD3 (OKT3), CD14 (M5E2), CD19 (HIB19), CD34 (8G12), CD38 (HIT2), human CD45 (HI30), murine CD45.1 (A20), CD123 (6H6), human IFN-g (4S.B3), human TNF-a (MAb11) and pan-HLA Class I (W6/32). Cell number was quantified using Precision Count Beads (Biolegend).

Immunohistochemical analysis. Formalin-fixed, paraffin-embedded tissue sections were deparaffinized and hydrated, and endogenous peroxidase activity was blocked with 0.3% hydrogen peroxidase solution, and nonspecific labeling was blocked in a 5% goat serum blocking solution. Two-color staining was performed using VectorLabs ImmPRESS Duet Double Staining System with a rabbit anti-human CD20 polyclonal antibody (Thermo-Fisher) and a mouse monoclonal antibody against Bcl-6 (clone PGB6P, Santa Cruz Biotechnology). Serial sections of the same tissue were stained for human IgM or IgG using specific rabbit polyclonal antibodies (Cell Marque) with the Super Sensitive Polymer-Horseradish Peroxidase Immunohistochemistry detection system (BioGenex) using diaminobenzidine color development. Sections were lightly counter-stained with hematoxylin to visualize cell nuclei.

Live cell imaging of interactions between iNKT cells and CBMC populations. T cells, B cells and monocytes were isolated from a CBMC sample and stained with Incucyte Cytolight Rapid Green reagent (Sartorius). $CD4^+$ iNKTs were stained with Incucyte Cytolight Rapid Red reagent (Sartorius). iNKT cells ($1x10^5$ cells per well) placed into replicate wells of a 48 well plate with cord T cells, B cells, or monocytes ($2x10^4$ cells per well) in 1 mL of media (RPMI, 10% BCS, 3% human serum, NEAA, Pen/Strep). Cellular interactions were analyzed over a 24 hour period in an Incucyte S3 Live-Cell Analysis system, with nine images per well taken every 15 minutes with a 20X objective lens. Images were analyzed

using Incucyte analysis software for both the number and total area of overlap between iNKT cells and the indicated cell population.

In vitro analysis of hematopoietic expansion. $CD34^+$ cells (HSPCs) were purified from CBMCs by magnetic sorting using positive selection. To assess the impact of secreted factors on HSPC differentiation, 2.5x104 HSPCs were seeded into the lower well of 24-well plates, and iNKT cells, cord monocytes, and/or cord T cells ($1.5x10^4$ cells each) were added to transwell inserts. Where indicated, a 1:1 ratio of CD3/CD28 Dynabeads (ThermoFisher Scientific) was added to activate the iNKT cells. The cells were cultured at 37 ºC and 5% CO_2 in X-VIVO15 serum-free medium (Lonza) containing 20 ng/ml each of Flt3-L, TPO, SCF, and IL-7 (Peprotech). After 10 days, cells from the lower well were stained with fluorescently labeled antibodies against CD45RA (Clone: HI100), CD33 (Clone: WM53), CD38 (Clone: HB-7), and CD34 (Clone: 581) and analyzed by flow cytometry using Precision Count Beads (Biolegend) to determine the number of cells bearing markers of differentiation. To assess the impact of exposure to T cell cytokines, $CD34^+$ HSPCs were isolated from an HLA-$A2^+$ CBMC sample. The HSPCs ($1x10^4$ cells) alone or in combination with $1x10^5$ CD34-depleted CBMCs (HLA-A2 negative sample) were placed into replicated wells of a 96-well plate. Where indicated, stimulating antibodies (anti-CD3 and anti-CD28) or blocking antibody (anti-IFN-g or anti-TNF-a) were added to a final concentration of 5 mg/ml. After 7 days of culture, the cells were resuspended and HLA-$A2^+$ cells were quantitated by flow cytometry.

Determination of iNKT cell production of GM-CSF and IL-3. iNKT cell cytokine production in response to CD1d molecules presenting titrated doses of a lipid antigen was assessed as previously described (Brigl et al., 2006; Wang et al., 2008). Briefly, high protein binding 96 well plates were coated with 10 mg/ml recombinant CD1d-Fc fusion protein. a-

GalCer lipid antigen suspended in DMSO was sonicated in a heated water bath for 45 minutes, then diluted in PBS and added to the wells at the indicated concentrations and incubated for 24h at 37 ^{o}C. The plates were washed first with PBS, then with T cell medium lacking IL-2. Polyclonal iNKT cells suspended in T cell medium lacking IL-2 were added at 5 x10^4 cells per well and incubated at 37 ^{o}C and 5% CO_2. Culture supernatants were harvested after 24h and concentrations of IL-3 and GM-CSF were determined by ELISA. Where indicated, monocytes and T cells were isolated from the same cord blood sample by magnetic sorting and co-cultured at a 1:1 ratio with allogeneic iNKT cells for 48h, and concentrations of IL-3 and GM-CSF in culture supernatants were determined by ELISA.

Quantitation of human IFN-g in murine plasma. Blood was collected by retro-orbital bleeding from isoflurane anesthetized mice at the indicated time points post-transplantation. Blood samples were diluted with a 1:1 ratio of PBS, then centrifuged at 400xg for 4 min to pellet the red blood cells, and the supernatant was collected. Supernatants were diluted 1:5 in ELISA assay buffer (PBS with 1 mg/ml BSA), and human IFN-g was detected from 3 replicate wells using an antibody pair (MD-1 and 4S.B3) purchased from BioLegend. IFN-g concentration was determined by interpolation from a standard curve of recombinant human IFN-g (Peprotech) that was tested in parallel.

In vitro analysis of NKT-monocyte suppression of cord T cells. Monocytes were positively selected from freshly isolated CBMCs using CD14 magnetic beads, then untouched $CD4^+$ T cells were isolated by magnetically depleting other subsets (Miltenyi Biotec). Cord T cells were labeled with 5 mM Cell Trace Violet (CTV) dye (ThermoFisher Scientific). Cord T cells (5x10^4/well) were cultured with autologous monocytes (2.5×10^4well) in the presence or absence of allogeneic iNKT cells (0.5×10^4/well) in culture medium (RPMI, 15% BCS, 3% human serum, Pen/Strep) containing 50 U/ml recombinant

human IL- 2 and 1 ng/ml recombinant human IL-7 (Peprotech) in a humidified incubator at 37 ºC with 5% CO_2. After 3-7 days of co-culture, the cells were stained with antibodies against CD3, CD14, and iNKT TCR, and after gating out iNKT cells and monocytes proliferation of the cord T cells of was assessed by flow cytometry to determine dilution CTV fluorescence intensity. Alternatively, the cells were stimulated with PMA/ionomycin in the presence of brefeldin A (Biolegend) for 4-6h, then fixed and permeabilized and stained intracellularly for IFN-g and TNF-a. To assess the impact of secreted factors produced by iNKT cells and monocytes, cord T cells were placed into the lower wells of transwell plates with anti-CD3 and anti-CD28 antibodies, in the presence or absence of transwell inserts containing monocytes and iNKT cells (5×10^4 cells of each). Where indicated, the specified cell populations (monocytes or T cells) were treated with inhibitor drugs or vehicle for 90 min at 37°C then washed twice before being added to the wells.

Analysis of secreted PGE_2. Monocytes were positively selected from freshly isolated CBMCs using CD14 magnetic beads. Cultured iNKT cells were placed in medium lacking IL-2 for 24 hours prior to the experiment to ensure they were in a resting state. Monocytes ($1x10^6$ cells) and iNKT cells ($1x10^6$ cells) were combined in 1 mL of culture medium (RPMI containing 15% BCS, 3% pooled human AB serum, 1% L-glutamine, 1% Penicillin/Streptomycin). After 24 hours of co-incubation at 37 ºC with 5% CO_2, culture supernatants were harvested and PGE_2 levels were quantitated in duplicate using the DetectX PGE_2 Multi-Format ELISA kit (Arbor Assays) following the manufacturer's protocol. For mass spectrometric determination of eicosanoids, cell-free culture supernatants were collected immediately after combining monocytes and iNKT cells ("Time 0") and after 24 hours of co-culture. The internal standard deuterated-PGE_2 (PGE_2-d4, Cayman Chemical) was added to each sample and incubated for 30 minutes on ice prior to extraction with two

volumes of ice-cold methanol. Samples were concentrated to 1 mL by N_2 gas evaporation and then rapidly acidified with 9 mL of pH 3.5 H_20 before loading onto C18 columns (Isolute, Biotage) that were previously conditioned with 6 mL MeOH followed by 6 mL neutral H_2O. Sample tubes were washed with 4 mL neutral water and loaded onto the same C18 column. The columns were then washed with 3 mL hexane and eluted using 6 mL methyl formate followed by 2 mL MeOH and concentrated to approximately 50 mL by N_2 gas evaporation. Samples were diluted to a final volume of 200 mL using 55:45 MeOH:H_20, and loaded onto an HPLC coupled to a mass spectrometer (Q Exactive; Thermo Sceintific) using a C18 Acquity BEH column (100mmx2.1mmx1.7µm) operated in negative ionization mode. Samples were eluted using a gradient of MeOH:H_2O:CH3COOH solvent that transitioned from 55:45:0.1 to 98:2:0.1 over a course of 28 minutes. Scans were collected from 3.5 to 20 minutes for mass-to-charge ratios (m/z) of 100 to 800 and analyzed using MAVEN open source software (omicX) in comparison to standards (Cayman Chemical) normalized to relative amounts of PGE_2-d4.

Chapter IV: Harnessing Invariant Natural Killer T Cells to Control Pathological Inflammation

Nikhila S. Bharadwaj, Jenny E. Gumperz.

This chapter was co-written with Dr. Jenny Gumperz and at the time of writing this thesis was accepted for publication as a mini-review in the journal Frontiers in Immunology.

ABSTRACT

Invariant natural killer T (iNKT) cells are a subset of innate T cells that are recognized for their potent immune modulatory functions. Over the last three decades, research in murine models and human observational studies have revealed that iNKT cells can act to limit inflammatory pathology in a variety of settings. Yet, since iNKT cells are multi-functional and can promote inflammation in some contexts, understanding the mechanistic basis for their anti-inflammatory effects is critical for effectively harnessing them for clinical use. Two contrasting mechanisms have emerged to explain the anti-inflammatory activity of iNKT cells: that they drive suppressive pathways mediated by other regulatory cells, and that they may cytolytically eliminate antigen presenting cells that promote excessive inflammatory responses. How these activities are controlled and separated from their pro-inflammatory functions remains a central question. Murine iNKT cells can be divided into four functional lineages that have either pro-inflammatory (NKT1, NKT17) or anti-inflammatory (NKT2, NKT10) cytokine profiles. However, in humans these subsets are not clearly evident, and instead most iNKT cells that are $CD4^+$ appear oriented towards polyfunctional (T_{H0}) cytokine production, while $CD4^-$ iNKT cells appear more predisposed towards cytolytic activity. Additionally, structurally distinct antigens have been shown to induce T_{H1}- or T_{H2}-biased responses by iNKT cells in murine models, but human iNKT cells may respond to differing levels of TCR stimulation in a way that does not neatly separate T_{H1}

and T_{H2} cytokine production. We discuss the implications of these differences for translational efforts focused on the anti-inflammatory activity of iNKT cells.

INTRODUCTION

iNKT cells are innate T lymphocytes that are present in all individuals and use a unique "semi-invariant" TCR, comprised of a canonically rearranged TCRa chain (TRAV10-TRAJ18) paired with TCRb chains utilizing TRBV25-1 in diverse rearrangements (53-55). The TCRs of iNKT cells are specific for CD1d, a non-classical antigen presenting molecule that has minimal polymorphism at the amino acid level in human populations (56). CD1d molecules are constitutively expressed by professional APCs, including B cells, monocytes, macrophages, and DCs (57), and also by non-hematopoietic cells (particularly epithelial cells) in a variety of tissues (58). CD1d molecules are specialized for presenting lipidic antigens, which are structurally conserved molecules that are not highly mutable (59). Antigens recognized by iNKT cells derive from both self and microbial sources (60). Self-lipids recognized by iNKT cells are constitutively presented by $CD1d^+$ APCs, and may also be up-regulated during inflammation or cellular stress (61). Hence, because of their status as 'donor-unrestricted' T cells that recognize conserved antigens and do not mediate alloreactivity, iNKT cells are ideal candidates for allogeneic cellular immunotherapies. Due to their self-lipid recognition iNKT cells can be used for adoptive cellular immunotherapies without added antigens. Alternatively, they can be specifically activated by synthetic mimetics of their lipid antigens.

Extensive studies have demonstrated remarkable potency of iNKT cells in limiting T_{H1}-driven pathology in multiple settings, including autoimmune diseases, inflammation associated with obesity, and graft versus host disease (GVHD) (reviewed in (62-64)). However, a central conundrum about iNKT cells is that they can also potently promote T_{H1}

responses. Their T_{H1}-promoting functions have been associated with enhanced host defense against infections and cancer (reviewed in (65, 66)), but also appear to play pathological roles in certain contexts, including atherosclerosis, sickle cell disease, and endotoxic shock (reviewed in (67-69)). Thus, in order to successfully exploit the potential of iNKT cells to treat inflammatory disease, it may be important to selectively engage their anti-inflammatory pathways.

How are the anti-inflammatory effects of iNKT cells mediated?

Two distinct mechanistic processes have been identified that may explain how iNKT cells limit T_{H1}-driven inflammation. The first is a regulatory axis characterized by iNKT cell production of T_{H2} (IL-4, IL-13) or regulatory (IL-10, TGFb) cytokines, and activation of anti-inflammatory cells including M2-polarized macrophages, myeloid-derived suppressor cells (MDSCs), and T_{regs} (Fig. 1A). The second is a cytolytic pathway involving iNKT-mediated killing of inflammatory antigen presenting cells (APCs) that activate T_{H1} effectors (Fig. 1B).

iNKT regulatory axis. Studies investigating insulitis in non-obese diabetic (NOD) mice were amongst the first to elucidate the regulatory activity of iNKT cells, with early work revealing a critical link to IL-4 and IL-10 production (70-73), and further analysis showing that they promote the differentiation of tolerogenic APCs that limit the activation of autoreactive T cells (74-77). A similar axis has been observed in murine models of diet-induced obesity, where adipose-resident iNKT cells play a powerful role in glucose tolerance by promoting macrophage polarization into a non-inflammatory M2 phenotype through secretion of IL-4 and IL-10 (78, 79), and by transactivating regulatory T cells via secretion of IL-2 (80). iNKT cells also contribute to the resolution phase of sterile inflammation in the liver by promoting monocyte transition into an anti-inflammatory phenotype through secretion of IL-4 (81, 82). In murine models of allogeneic hematopoietic transplantation, iNKT cells protect against

GVHD through IL-4 dependent mechanisms (83-85), and by promoting the regulatory functions of myeloid-derived suppressor cells (MDSCs) while driving the expansion of Treg cells via secretion of IL-2 (86-88).

Analyses of human iNKT cells have suggested that they may participate in similar regulatory processes. IL-10 producing iNKT cells recently identified in the intestinal lamina propria of Crohn's Disease patients showed suppressive activity towards pathogenic CD4+ T cells, and the frequency of IL-10 producing iNKT cells in colon tissue of these patients correlated inversely with TH1 and TH17 cell frequency, and was associated with reduced disease severity, higher TGFB gene expression, and lower levels of inflammatory proteins (89). Moreover, co-culture of human Tregs with iNKT cells led to increased Treg FOXP3 expression, enhanced IL-10 secretion, and more profound inhibition of conventional T cell proliferation (90).

Human iNKT cells can also mediate potent suppression of T cell IFN-g production by modulating the functions of monocytic cells. Our research group previously showed that GM-CSF and IL-13 secretion by human iNKT cells induced monocytes to differentiate into tolerogenic APCs that produced high levels of IL-10, expressed the checkpoint inhibitors PDL-1 and PDL-2, and potently suppressed T cell proliferation and IFN-g secretion (91, 92). The regulatory phenotype of the APCs was due to iNKT cell release of extracellular ATP, which signaled through the P2X7 receptor on the monocytes to induce upregulation of PD-L1 and PD-L2 (93). This iNKT-monocyte interaction resembles a pathway observed in a murine model in which IL-13 secreted by CD1d-restricted T cells promoted monocyte expression of TGFb, which led to suppression of T cell effector responses (94, 95), although the role of TGFb in the human iNKT-monocyte pathway remains unclear.

We also used a xenotransplantation model of hematopoietic engraftment to investigate the impact of the human iNKT-monocyte pathway in vivo. The addition of allogeneic adult iNKT cells to human cord blood mononuclear cell grafts resulted in dramatically improved engraftment, which was due to iNKT cells inducing cord blood monocytes to secrete prostaglandin E_2, which potently suppressed T cell IFN-g production (38). Since hematopoietic engraftment is suppressed by excessive IFN-g (96), this analysis shows that human iNKT cells can engage powerful regulatory pathways that limit adverse effects of human T_{H1} activation in vivo.

iNKT cytolytic activity. A number of studies have suggested that iNKT cells may also control inflammation by eliminating pro-inflammatory APCs through a mechanism involving CD1d-dependent activation of the iNKT cells and lysis of APCs by cytotoxic granule deposition (97-101). Human iNKT cells were found to kill human monocyte-derived DCs generated in vitro and also freshly isolated blood DCs, but did not kill freshly isolated monocytes or plasmacytoid DCs, suggesting they specifically target certain types of APCs (97, 100). In another analysis, human iNKT cells preferentially eliminated monocyte-derived DCs that produced high levels of IL-12 while DCs that produced mainly IL-10 were spared, resulting in a DC population that limited TH1 activation (99). Together these studies suggest that this cytolytic pathway selectively targets pro-inflammatory APCs, and might thereby limit pathological inflammation. Consistent with this, in mice infected with a highly pathogenic strain of influenza A virus, iNKT cells were associated with reduced accumulation of inflammatory monocytes in the lungs (101). iNKT cell activity in this model was associated with reduced levels of MCP-1 (a chemokine that recruits monocytes and CD4+ T cells), reduced damage to lung tissue, and improved survival even though viral loads were not affected (101). The effect of iNKT cells was thought to be due to their cytolytic

activity against influenza-infected monocytes, suggesting that iNKT cells may limit pathological inflammation during viral infections by eliminating inflammatory APCs. However, it is important to note that in all of these studies the iNKT cells were experimentally exposed to strong TCR stimulation prior to analysis of their cytolytic activity. Therefore, the physiological conditions that might lead to APC-targeted cytolytic activity by iNKT cells remain unclear.

How are iNKT cells activated, physiologically?

iNKT cells can be activated in two ways: either through TCR-mediated recognition of antigen presented by CD1d, or through TCR-independent pathways such as exposure to the cytokines IL-12 or IL-18, or LFA-1 ligation by high-density ICAM-1 (102-105). Notably, TCR-independent pathways selectively induce iNKT cells to produce IFN-g and not T_{H2} or regulatory cytokines (103, 105), and iNKT cells require a TCR signal for cytolysis of target cells (106-108). Thus, the anti-inflammatory activities of iNKT cells are probably highly dependent on TCR-recognition of antigens presented by CD1d molecules. Since it is clear that iNKT cells can mediate regulatory effects in the absence of infectious challenges, the antigens required for their anti-inflammatory pathways must be constitutively or chronically present. However, the sources and nature of the antigens that physiologically activate iNKT cells, and correspondingly the processes that contribute to their increased or decreased activation in different contexts, remain an ongoing area of inquiry.

Sources of antigen. Due to their shared use of a canonically rearranged TCRa chain, all iNKT cells recognize an unusual type of glycolipid in which the sugar head group is present in an a-anomeric configuration. Certain microbes produce glycolipids of this type that are potent antigens for iNKT cells (reviewed in (60)). Recent studies indicate that bacterial

species that can be found within the normal gut microbiota can produce similar antigenic lipids (109, 110), although these may be counter-regulated by related forms produced by other bacteria that are antagonists (111). These studies suggest that, particularly at mucosal sites, TCR-dependent activation of iNKT cells may fluctuate according to the composition of the microbial community.

iNKT cells can also recognize self-lipids as antigens. Mammalian cells do not directly synthesize the a-linked glycolipids recognized by iNKT cells, but the b-linked forms they produce may be converted at low frequencies to a-linked forms that are strongly antigenic (112, 113). Additionally, iNKT cells can recognize mammalian b-linked glycolipids as weak agonists (114). Some antigenic self-lipids, including lysophospholipids and glycosylated sphingolipid species, are specifically upregulated during inflammation or cellular stress (115-120). Conversely, some non-antigenic self-lipids, such as sphingomyelin, may inhibit presentation of antigenic species (117). Together, the available data suggest that antigenic self-lipids are constitutively present, but are maintained in a manner that is only weakly agonistic for iNKT cells, and that during inflammation or cellular stress the abundance or nature of the antigenic self-lipids changes in a way that provides stronger TCR signals to iNKT cells.

What determines the nature of the functional response mediated by iNKT cells?

If iNKT cells are to be successfully employed clinically to limit inflammatory pathology, a key question is how they end up generating anti- rather than pro-inflammatory responses. Since TCR-independent signals selectively promote iNKT cell IFN-g secretion, when these signals are present iNKT cells probably predominantly promote inflammatory responses (102, 105, 121, 122). In contrast, the TCR-dependent activation pathway can promote either pro-inflammatory or anti-inflammatory outcomes (reviewed in (123)), and it has been of

considerable interest to understand how TCR-mediated activation of iNKT cells leads to these contrasting effects. Two central factors have emerged: first, that the iNKT cell population contains multiple functionally distinct subsets; and second, that iNKT cell functional responses vary according to antigen characteristics.

Distinct subsets. In contrast to conventional T cells that become polarized into different effector phenotypes by priming in the periphery, iNKT cells are already cytokine competent as they exit the thymus (124). Murine iNKT cells are segregated into four functionally distinct subsets based on their expression of master-regulator transcription factors that govern cytokine production (Tbet, GATA3, RORgT, E4BP4) and on differences in expression levels of PLZF (promyelocytic leukemia zinc finger), a transcription factor that promotes cellular characteristics associated with innate lymphocytes (80, 125-128). NKT1 cells have a TH1 cytokine profile, often express a cytotoxic effector program, and are PLZFloTbethi; NKT2 cells are characterized by high levels of IL-4 secretion and are PLZFhiGATA3+; NKT17 cells produce IL-17 and express RORgT with intermediate levels of PLZF; NKT10 cells produce IL-10, are preferentially found within adipose tissues, and are negative for PLZF but express E4BP4 (Fig. 2A). NKT1, NKT2, and NKT17 lineages are generated during thymic selection, and are thought to home to distinct tissues (129). In contrast, NKT10 cells may originate from other subsets and differentiate into a regulatory phenotype as a result of exposure to factors in adipose tissues (79). The identification of these iNKT sub-lineages has led to the paradigm that the anti-inflammatory effects of iNKT cells are due to NKT2 or NKT10 cells, which become activated in different situations than NKT1 and NKT17 subsets as a result of differences in tissue localization.

In contrast, it has thus far not been straightforward to categorize human iNKT cells into NKT1, NKT2, and NKT17 lineages matching those in mice. Similar to their murine

counterparts, most human iNKT cells express PLZF (130-132), and are characterized by an innate-like transcriptional profile that results in a "poised-effector" status allowing them to rapidly mediate functional responses (133). Multi-parameter flow cytometric analyses and gene expression studies have revealed human iNKT cells to express a diverse selection of cytokines and chemokines (134-138). Human iNKT cells can be segregated into two major subsets according to CD4 expression (134, 135). Those that express CD4 often appear to co-produce GM-CSF, IL-13, TNF-a, IFN-g, IL-4, and IL-2, while those lacking CD4 appear more specialized for cytolysis (Fig. 2C). These two major populations are most likely sub-divided into further subsets characterized by additional markers (e.g. CD8a, CD161, CD62L) with distinctions in functional characteristics, but it is not clear that these subsets equate to the NKT1, NKT2, or NKT17 lineages observed in mice (139, 140). It is also not clear whether anti-inflammatory activity segregates according to CD4+ or CD4- status of human iNKT cells, although CD4+ iNKT cells are the ones that have been found to induce regulatory functions in monocytic cells, and the CD4- subset has appeared more likely to kill DCs.

Antigenic modulation. The prototypical iNKT antigen is called a-galactosylceramide (a-GalCer) (141), and synthetic forms of this lipid have proved extremely valuable as pharmacological agents that activate iNKT cells in a highly specific manner (142). Observations that structural variants of a-GalCer can produce substantially different immunological outcomes in vivo have led to interest in using these agents to selectively tune iNKT responses towards pro- or anti-inflammatory functions (142). Administration of α-GalCer to mice potently stimulates iNKT cells, and induces a mixed response where TH1, TH2, and regulatory cytokines are all produced, although with different kinetics (143). In contrast, certain analogues of α-GalCer have been shown to produce a TH2-biased cytokine

response (144, 145), while other variants produce a highly TH1-biased response (146) (Fig. 2B). The mechanisms underlying these differential responses appear complex. One component may be that certain variants induce biased cytokine production from iNKT cells themselves (147), while another important element likely relates to whether or not antigen-driven interactions between iNKT cells and APCs result in release of cytokines (e.g. IL-12) that activate a secondary IFN-g response by NK cells (146, 148). A key factor may be the relative duration of antigen presentation by CD1d molecules, with more durable antigens being associated with TH1-biased responses (149). It is not clear whether antigen variants selectively activate different iNKT cell subsets, or whether they bias the cytokine profile produced within a given subset (for example, by inducing higher IL-4 production by NKT1 cells, or increased IFN-g by NKT2 or NKT17 cells). It is also not known whether any structural variants selectively promote IL-10 production.

Whether human iNKT cell responses can be modulated similarly using a-GalCer structural variants remains an open question. It has become clear that differences TCR differences between murine and human iNKT cells result in significant discrepancies in TCR-signaling strength induced by lipid variants (150). Perhaps more importantly, polyfunctional human iNKT cells show a hierarchy of cytokine production in response to TCR stimulation that does not neatly segregate into clear T_{H1} or T_{H2} patterns. Weak TCR stimulation of human iNKT cells preferentially induces production of IL-3, GM-CSF, and IL-13, with increasing stimulation leading first to IFN-g, then IL-4, then IL-2 (38, 151, 152) (Fig. 2D). Secondary induction of NK cell IFN-g secretion was associated with activation of human iNKT cells by strong TCR agonists (152). It is therefore not clear that it will be feasible to selectively polarize human immune responses towards IL-4 production through the use of specific lipid

antigen variants, although it may be possible to drive IL-13 production through administration of weak agonists.

DISCUSSION

The potential of engaging iNKT cells therapeutically to treat T_{H1}-inflammatory pathology is well supported by pre-clinical studies in murine models, in vitro experiments using human cells, and ex vivo analyses of human subjects, but clinical data has been limited. Recently, however, a pilot clinical trial using allogeneic iNKT cells as a cellular immunotherapy to treat patients who were intubated with acute respiratory distress syndrome (ARDS) secondary to SARS-CoV-2 infection has shown highly promising results, with 77% survival of treated patients compared to a national average of 40% survival for other intubated SARS-CoV-2 patients during the same period of enrollment (153). Understanding whether such iNKT cell therapies work through one of the regulatory pathways shown in Figure 1A, or through elimination of inflammatory cells via cytolysis as depicted in Figure 1B, has important implications. For example, if APC killing is a key component it may be necessary to deliver a strong TCR signal to the iNKT cells to prime their cytolytic activity. Alternatively, if a regulatory pathway is involved it may be beneficial to generate iNKT cells that are biased towards production of T_{H2} cytokines or IL-10, depending on the pathway.

Also, critical to developing effective iNKT cell therapies is to determine whether human iNKT cells include stable regulatory subsets, or whether polyfunctional iNKT cells are converted into a regulatory phenotype through particular signals. If a stable NKT10 lineage exists in humans, an attractive option might be to specifically engage these cells for immunotherapy. Alternatively, if human iNKT cells generally retain functional plasticity, it may be important to identify methods to specifically promote their regulatory functions. To this end, a recent study found that the presence of IL-7 during in vitro expansion of human

iNKT cells resulted in a $CD4^+$ population with enhanced T_{H2} cytokine production (154), while exposure to short chain fatty acids, palmitate, or the mTOR inhibitor rapamycin may induce a regulatory phenotype (79, 89, 155).

Another important consideration is that iNKT immunotherapy that engages T_{H2} pathways would likely be contraindicated in certain inflammatory diseases, including asthma, chronic obstructive pulmonary disease, and ulcerative colitis, where T_{H2} cytokine production by iNKT cells has been associated with disease-exacerbating effects (reviewed in (156-158)). Finally, key areas of further investigation will be to better understand the antigens that physiologically or pharmacologically activate human iNKT cells, and to determine whether these are differentially presented in different tissues or by distinct APCs.

FIGURES

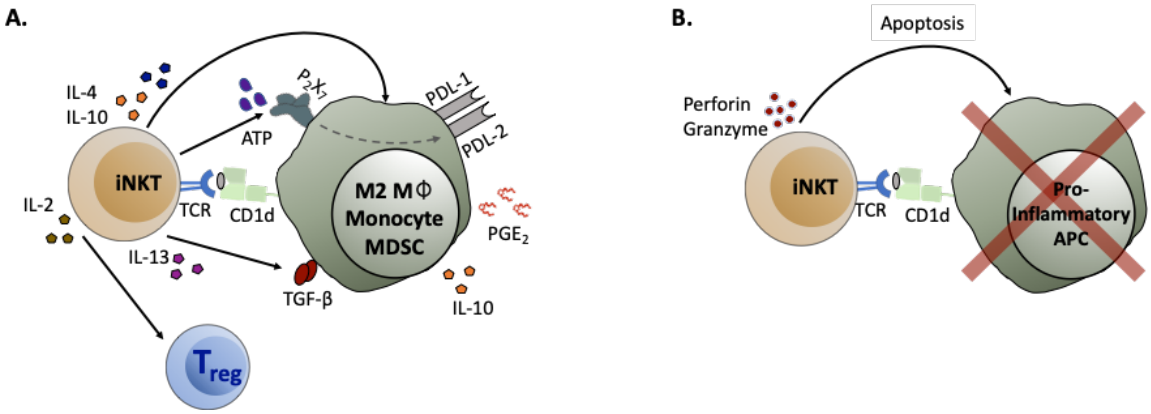

Figure 1. iNKT cell anti-inflammatory mechanisms. (**A**) iNKT cells interact with myeloid cell types to initiate the activation of regulatory pathways. Recognition of antigens presented by CD1d molecules expressed by myeloid cells induces iNKT cells to produce cytokines like IL-4, IL-10, or IL-13, that in turn act on the APCs. IL-4 and IL-10 promote macrophage differentiation into an M2 phenotype. IL-13 promotes monocyte differentiation into APCs that express suppressive cytokines such as IL-10 and TGF-b. Secretion of ATP by iNKT cells leads to upregulation of the checkpoint inhibitors PD-L1 and PD-L2, and iNKT interaction with monocytes induces secretion of PGE_2 by mechanisms that have not yet been determined. Additionally, IL-2 produced by iNKT cells helps to drive the expansion of T_{regs}. (**B**) iNKT cells can lyse pro-inflammatory APCs, leading to reduced T cell activation. In this case, recognition of antigens presented by CD1d molecules activates iNKT cells to release cytolytic granules that induce apoptosis of pro-inflammatory APCs.

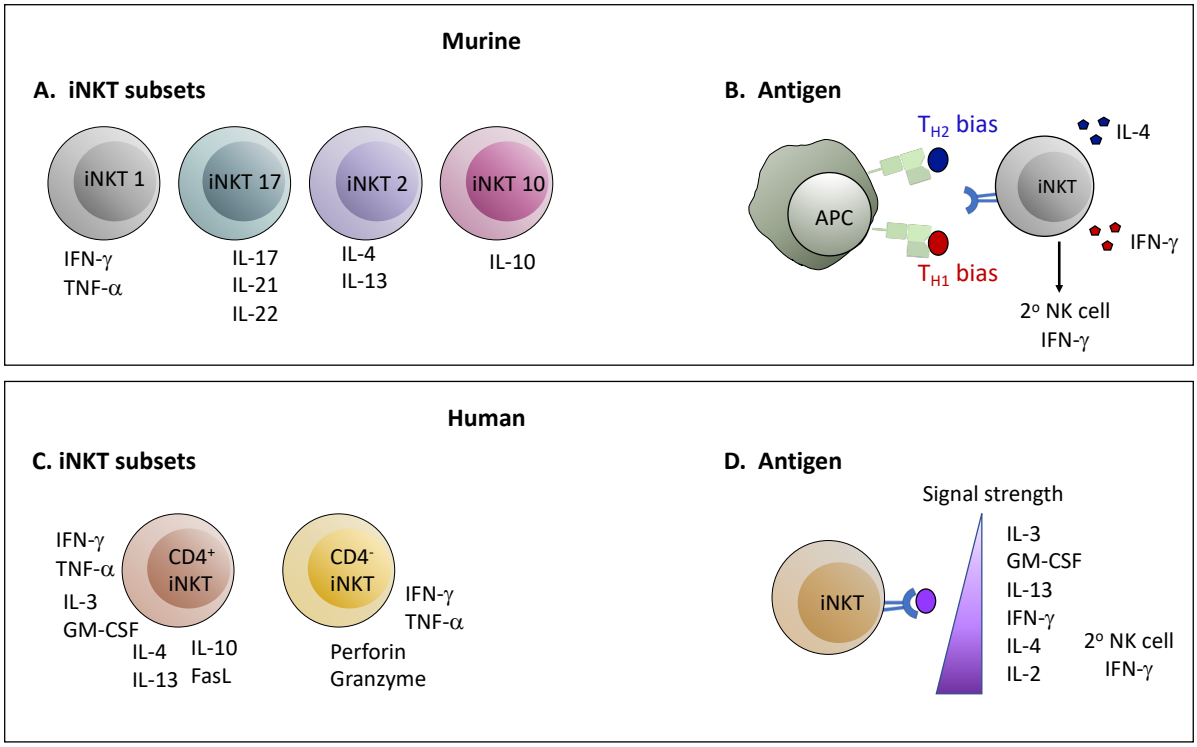

Figure 2. Determinants of the nature of the functional response mediated by iNKT cells. In both mice and humans the nature of the response mediated by iNKT cells may depend on the subset of iNKT cells activated or on the characteristics of the antigenic stimulation leading to activation. However, there are important differences between mice and humans in each of these parameters. (**A and C**) Murine iNKT cells can be classified into four lineages with functionally segregated cytokine profiles; whereas the two major subsets of human iNKT cells are characterized by comparatively polyfunctional cytokine production ($CD4^+$) or a more T_{H1}/cytotoxic profile ($CD4^-$). (**B and D**) Structural features of lipid antigens can bias murine iNKT cell responses towards either a T_{H1} or T_{H2} output, whereas human iNKT cell cytokine production proceeds in a hierarchical manner depending on the strength of the TCR signal. Antigens that stimulate a T_{H1}-biased response in mice typically also produce a strong secondary wave of IFN-g production by NK cells, whereas strong agonists produce this effect from human iNKT cells.

Chapter V: Discussion, Hypothesis and Future directions

iNKT cells are often seen mediating completely opposite functional outcomes in different disease models. They are known to offer protective immunity against certain infections and cancer. On the contrary, in autoimmune disease models mediate immunoregulatory functions. For successful use of iNKT cells clinically, it is important to understand factors that regulate iNKT cell function, whether it is immune activating or immune tolerizing.

We have shown that human derived $CD4^+$ iNKT cells can promote engraftment by silencing T cell inflammation (Chapter III). Mechanistically we identified that iNKT cells induced monocytes to produce PGE_2, a lipid mediator that can have a strong impact on T cell inflammation. We also showed that CD4 T cells, when exposed to homeostatic signals upregulate their metabolic activity and differentiate into MP cells which allows them to efficiently respond to a subsequent immunological challenge (Chapter I). What our experiments did not explore is how PGE_2 impacts other aspects of MP cells including the general differentiation status and their metabolic profile. It is also not clear if effects of PGE2 on T cells are lasting, and how it impacts their ability to respond to a subsequent immunological challenge post exposure.

Prior work on impact of PGE2 on T cells has been contradictory. One study showed that exposure to PGE2 promotes differentiation of activated T cells into terminally dysfunctional T cells (1). However, another study found that PGE2 treatment in presence of IL-7 promoted differentiation of antigen specific T cells into stem like memory T cells. These PGE2 treated cells favored oxidative phosphorylation over glycolysis unlike traditionally activated effector cells (2). Both studies mentioned above were performed using mouse CD8 T cells so the impact of PGE2 on metabolic status of polyclonal CD4 MP T cells that are activated

independently of a pathogen is not clear. Exploring the impact of iNKT induced monocyte derived PGE2 on MP cell function will help us understand overall implication of our iNKT immunotherapy and how it might impact potential GVL and GVHD response.

Another key unresolved question is if the iNKT-monocyte mediated suppressive effect seen in our model is dependent on use of a specific type of iNKT cell subset. Like conventional T cells, Mouse iNKT cells can be neatly categorized into lineages based the cytokines they produce. Recently, a group showed that iNKT subset that secreted Th2 cytokines were better at suppressing GVHD and iNKT cells that were predominantly Th1 like were better at mediating anti-tumor response (3). However, translation of these findings to human iNKT cells has not been straightforward. Human iNKT cells are usually polyfunctional, meaning they efficiently can make T helper type 1 (Th1) cytokines like IFNγ and TNFα, but also make T helper type 2 (Th2) cytokines such as IL-13 and IL-4 (Fig 1A). In our system, iNKT cells are able to induce T cell suppression irrespective of their ability to make copious amounts of Th1 cytokines. We further confirmed this by generating clonal iNKT cell lines and investigating if iNKT cell suppressive interaction with monocytes are dependent on iNKT cell cytokine profile.

Similar to polyclonal iNKT cell lines, majority iNKT clonal iNKT cell line end up being able to produce both Th1 and Th2 cytokines (Table 1). We also tested their suppressive function by evaluating IFNγ secretion by MP cells. Surprisingly, all of the iNKT clones, including WINK2b.6 clone, which was a Th1 biased iNKT cell clone, were able to suppress IFNγ production by MP cells (Fig 2). Based on results from these experiments, it seems like the suppressive effects of iNKT cells might not be dependent on their ability to make any Th2 cytokines. Unfortunately, we were unable to generate a clone that was biased towards Th2 cytokine profile. However, this could be addressed indirectly by blocking IFNγ and TNFα

using blocking antibodies during their interaction with monocytes. In addition, IL-10 can be important in mediating T cell suppression. Murine and human studies have identified IL-10 producing NKT cells that are more immunoregulatory in the context of inflammatory diseases (4-6). The IL-10 status of our generated clones is unknown.

Alternatively, it could be hypothesized that iNKT-mono suppression axis is dependent on a non-cytokine factor produced by iNKT cells. All immune cells are capable for metabolizing arachidonic acid that can result in production of eicosanoids like PGE2. Our published work showed that iNKT induced monocyte derived PGE2 had a significant impact on T cell suppression (Chapter III). However, we found that during the iNKT-monocyte interaction, if iNKT cells were treated with dexamethasone (a drug that inhibits production of PGE2), there was still partial recovery of T cell function (Fig 3). These results suggest that eicosanoids produced by iNKT cells might play a role in the suppressive interaction. Based on these preliminary experiments, I would hypothesize that iNKT-monocyte interaction induces iNKT cells to secrete small amounts of PGE2 which in turn activates COX2 in monocytes to produce more PGE2. This positive feedback loop might regulate T cell suppression in our system.

iNKT cell metabolism could be another potential factor that regulates their tolerogenic activity. Recent metabolic studies have revealed that iNKT cells might be unique in terms of their energy consumption. Compared to conventional CD4 T cells, iNKT are less dependent on glycolysis and show increased mitochondrial activity (7). It is possible that reactive oxygen species produced by iNKT cells stimulate monocytes to secrete PGE2.

To summarize, my PhD works has focused on gaining mechanistic insight into, A) T cell differentiation in the context of HSCT; B) How iNKT cells limit T cell inflammation and

promote HSC engraftment. We also identified a novel role of integrin stimulation in differentiation of stem like effector cells. Further experiments are needed to explore and confirm bigger implications of these pathways in regulating anti-tumor responses and also pathological responses in diseases like GVHD.

FIGURES

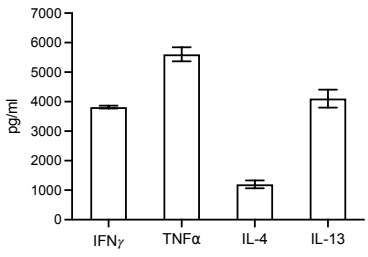

Figure 1. Cytokine profile of human iNKT cells. Polyclonal iNKT cells were stimulated with anti-CD3/CD28. Culture supernatants were collected after 24hrs and levels of cytokine production evaluated by ELISA.

Table 1

Cytokine profile of human $CD4^+$ iNKT clones

iNKT clones	IFN-γ	TNF-α	IL-4	IL-13
WINK3b.1	++++	++++	++	+++
WINK3b.2	++++	++++	+++	++
WINK3b.4	++++	++++	+	+
WINK3b.5	++++	++++	+	+
WINK3b.6	+++	++++	++	+++
WINK3b.7	++	++++	++	++
WINK3b.8	++++	++++	+	++
WINK3b.9	++++	++++	+	++
WINK3b.10	++++	++++	++++	++++
WINK3b.13	++++	++++	+++	+++
WINK3b.14	++++	++++	+	+
WINK2b.3	++++	++++	++++	+++
WINK2b.4	++++	++++	++++	+++
WINK2b.6	++++	++++	-	-
WID3b.1	++++	++++	++++	+++

Isolated clonal iNKT cell lines were stimulated with PMA/ionomycin and stained intracellularly to evaluate cytokine production.

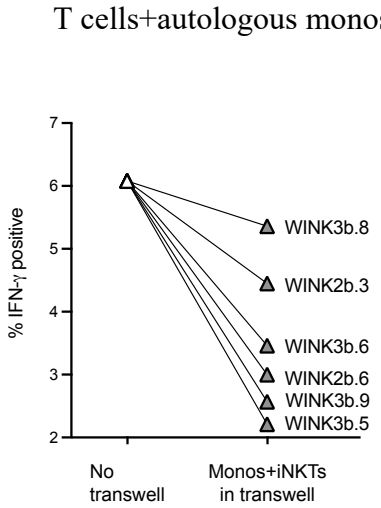

Figure 2. Suppressive effects of clonal iNKT cells. Isolated $CD4^+$ cord blood T cells were cultured for 5 days autologous monocytes in the presence or absence of transwell inserts containing iNKT cells and monocytes. Plot shows percentage of T cells staining positively for intracellular IFN-γ after PMA/ionomycin stimulation. Results shown here are taken from T cells and monocytes isolated from one cord sample. Experiment was repeated at least using 4 different cord samples to ensure reproducibility.

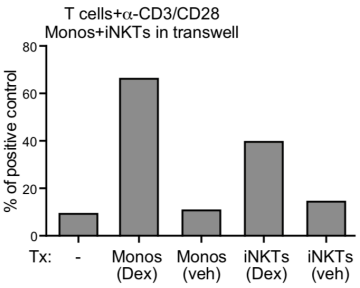

Figure 3. Role of iNKT cell derived eicosanoids. Isolated $CD4^+$ cord blood T cells were cultured for 3–5 d with anti-CD3 and anti-CD28 antibodies in the presence of transwell inserts containing iNKT cells and cord blood monocytes, then stimulated with PMA/ionomycin. Before co-culture, either the monocytes or the NKT cells were pretreated with dexamethasone (500 ng/ml). Plot shows IFN-γ production from the transwell co-cultures

as a percent of the response by positive control T cells that were cultured with anti-CD3/CD28 alone.

References

References for Introduction

1. Auletta J.J., Kou J., Chen M., Shaw B.E. Current use and outcome of hematopoietic stem cell transplantation: CIBMTR US summary slides, 2021.

2. Metheny, Leland et al. “Cord Blood Transplantation: Can We Make it Better?.” *Frontiers in oncology* vol. 3 238. 17 Sep. 2013, doi:10.3389/fonc.2013.00238

3. Rocha, V et al. “Comparison of outcomes of unrelated bone marrow and umbilical cord blood transplants in children with acute leukemia.” *Blood* vol. 97,10 (2001): 2962-71. doi:10.1182/blood.v97.10.2962

4. Ruggeri, Annalisa et al. “Engraftment kinetics and graft failure after single umbilical cord blood transplantation using a myeloablative conditioning regimen.” *Haematologica* vol. 99,9 (2014): 1509-15. doi:10.3324/haematol.2014.109280

5. Fuchs, Ephraim J et al. “Double unrelated umbilical cord blood vs HLA-haploidentical bone marrow transplantation: the BMT CTN 1101 trial.” *Blood* vol. 137,3 (2021): 420-428. doi:10.1182/blood.2020007535

6. Wagner JE, Eapen M, Carter SL, Haut PR, Peres E, Schultz KR, et al. No Survival Advantage after Double Umbilical Cord Blood (UCB) Compared to Single UCB Transplant in Children with Hematological Malignancy: Results of the Blood and Marrow Transplant Clinical Trials Network (BMT CTN 0501) Randomized Trial [Presentation]. ASH; (2012).

7. Yang, Liping et al. “IFN-gamma negatively modulates self-renewal of repopulating human hemopoietic stem cells.” *Journal of immunology (Baltimore, Md. : 1950)* vol. 174,2 (2005): 752-7. doi:10.4049/jimmunol.174.2.752

8. Qin, Yuhong, and Cai Zhang. “The Regulatory Role of IFN-γ on the Proliferation and Differentiation of Hematopoietic Stem and Progenitor Cells.” *Stem cell reviews and reports* vol. 13,6 (2017): 705-712. doi:10.1007/s12015-017-9761-1

9. Gumperz, Jenny E. “Antigen specificity of semi-invariant CD1d-restricted T cell receptors: the best of both worlds?.” *Immunology and cell biology* vol. 82,3 (2004): 285-94. doi:10.1111/j.0818-9641.2004.01257.x

10. Mattner, Jochen et al. “Exogenous and endogenous glycolipid antigens activate NKT cells during microbial infections.” *Nature* vol. 434,7032 (2005): 525-9. doi:10.1038/nature03408

11. Kinjo, Yuki et al. “Invariant natural killer T cells recognize glycolipids from pathogenic Gram-positive bacteria.” *Nature immunology* vol. 12,10 966-74. 4 Sep. 2011, doi:10.1038/ni.2096

12. Wolf, Benjamin J et al. “Novel Approaches to Exploiting Invariant NKT Cells in Cancer Immunotherapy.” *Frontiers in immunology* vol. 9 384. 2 Mar. 2018, doi:10.3389/fimmu.2018.00384

13. Brennan, Patrick J et al. “Invariant natural killer T cells: an innate activation scheme linked to diverse effector functions.” *Nature reviews. Immunology* vol. 13,2 (2013): 101-17. doi:10.1038/nri3369

14. Qin, Yingyu et al. “Invariant NKT cells facilitate cytotoxic T-cell activation via direct recognition of CD1d on T cells.” *Experimental & molecular medicine* vol. 51,10 1-9. 25 Oct. 2019, doi:10.1038/s12276-019-0329-9

15. Ikehara, Y et al. “CD4(+) Valpha14 natural killer T cells are essential for acceptance of rat islet xenografts in mice.” *The Journal of clinical investigation* vol. 105,12 (2000): 1761-7. doi:10.1172/JCI8922

16. Pratschke, Johann et al. “Role of NK and NKT cells in solid organ transplantation.” *Transplant international : official journal of the European Society for Organ Transplantation* vol. 22,9 (2009): 859-68. doi:10.1111/j.1432-2277.2009.00884.x

17. Wang, B et al. “CD1-restricted NK T cells protect nonobese diabetic mice from developing diabetes.” *The Journal of experimental medicine* vol. 194,3 (2001): 313-20. doi:10.1084/jem.194.3.313

18. Beaudoin, Lucie et al. “NKT cells inhibit the onset of diabetes by impairing the development of pathogenic T cells specific for pancreatic beta cells.” *Immunity* vol. 17,6 (2002): 725-36. doi:10.1016/s1074-7613(02)00473-9

19. Forestier, Claire et al. “Improved outcomes in NOD mice treated with a novel Th2 cytokine-biasing NKT cell activator.” *Journal of immunology (Baltimore, Md. : 1950)* vol. 178,3 (2007): 1415-25. doi:10.4049/jimmunol.178.3.1415

20. Schneidawind, Dominik et al. “Third-party CD4+ invariant natural killer T cells protect from murine GVHD lethality.” *Blood* vol. 125,22 (2015): 3491-500. doi:10.1182/blood-2014-11-612762

21. Rubio, Marie-Thérèse et al. “Early posttransplantation donor-derived invariant natural killer T-cell recovery predicts the occurrence of acute graft-versus-host disease and overall survival.” *Blood* vol. 120,10 (2012): 2144-54. doi:10.1182/blood-2012-01-404673

22. de Lalla, Claudia et al. “Invariant NKT cell reconstitution in pediatric leukemia patients given HLA-haploidentical stem cell transplantation defines distinct CD4+ and CD4- subset dynamics and correlates with remission state.” *Journal of immunology (Baltimore, Md. : 1950)* vol. 186,7 (2011): 4490-9. doi:10.4049/jimmunol.1003748

23. Mavers, Melissa et al. “Invariant Natural Killer T Cells As Suppressors of Graft-versus-Host Disease in Allogeneic Hematopoietic Stem Cell Transplantation.” *Frontiers in immunology* vol. 8 900. 31 Jul. 2017, doi:10.3389/fimmu.2017.00900

24. Krovi, S Harsha, and Laurent Gapin. “Invariant Natural Killer T Cell Subsets-More Than Just Developmental Intermediates.” *Frontiers in immunology* vol. 9 1393. 20 Jun. 2018, doi:10.3389/fimmu.2018.01393

25. Maas-Bauer K, Lohmeyer JK, Hirai T, Ramos TL, Fazal FM, Litzenburger UM, et al. Invariant natural killer T-cell subsets have diverse graft-versus-host-disease-preventing and antitumor effects. Blood. 2021;138(10):858-70.

26. Pillai AB, George TI, Dutt S, Strober S. Host natural killer T cells induce an interleukin-4-dependent expansion of donor CD4+CD25+Foxp3+ T regulatory cells that protects against graft-versus-host disease. Blood. 2009;113(18):4458-67.

27. Hashimoto D, Asakura S, Miyake S, Yamamura T, Van Kaer L, Liu C, et al. Stimulation of host NKT cells by synthetic glycolipid regulates acute graft-versus-host disease by inducing Th2 polarization of donor T cells. J Immunol. 2005;174(1):551-6

28. Hussain, Tabinda, and Kylie M Quinn. “Similar but different: virtual memory CD8 T cells as a memory-like cell population.” *Immunology and cell biology* vol. 97,7 (2019): 675-684. doi:10.1111/imcb.12277

29. Kawabe, Takeshi et al. “Memory-phenotype $CD4^+$ T cells spontaneously generated under steady-state conditions exert innate T_H1-like effector function.” *Science immunology* vol. 2,12 (2017): eaam9304. doi:10.1126/sciimmunol.aam9304

30. Kawabe, Takeshi, and Alan Sher. “Memory-phenotype CD4+ T cells: a naturally arising T lymphocyte population possessing innate immune function.” *International immunology* vol. 34,4 (2022): 189-196. doi:10.1093/intimm/dxab108

31. Kawabe, Takeshi et al. “Redefining the Foreign Antigen and Self-Driven Memory $CD4^+$ T-Cell Compartments *via* Transcriptomic, Phenotypic, and Functional Analyses.” *Frontiers in immunology* vol. 13 870542. 30 May. 2022, doi:10.3389/fimmu.2022.870542

32. Moon, James J et al. “Naive CD4(+) T cell frequency varies for different epitopes and predicts repertoire diversity and response magnitude.” *Immunity* vol. 27,2 (2007): 203-13. doi:10.1016/j.immuni.2007.07.007

33. Kim, Kwang Soon et al. “Dietary antigens limit mucosal immunity by inducing regulatory T cells in the small intestine.” *Science (New York, N.Y.)* vol. 351,6275 (2016): 858-63. doi:10.1126/science.aac5560

34. White, Jason T et al. “Virtual memory T cells develop and mediate bystander protective immunity in an IL-15-dependent manner.” *Nature communications* vol. 7 11291. 21 Apr. 2016, doi:10.1038/ncomms11291

35. Tan, J T et al. “IL-7 is critical for homeostatic proliferation and survival of naive T cells.” *Proceedings of the National Academy of Sciences of the United States of America* vol. 98,15 (2001): 8732-7. doi:10.1073/pnas.161126098

36. Masse, Guillemette X et al. “gamma(c) cytokines provide multiple homeostatic signals to naive CD4(+) T cells.” *European journal of immunology* vol. 37,9 (2007): 2606-16. doi:10.1002/eji.200737234

37. Jin, Jie-Hua et al. “Virtual memory CD8+ T cells restrain the viral reservoir in HIV-1-infected patients with antiretroviral therapy through derepressing KIR-mediated inhibition.” *Cellular & molecular immunology*vol. 17,12 (2020): 1257-1265. doi:10.1038/s41423-020-0408-9

38. Lin, J S et al. “Virtual memory CD8 T cells expanded by helminth infection confer broad protection against bacterial infection.” *Mucosal immunology* vol. 12,1 (2019): 258-264. doi:10.1038/s41385-018-0100-x

For Chapter I

1. T. E. Boursalian, J. Golob, D. M. Soper, C. J. Cooper, P. J. Fink, Continued maturation of thymic emigrants in the periphery. *Nat Immunol* **5**, 418-425 (2004).
2. C. A. Cunningham, E. Y. Helm, P. J. Fink, Reinterpreting recent thymic emigrant function: defective or adaptive? *Curr Opin Immunol* **51**, 1-6 (2018).
3. C. J. Haines *et al.*, Human CD4+ T cell recent thymic emigrants are identified by protein tyrosine kinase 7 and have reduced immune function. *J Exp Med* **206**, 275-285 (2009).
4. G. Trinchieri *et al.*, Natural killer cell stimulatory factor (NKSF) or interleukin-12 is a key regulator of immune response and inflammation. *Prog Growth Factor Res* **4**, 355-368 (1992).
5. S. L. Swain, CD4 T cell development and cytokine polarization: an overview. *J Leukoc Biol* **57**, 795-798 (1995).
6. M. Moser, K. M. Murphy, Dendritic cell regulation of TH1-TH2 development. *Nat Immunol* **1**, 199-205 (2000).
7. J. Zhu, H. Yamane, W. E. Paul, Differentiation of effector CD4 T cell populations (*). *Annu Rev Immunol* **28**, 445-489 (2010).
8. H. Gudmundsdottir, L. A. Turka, A closer look at homeostatic proliferation of CD4+ T cells: costimulatory requirements and role in memory formation. *J Immunol* **167**, 3699-3707 (2001).
9. J. Sprent, C. D. Surh, Normal T cell homeostasis: the conversion of naive cells into memory- phenotype cells. *Nat Immunol* **12**, 478-484 (2011).
10. T. Kawabe, A. Sher, Memory-phenotype CD4 + T cells: a naturally arising T lymphocyte population possessing innate immune function. *Int Immunol*, (2021).
11. L. F. Su, B. A. Kidd, A. Han, J. J. Kotzin, M. M. Davis, Virus-specific CD4(+) memory- phenotype T cells are abundant in unexposed adults. *Immunity* **38**, 373-383 (2013).
12. T. Kawabe *et al.*, Memory-phenotype CD4(+) T cells spontaneously generated under steady- state conditions exert innate TH1-like effector function. *Sci Immunol* **2**, (2017).
13. C. King, A. Ilic, K. Koelsch, N. Sarvetnick, Homeostatic expansion of T cells during immune insufficiency generates autoimmunity. *Cell* **117**, 265-277 (2004).
14. K. Khiong *et al.*, Homeostatically proliferating CD4 T cells are involved in the pathogenesis of an Omenn syndrome murine model. *J Clin Invest* **117**, 1270-1281 (2007).
15. V. F. Moxham *et al.*, Homeostatic proliferation of lymphocytes results in augmented memory-like function and accelerated allograft rejection. *J Immunol* **180**, 3910-3918 (2008).
16. J. L. Jones *et al.*, Human autoimmunity after lymphocyte depletion is caused by homeostatic T-cell proliferation. *Proc Natl Acad Sci U S A* **110**, 20200-20205 (2013).
17. P. Scott, IFN-gamma modulates the early development of Th1 and Th2 responses in a murine model of cutaneous leishmaniasis. *J Immunol* **147**, 3149-3155 (1991).
18. B. Min, W. E. Paul, Endogenous proliferation: burst-like CD4 T cell proliferation in lymphopenic settings. *Semin Immunol* **17**, 201-207 (2005).

19. B. Min, H. Yamane, J. Hu-Li, W. E. Paul, Spontaneous and homeostatic proliferation of CD4 T cells are regulated by different mechanisms. *J Immunol* **174**, 6039-6044 (2005).
20. A. Le Campion *et al.*, Naive T cells proliferate strongly in neonatal mice in response to self- peptide/self-MHC complexes. *Proc Natl Acad Sci U S A* **99**, 4538-4543 (2002).
21. W. C. Kieper *et al.*, Recent immune status determines the source of antigens that drive homeostatic T cell expansion. *J Immunol* **174**, 3158-3163 (2005).
22. J. S. Do, B. Min, Differential requirements of MHC and of DCs for endogenous proliferation of different T-cell subsets in vivo. *Proc Natl Acad Sci U S A* **106**, 20394-20398 (2009).
23. T. Onoe *et al.*, Homeostatic expansion and phenotypic conversion of human T cells depend on peripheral interactions with APCs. *J Immunol* **184**, 6756-6765 (2010).
24. T. Kawabe *et al.*, Homeostatic proliferation of naive CD4+ T cells in mesenteric lymph nodes generates gut-tropic Th17 cells. *J Immunol* **190**, 5788-5798 (2013).
25. K. S. Kim *et al.*, Dietary antigens limit mucosal immunity by inducing regulatory T cells in the small intestine. *Science* **351**, 858-863 (2016).
26. S. A. Younes *et al.*, Memory phenotype CD4 T cells undergoing rapid, nonburst-like, cytokine-driven proliferation can be distinguished from antigen-experienced memory cells. *PLoS Biol* **9**, e1001171 (2011).
27. N. K. Tchao, L. A. Turka, Lymphodepletion and homeostatic proliferation: implications for transplantation. *Am J Transplant* **12**, 1079-1090 (2012).
28. B. E. Anderson *et al.*, Memory CD4+ T cells do not induce graft-versus-host disease. *J Clin Invest* **112**, 101-108 (2003).
29. 29. B. J. Chen, X. Cui, G. D. Sempowski, C. Liu, N. J. Chao, Transfer of allogeneic CD62L- memory T cells without graft-versus-host disease. *Blood* **103**, 1534-1541 (2004).
30. 30. S. Dutt *et al.*, Naive and memory T cells induce different types of graft-versus-host disease. *J Immunol* **179**, 6547-6554 (2007).
31. H. Wang, Y. G. Yang, The complex and central role of interferon-gamma in graft-versus- host disease and graft-versus-tumor activity. *Immunol Rev* **258**, 30-44 (2014).
32. Y. G. Yang, H. Wang, W. Asavaroengchai, B. R. Dey, Role of Interferon-gamma in GVHD and GVL. *Cell Mol Immunol* **2**, 323-329 (2005).
33. W. Dummer *et al.*, T cell homeostatic proliferation elicits effective antitumor autoimmunity. *J Clin Invest* **110**, 185-192 (2002).
34. 34. S. Kohler, A. Thiel, Life after the thymus: CD31+ and CD31- human naive CD4+ T-cell subsets. *Blood* **113**, 769-774 (2009).
35. 35. R. D. Jacks *et al.*, Cell intrinsic characteristics of human cord blood naive CD4T cells. *Immunol Lett* **193**, 51-57 (2018).
36. 36. L. Chen, A. C. Cohen, D. B. Lewis, Impaired allogeneic activation and T-helper 1 differentiation of human cord blood naive CD4 T cells. *Biol Blood Marrow Transplant* **12**, 160-171 (2006).
37. N. J. Hess, A. W. Hudson, P. Hematti, J. E. Gumperz, Early T Cell Activation Metrics Predict Graft-versus-Host Disease in a Humanized Mouse Model of Hematopoietic Stem Cell Transplantation. *J Immunol* **205**, 272-281 (2020).
38. N. J. Hess *et al.*, iNKT cells coordinate immune pathways to enable engraftment in nonconditioned hosts. *Life Sci Alliance* **4**, (2021). \

39. N. A. Zumwalde *et al.*, Adoptively transferred Vgamma9Vdelta2 T cells show potent antitumor effects in a preclinical B cell lymphomagenesis model. *JCI Insight* **2**, (2017).
40. M. Afkarian *et al.*, T-bet is a STAT1-induced regulator of IL-12R expression in naive CD4+ T cells. *Nat Immunol* **3**, 549-557 (2002).
41. S. J. Szabo *et al.*, A novel transcription factor, T-bet, directs Th1 lineage commitment. *Cell* **100**, 655-669 (2000).
42. P. R. Rogers, H. M. Grey, M. Croft, Modulation of naive CD4 T cell activation with altered peptide ligands: the nature of the peptide and presentation in the context of costimulation are critical for a sustained response. *J Immunol* **160**, 3698-3704 (1998).
43. C. H. Chang *et al.*, Posttranscriptional control of T cell effector function by aerobic glycolysis. *Cell* **153**, 1239-1251 (2013).
44. M. Peng *et al.*, Aerobic glycolysis promotes T helper 1 cell differentiation through an epigenetic mechanism. *Science* **354**, 481-484 (2016).
45. J. Storek, R. P. Witherspoon, R. Storb, T cell reconstitution after bone marrow transplantation into adult patients does not resemble T cell development in early life. *Bone Marrow Transplant* **16**, 413-425 (1995).
46. C. L. Mackall *et al.*, Distinctions between CD8+ and CD4+ T-cell regenerative pathways result in prolonged T-cell subset imbalance after intensive chemotherapy. *Blood* **89**, 3700- 3707 (1997).
47. H. H. Smits *et al.*, Intercellular adhesion molecule-1/LFA-1 ligation favors human Th1 development. *J Immunol* **168**, 1710-1716 (2002).
48. S. A. Jenks, B. J. Eisfelder, J. Miller, LFA-1 co-stimulation inhibits T(h)2 differentiation by down-modulating IL-4 responsiveness. *Int Immunol* **17**, 315-323 (2005).
49. J. J. Bird *et al.*, Helper T cell differentiation is controlled by the cell cycle. *Immunity* **9**, 229- 237 (1998).
50. S. L. Reiner, A. C. Mullen, A. S. Hutchins, E. L. Pearce, Helper T cell differentiation and the problem of cellular inheritance. *Immunol Res* **27**, 463-468 (2003).
51. K. Maeda, M. H. Kosco-Vilbois, G. F. Burton, A. K. Szakal, J. G. Tew, Expression of the intercellular adhesion molecule-1 on high endothelial venules and on non-lymphoid antigen handling cells: interdigitating cells, antigen transporting cells and follicular dendritic cells. *Cell Tissue Res* **279**, 47-54 (1995).
52. T. N. Ramos, D. C. Bullard, S. R. Barnum, ICAM-1: isoforms and phenotypes. *J Immunol* **192**, 4469-4474 (2014).

For Chapter II

1. Xia, Anliang et al. “T Cell Dysfunction in Cancer Immunity and Immunotherapy.” *Frontiers in immunology* vol. 10 1719. 19 Jul. 2019, doi:10.3389/fimmu.2019.01719

2. Thommen, Daniela S, and Ton N Schumacher. “T Cell Dysfunction in Cancer.” *Cancer cell* vol. 33,4 (2018): 547-562. doi:10.1016/j.ccell.2018.03.012

3. Liu, Qingjun et al. “Memory T cells: strategies for optimizing tumor immunotherapy.” *Protein & cell* vol. 11,8 (2020): 549-564. doi:10.1007/s13238-020-00707-9

4. Chung, David J et al. “T-cell Exhaustion in Multiple Myeloma Relapse after Autotransplant: Optimal Timing of Immunotherapy.” *Cancer immunology research* vol. 4,1 (2016): 61-71. doi:10.1158/2326-6066.CIR-15-0055

5. Gumber, Diana, and Leo D Wang. “Improving CAR-T immunotherapy: Overcoming the challenges of T cell exhaustion.” *EBioMedicine* vol. 77 (2022): 103941. doi:10.1016/j.ebiom.2022.103941

6. Mondino, Anna, and Teresa Manzo. “To Remember or to Forget: The Role of Good and Bad Memories in Adoptive T Cell Therapy for Tumors.” *Frontiers in immunology* vol. 11 1915. 27 Aug. 2020, doi:10.3389/fimmu.2020.01915

7. Klebanoff, Christopher A et al. “Sorting through subsets: which T-cell populations mediate highly effective adoptive immunotherapy?.” *Journal of immunotherapy (Hagerstown, Md. : 1997)* vol. 35,9 (2012): 651-60. doi:10.1097/CJI.0b013e31827806e6

8. Roberto, Alessandra et al. “Role of naive-derived T memory stem cells in T-cell reconstitution following allogeneic transplantation.” *Blood* vol. 125,18 (2015): 2855-64. doi:10.1182/blood-2014-11-608406

9. Cieri, Nicoletta et al. “Generation of human memory stem T cells after haploidentical T-replete hematopoietic stem cell transplantation.” *Blood* vol. 125,18 (2015): 2865-74. doi:10.1182/blood-2014-11-608539

10. Gattinoni, Luca et al. “A human memory T cell subset with stem cell-like properties.” *Nature medicine* vol. 17,10 1290-7. 18 Sep. 2011, doi:10.1038/nm.2446

11. Li, Yujie et al. “Immunotherapeutic Potential of T Memory Stem Cells.” *Frontiers in oncology* vol. 11 723888. 17 Sep. 2021, doi:10.3389/fonc.2021.723888

12. Alizadeh, Darya et al. “IL15 Enhances CAR-T Cell Antitumor Activity by Reducing mTORC1 Activity and Preserving Their Stem Cell Memory Phenotype.” *Cancer immunology research* vol. 7,5 (2019): 759-772. doi:10.1158/2326-6066.CIR-18-0466

13. Frumento, Guido et al. “Homeostatic Cytokines Drive Epigenetic Reprogramming of Activated T Cells into a "Naive-Memory" Phenotype.” *iScience* vol. 23,4 (2020): 100989. doi:10.1016/j.isci.2020.100989

References for Chapter III

Arumugham, V.B., and C.T. Baldari. 2017. cAMP: a multifaceted modulator of immune synapse assembly and T cell activation. *J Leukoc Biol* 101:1301-1316.

Ballen, K.K., E. Gluckman, and H.E. Broxmeyer. 2013. Umbilical cord blood transplantation: the first 25 years and beyond. *Blood* 122:491-498.

Beziat, V., S. Nguyen, M. Exley, A. Achour, T. Simon, P. Chevallier, A. Sirvent, S. Vigouroux, P. Debre, B. Rio, and V. Vieillard. 2010. Shaping of iNKT cell repertoire after unrelated cord blood transplantation. *Clinical immunology* 135:364-373.

Bishop, M.R., E.P. Alyea, 3rd, M.S. Cairo, J.H. Falkenburg, C.H. June, N. Kroger, R.F. Little, J.S. Miller, S.Z. Pavletic, D.L. Porter, S.R. Riddell, K. van Besien, A.S. Wayne, D.J. Weisdorf, R.S. Wu, and S. Giralt. 2011. National Cancer Institute's First International Workshop on the Biology, Prevention, and Treatment of Relapse after Allogeneic Hematopoietic Stem Cell Transplantation: summary and recommendations from the organizing committee. *Biol Blood Marrow Transplant* 17:443-454.

Brigl, M., and M.B. Brenner. 2004. CD1: Antigen Presentation and T Cell Function. *Annu Rev Immunol* 22:817-890.

Brigl, M., L. Bry, S.C. Kent, J.E. Gumperz, and M.B. Brenner. 2003. Mechanism of CD1d-restricted natural killer T cell activation during microbial infection. *Nat Immunol* 4:1230-1237.

Brigl, M., R.V. Tatituri, G.F. Watts, V. Bhowruth, E.A. Leadbetter, N. Barton, N.R. Cohen, F.F. Hsu, G.S. Besra, and M.B. Brenner. 2011. Innate and cytokine-driven signals, rather than microbial antigens, dominate in natural killer T cell activation during microbial infection. *J Exp Med* 208:1163-1177.

Brigl, M., P. van den Elzen, X. Chen, J.H. Meyers, D. Wu, C.H. Wong, F. Reddington, P.A. Illarianov, G.S. Besra, M.B. Brenner, and J.E. Gumperz. 2006. Conserved and heterogeneous lipid antigen specificities of CD1d-restricted NKT cell receptors. *J Immunol* 176:3625-3634.

Brown, J.A., and V.A. Boussiotis. 2008. Umbilical cord blood transplantation: basic biology and clinical challenges to immune reconstitution. *Clinical immunology* 127:286-297.

Casorati, G., C. de Lalla, and P. Dellabona. 2012. Invariant natural killer T cells reconstitution and the control of leukemia relapse in pediatric haploidentical hematopoietic stem cell transplantation. *Oncoimmunology* 1:355-357.

Cassidy, J.T., and G.L. Nordby. 1975. Human serum immunoglobulin concentrations: prevalence of immunoglobulin deficiencies. *J Allergy Clin Immunol* 55:35-48.

Chaidos, A., S. Patterson, R. Szydlo, M.S. Chaudhry, F. Dazzi, E. Kanfer, D. McDonald, D. Marin, D. Milojkovic, J. Pavlu, J. Davis, A. Rahemtulla, K. Rezvani, J. Goldman, I. Roberts, J. Apperley, and A. Karadimitris. 2012. Graft invariant natural killer T-cell dose predicts risk of acute graft-versus-host disease in allogeneic hematopoietic stem cell transplantation. *Blood* 119:5030-5036.

Chang, D.H., H. Deng, P. Matthews, J. Krasovsky, G. Ragupathi, R. Spisek, A. Mazumder, D.H. Vesole, S. Jagannath, and M.V. Dhodapkar. 2008. Inflammation-associated

lysophospholipids as ligands for CD1d-restricted T cells in human cancer. *Blood* 112:1308-1316.

Chang, P.P., P. Barral, J. Fitch, A. Pratama, C.S. Ma, A. Kallies, J.J. Hogan, V. Cerundolo, S.G. Tangye, R. Bittman, S.L. Nutt, R. Brink, D.I. Godfrey, F.D. Batista, and C.G. Vinuesa. 2011. Identification of Bcl-6-dependent follicular helper NKT cells that provide cognate help for B cell responses. *Nat Immunol* 13:35-43.

Chen, X., X. Wang, J.M. Keaton, F. Reddington, P.A. Illarionov, G.S. Besra, and J.E. Gumperz. 2007. Distinct endosomal trafficking requirements for presentation of autoantigens and exogenous lipids by human CD1d molecules. *J Immunol* 178:6181-6190.

Chen, Y.B., T. Wang, M.T. Hemmer, C. Brady, D.R. Couriel, A. Alousi, J. Pidala, A. Urbano-Ispizua, S.W. Choi, T. Nishihori, T. Teshima, Y. Inamoto, B. Wirk, D.I. Marks, H. Abdel-Azim, L. Lehmann, L. Yu, M. Bitan, M.S. Cairo, M. Qayed, R. Salit, R.P. Gale, R. Martino, S. Jaglowski, A. Bajel, B. Savani, H. Frangoul, I.D. Lewis, J. Storek, M. Askar, M.A. Kharfan-Dabaja, M. Aljurf, O. Ringden, R. Reshef, R.F. Olsson, S. Hashmi, S. Seo, T.R. Spitzer, M.L. MacMillan, A. Lazaryan, S.R. Spellman, M. Arora, and C.S. Cutler. 2017. GvHD after umbilical cord blood transplantation for acute leukemia: an analysis of risk factors and effect on outcomes. *Bone Marrow Transplant* 52:400-408.

Cosgun, K.N., S. Rahmig, N. Mende, S. Reinke, I. Hauber, C. Schafer, A. Petzold, H. Weisbach, G. Heidkamp, A. Purbojo, R. Cesnjevar, A. Platz, M. Bornhauser, M. Schmitz, D. Dudziak, J. Hauber, J. Kirberg, and C. Waskow. 2014. Kit regulates HSC engraftment across the human-mouse species barrier. *Cell Stem Cell* 15:227-238.

Czechowicz, A., R. Palchaudhuri, A. Scheck, Y. Hu, J. Hoggatt, B. Saez, W.W. Pang, M.K. Mansour, T.A. Tate, Y.Y. Chan, E. Walck, G. Wernig, J.A. Shizuru, F. Winau, D.T. Scadden, and D.J. Rossi. 2019. Selective hematopoietic stem cell ablation using CD117-antibody-drug-conjugates enables safe and effective transplantation with immunity preservation. *Nat Commun* 10:617.

de Lalla, C., A. Rinaldi, D. Montagna, L. Azzimonti, M.E. Bernardo, L.M. Sangalli, A.M. Paganoni, R. Maccario, A. Di Cesare-Merlone, M. Zecca, F. Locatelli, P. Dellabona, and G. Casorati. 2011. Invariant NKT Cell Reconstitution in Pediatric Leukemia Patients Given HLA-Haploidentical Stem Cell Transplantation Defines Distinct CD4+ and CD4- Subset Dynamics and Correlates with Remission State. *J Immunol* 186:4490-4499.

Dekker, L., C. de Koning, C. Lindemans, and S. Nierkens. 2020. Reconstitution of T Cell Subsets Following Allogeneic Hematopoietic Cell Transplantation. *Cancers (Basel)* 12:

Du, J., K. Paz, G. Thangavelu, D. Schneidawind, J. Baker, R. Flynn, O. Duramad, C. Feser, A. Panoskaltsis-Mortari, R.S. Negrin, and B.R. Blazar. 2017. Invariant natural killer T cells ameliorate murine chronic GVHD by expanding donor regulatory T cells. *Blood* 129:3121-3125.

Durand, E.M., and L.I. Zon. 2010. Newly emerging roles for prostaglandin E2 regulation of hematopoiesis and hematopoietic stem cell engraftment. *Current opinion in hematology* 17:308-312.

Exton, J.H. 1994. Phosphatidylcholine breakdown and signal transduction. *Biochim Biophys Acta* 1212:26-42.

Fox, L.M., D.G. Cox, J.L. Lockridge, X. Wang, X. Chen, L. Scharf, D.L. Trott, R.M. Ndonye, N. Veerapen, G.S. Besra, A.R. Howell, M.E. Cook, E.J. Adams, W.H. Hildebrand,

and J.E. Gumperz. 2009. Recognition of lyso-phospholipids by human natural killer T lymphocytes. *PLoS Biol* 7:e1000228.

Funk, C.D. 2001. Prostaglandins and leukotrienes: advances in eicosanoid biology. *Science* 294:1871-1875.

Han, M., L.I. Hannick, M. DiBrino, and M.A. Robinson. 1999. Polymorphism of human CD1 genes. *Tissue Antigens* 54:122-127.

Haraguchi, K., T. Takahashi, K. Hiruma, Y. Kanda, Y. Tanaka, S. Ogawa, S. Chiba, O. Miura, H. Sakamaki, and H. Hirai. 2004. Recovery of Valpha24+ NKT cells after hematopoietic stem cell transplantation. *Bone Marrow Transplant* 34:595-602.

Hegde, S., E. Jankowska-Gan, D.A. Roenneburg, J. Torrealba, W.J. Burlingham, and J.E. Gumperz. 2009. Human NKT cells promote monocyte differentiation into suppressive myeloid antigen-presenting cells. *J Leukoc Biol* 86:757-768.

Hegde, S., J.L. Lockridge, Y.A. Becker, S. Ma, S.C. Kenney, and J.E. Gumperz. 2011. Human NKT cells direct the differentiation of myeloid APCs that regulate T cell responses via expression of programmed cell death ligands. *J Autoimmun* 37:28-38.

Hess, N.J., A.W. Hudson, P. Hematti, and J.E. Gumperz. 2020a. Early T Cell Activation Metrics Predict Graft-versus-Host Disease in a Humanized Mouse Model of Hematopoietic Stem Cell Transplantation. *J Immunol* 205:272-281.

Hess, N.J., P.N. Lindner, J. Vazquez, S. Grindel, A.W. Hudson, A.K. Stanic, A. Ikeda, P. Hematti, and J.E. Gumperz. 2020b. Different Human Immune Lineage Compositions Are Generated in Non-Conditioned NBSGW Mice Depending on HSPC Source. *Front Immunol* 11:573406.

Jahnke, S., H. Schmid, K.A. Secker, J. Einhaus, S. Duerr-Stoerzer, H. Keppeler, I. Schober-Melms, R. Baur, M. Schumm, R. Handgretinger, W. Bethge, L. Kanz, C. Schneidawind, and D. Schneidawind. 2019. Invariant NKT Cells From Donor Lymphocyte Infusions (DLI-iNKTs) Promote ex vivo Lysis of Leukemic Blasts in a CD1d-Dependent Manner. *Front Immunol* 10:1542.

Jangalwe, S., L.D. Shultz, A. Mathew, and M.A. Brehm. 2016. Improved B cell development in humanized NOD-scid IL2Rgamma(null) mice transgenically expressing human stem cell factor, granulocyte-macrophage colony-stimulating factor and interleukin-3. *Immun Inflamm Dis* 4:427-440.

Juric, M.K., S. Ghimire, J. Ogonek, E.M. Weissinger, E. Holler, J.J. van Rood, M. Oudshoorn, A. Dickinson, and H.T. Greinix. 2016. Milestones of Hematopoietic Stem Cell Transplantation - From First Human Studies to Current Developments. *Front Immunol* 7:470.

Keating, A.K., J. Langenhorst, J.E. Wagner, K.M. Page, P. Veys, R.F. Wynn, H. Stefanski, R. Elfeky, R. Giller, R. Mitchell, F. Milano, T.A. O'Brien, A. Dahlberg, C. Delaney, J. Kurtzberg, M.R. Verneris, and J.J. Boelens. 2019. The influence of stem cell source on transplant outcomes for pediatric patients with acute myeloid leukemia. *Blood Adv* 3:1118-1128.

Kotsianidis, I., J.D. Silk, E. Spanoudakis, S. Patterson, A. Almeida, R.R. Schmidt, C. Tsatalas, G. Bourikas, V. Cerundolo, I.A. Roberts, and A. Karadimitris. 2006. Regulation of hematopoiesis in vitro and in vivo by invariant NKT cells. *Blood* 107:3138-3144.

Leite-de-Moraes, M.C., M. Lisbonne, A. Arnould, F. Machavoine, A. Herbelin, M. Dy, and E. Schneider. 2002. Ligand-activated natural killer T lymphocytes promptly produce IL-3 and GM-CSF in vivo: relevance to peripheral myeloid recruitment. *Eur J Immunol* 32:1897-1904.

Li, L., H.T. Kim, A. Nellore, N. Patsoukis, V. Petkova, S. McDonough, I. Politikos, S. Nikiforow, R. Soiffer, J.H. Antin, K. Ballen, C. Cutler, J. Ritz, and V.A. Boussiotis. 2014. Prostaglandin E2 promotes survival of naive UCB T cells via the Wnt/beta-catenin pathway and alters immune reconstitution after UCBT. *Blood Cancer J* 4:e178.

Lopez-Sagaseta, J., L.V. Sibener, J.E. Kung, J. Gumperz, and E.J. Adams. 2012. Lysophospholipid presentation by CD1d and recognition by a human Natural Killer T-cell receptor. *Embo J* 31:2047-2059.

Lucchini, G., M.A. Perales, and P. Veys. 2015. Immune reconstitution after cord blood transplantation: peculiarities, clinical implications and management strategies. *Cytotherapy* 17:711-722.

Luis, T.C., C.S. Tremblay, M.G. Manz, T.E. North, K.Y. King, and G.A. Challen. 2016. Inflammatory signals in HSPC development and homeostasis: Too much of a good thing? *Exp Hematol* 44:908-912.

Mavers, M., K. Maas-Bauer, and R.S. Negrin. 2017. Invariant Natural Killer T Cells As Suppressors of Graft-versus-Host Disease in Allogeneic Hematopoietic Stem Cell Transplantation. *Front Immunol* 8:900.

McIntosh, B.E., M.E. Brown, B.M. Duffin, J.P. Maufort, D.T. Vereide, Slukvin, II, and J.A. Thomson. 2015. Nonirradiated NOD,B6.SCID Il2rgamma-/- Kit(W41/W41) (NBSGW) mice support multilineage engraftment of human hematopoietic cells. *Stem Cell Reports* 4:171-180.

Navarro-Alvarez, N., and Y.G. Yang. 2011. CD47: a new player in phagocytosis and xenograft rejection. *Cell Mol Immunol* 8:285-288.

Negrin, R.S. 2019. Immune regulation in hematopoietic cell transplantation. *Bone Marrow Transplant* 54:765-768.

North, T.E., W. Goessling, C.R. Walkley, C. Lengerke, K.R. Kopani, A.M. Lord, G.J. Weber, T.V. Bowman, I.H. Jang, T. Grosser, G.A. Fitzgerald, G.Q. Daley, S.H. Orkin, and L.I. Zon. 2007. Prostaglandin E2 regulates vertebrate haematopoietic stem cell homeostasis. *Nature* 447:1007-1011.

Ramadan, A., and S. Paczesny. 2015. Various forms of tissue damage and danger signals following hematopoietic stem-cell transplantation. *Front Immunol* 6:14.

Rongvaux, A., T. Willinger, J. Martinek, T. Strowig, S.V. Gearty, L.L. Teichmann, Y. Saito, F. Marches, S. Halene, A.K. Palucka, M.G. Manz, and R.A. Flavell. 2014. Development and function of human innate immune cells in a humanized mouse model. *Nat Biotechnol* 32:364-372.

Schmid, H., C. Schneidawind, S. Jahnke, F. Kettemann, K.A. Secker, S. Duerr-Stoerzer, H. Keppeler, L. Kanz, P.B. Savage, and D. Schneidawind. 2018. Culture-Expanded Human Invariant Natural Killer T Cells Suppress T-Cell Alloreactivity and Eradicate Leukemia. *Front Immunol* 9:1817.

Schneidawind, D., J. Baker, A. Pierini, C. Buechele, R.H. Luong, E.H. Meyer, and R.S. Negrin. 2015. Third-party CD4+ invariant natural killer T cells protect from murine GVHD lethality. *Blood* 125:3491-3500.

Schneidawind, D., A. Pierini, M. Alvarez, Y. Pan, J. Baker, C. Buechele, R.H. Luong, E.H. Meyer, and R.S. Negrin. 2014. CD4+ invariant natural killer T cells protect from murine GVHD lethality through expansion of donor CD4+CD25+FoxP3+ regulatory T cells. *Blood* 124:3320-3328.

Schneidawind, D., A. Pierini, and R.S. Negrin. 2013. Regulatory T cells and natural killer T cells for modulation of GVHD following allogeneic hematopoietic cell transplantation. *Blood* 122:3116-3121.

Sharma, A., S.M. Lawry, B.S. Klein, X. Wang, N.M. Sherer, N.A. Zumwalde, and J.E. Gumperz. 2018. LFA-1 Ligation by High-Density ICAM-1 Is Sufficient To Activate IFN-gamma Release by Innate T Lymphocytes. *J Immunol* 201:2452-2461.

Shultz, L.D., B.L. Lyons, L.M. Burzenski, B. Gott, X. Chen, S. Chaleff, M. Kotb, S.D. Gillies, M. King, J. Mangada, D.L. Greiner, and R. Handgretinger. 2005. Human lymphoid and myeloid cell development in NOD/LtSz-scid IL2R gamma null mice engrafted with mobilized human hemopoietic stem cells. *J Immunol* 174:6477-6489.

Shultz, L.D., P.A. Schweitzer, S.W. Christianson, B. Gott, I.B. Schweitzer, B. Tennent, S. McKenna, L. Mobraaten, T.V. Rajan, D.L. Greiner, and et al. 1995. Multiple defects in innate and adaptive immunologic function in NOD/LtSz-scid mice. *J Immunol* 154:180-191.

Sippel, T.R., S. Radtke, T.M. Olsen, H.P. Kiem, and A. Rongvaux. 2019. Human hematopoietic stem cell maintenance and myeloid cell development in next-generation humanized mouse models. *Blood Adv* 3:268-274.

Toubai, T., N.D. Mathewson, J. Magenau, and P. Reddy. 2016. Danger Signals and Graft-versus-host Disease: Current Understanding and Future Perspectives. *Front Immunol* 7:539.

Tsai, S.B., H. Liu, T. Shore, Y. Fan, M. Bishop, M.M. Cushing, U. Gergis, L. Godley, J. Kline, R.A. Larson, G. Martinez, S. Mayer, O. Odenike, W. Stock, A. Wickrema, K. van Besien, and A.S. Artz. 2016. Frequency and Risk Factors Associated with Cord Graft Failure after Transplant with Single-Unit Umbilical Cord Cells Supplemented by Haploidentical Cells with Reduced-Intensity Conditioning. *Biol Blood Marrow Transplant* 22:1065-1072.

van der Maas, N.G., D. Berghuis, M. van der Burg, and A.C. Lankester. 2019. B Cell Reconstitution and Influencing Factors After Hematopoietic Stem Cell Transplantation in Children. *Front Immunol* 10:782.

Wang, W., H. Fujii, H.J. Kim, K. Hermans, T. Usenko, S. Xie, Z.J. Luo, J. Ma, C.L. Celso, J.E. Dick, T. Schroeder, J. Krueger, D. Wall, R.M. Egeler, and P.W. Zandstra. 2017. Enhanced human hematopoietic stem and progenitor cell engraftment by blocking donor T cell-mediated TNFalpha signaling. *Sci Transl Med* 9:

Wang, X., K.A. Bishop, S. Hegde, L.A. Rodenkirch, J.W. Pike, and J.E. Gumperz. 2012. Human invariant natural killer T cells acquire transient innate responsiveness via histone H4 acetylation induced by weak TCR stimulation. *J Exp Med* 209:987-1000.

Wang, X., X. Chen, L. Rodenkirch, W. Simonson, S. Wernimont, R.M. Ndonye, N. Veerapen, D. Gibson, A.R. Howell, G.S. Besra, G.F. Painter, A. Huttenlocher, and J.E.

Gumperz. 2008. Natural killer T-cell autoreactivity leads to a specialized activation state. *Blood* 112:4128-4138.

Waskow, C., V. Madan, S. Bartels, C. Costa, R. Blasig, and H.R. Rodewald. 2009. Hematopoietic stem cell transplantation without irradiation. *Nat Methods* 6:267-269.

Willinger, T., A. Rongvaux, H. Takizawa, G.D. Yancopoulos, D.M. Valenzuela, A.J. Murphy, W. Auerbach, E.E. Eynon, S. Stevens, M.G. Manz, and R.A. Flavell. 2011. Human IL-3/GM-CSF knock-in mice support human alveolar macrophage development and human immune responses in the lung. *Proc Natl Acad Sci U S A* 108:2390-2395.

Xu, X., G.M. Pocock, A. Sharma, S.L. Peery, J.S. Fites, L. Felley, R. Zarnowski, D. Stewart, E. Berthier, B.S. Klein, N.M. Sherer, and J.E. Gumperz. 2016. Human iNKT Cells Promote Protective Inflammation by Inducing Oscillating Purinergic Signaling in Monocyte-Derived DCs. *Cell Rep* 16:3273-3285.

Yang, F., D. Lu, Y. Hu, X. Huang, H. Huang, J. Chen, D. Wu, J. Wang, C. Wang, M. Han, and H. Chen. 2017. Risk Factors for Graft-Versus-Host Disease After Transplantation of Hematopoietic Stem Cells from Unrelated Donors in the China Marrow Donor Program. *Ann Transplant* 22:384-401.

Yurino, A., K. Takenaka, T. Yamauchi, T. Nunomura, Y. Uehara, F. Jinnouchi, K. Miyawaki, Y. Kikushige, K. Kato, T. Miyamoto, H. Iwasaki, Y. Kunisaki, and K. Akashi. 2016. Enhanced Reconstitution of Human Erythropoiesis and Thrombopoiesis in an Immunodeficient Mouse Model with Kit(Wv) Mutations. *Stem Cell Reports* 7:425-438.

For Chapter IV

1. Gumperz JE. Antigen specificity of semi-invariant CD1d-restricted T cell receptors: the best of both worlds? Immunol Cell Biol. 2004;82(3):285-94.

2. Zajonc DM, Kronenberg M. Carbohydrate specificity of the recognition of diverse glycolipids by natural killer T cells. Immunol Rev. 2009;230(1):188-200.

3. Van Rhijn I, Godfrey DI, Rossjohn J, Moody DB. Lipid and small-molecule display by CD1 and MR1. Nat Rev Immunol. 2015;15(10):643-54.

4. Oteo M, Parra JF, Mirones I, Gimenez LI, Setien F, Martinez-Naves E. Single strand conformational polymorphism analysis of human CD1 genes in different ethnic groups. Tissue Antigens. 1999;53(6):545-50.

5. Exley M, Garcia J, Wilson SB, Spada F, Gerdes D, Tahir SM, et al. CD1d structure and regulation on human thymocytes, peripheral blood T cells, B cells and monocytes. Immunology. 2000;100(1):37-47.

6. Canchis PW, Bhan AK, Landau SB, Yang L, Balk SP, Blumberg RS. Tissue distribution of the non-polymorphic major histocompatibility complex class I-like molecule, CD1d. Immunology. 1993;80(4):561-5.

7. Moody DB, Cotton RN. Four pathways of CD1 antigen presentation to T cells. Curr Opin Immunol. 2017;46:127-33.

8. McEwen-Smith RM, Salio M, Cerundolo V. CD1d-dependent endogenous and exogenous lipid antigen presentation. Curr Opin Immunol. 2015;34:116-25.

9. Salio M, Cerundolo V. Linking inflammation to natural killer T cell activation. PLoS Biol. 2009;7(10):e1000226.

10. Van Kaer L, Wu L. Therapeutic Potential of Invariant Natural Killer T Cells in Autoimmunity. Front Immunol. 2018;9:519.

11. Rakhshandehroo M, Kalkhoven E, Boes M. Invariant natural killer T cells in adipose tissue: novel regulators of immune-mediated metabolic disease. Cell Mol Life Sci. 2013;70(24):4711-27.

12. Negrin RS. Immune regulation in hematopoietic cell transplantation. Bone Marrow Transplant. 2019;54(Suppl 2):765-8.

13. Kinjo Y, Takatsuka S, Kitano N, Kawakubo S, Abe M, Ueno K, et al. Functions of CD1d-Restricted Invariant Natural Killer T Cells in Antimicrobial Immunity and Potential Applications for Infection Control. Front Immunol. 2018;9:1266.

14. Shimizu K, Iyoda T, Yamasaki S, Kadowaki N, Tojo A, Fujii AS. NK and NKT Cell-Mediated Immune Surveillance against Hematological Malignancies. Cancers (Basel). 2020;12(4).

15. Felley L, Gumperz JE. Are human iNKT cells keeping tabs on lipidome perturbations triggered by oxidative stress in the blood? Immunogenetics. 2016;68(8):611-22.

16. Field JJ, Nathan DG, Linden J. Targeting iNKT cells for the treatment of sickle cell disease. Clinical immunology. 2011;140(2):177-83.

17. Leung B, Harris HW. NKT cells: the culprits of sepsis? J Surg Res. 2011;167(1):87-95.

18. Hammond KJ, Poulton LD, Palmisano LJ, Silveira PA, Godfrey DI, Baxter AG. alpha/beta-T cell receptor (TCR)+CD4-CD8- (NKT) thymocytes prevent insulin-dependent diabetes mellitus in nonobese diabetic (NOD)/Lt mice by the influence of interleukin (IL)-4 and/or IL-10. J Exp Med. 1998;187(7):1047-56.

19. Lehuen A, Lantz O, Beaudoin L, Laloux V, Carnaud C, Bendelac A, et al. Overexpression of natural killer T cells protects Valpha14- Jalpha281 transgenic nonobese diabetic mice against diabetes. J Exp Med. 1998;188(10):1831-9.

20. Hong S, Wilson MT, Serizawa I, Wu L, Singh N, Naidenko OV, et al. The natural killer T-cell ligand alpha-galactosylceramide prevents autoimmune diabetes in non-obese diabetic mice. Nat Med. 2001;7(9):1052-6.

21. Falcone M, Facciotti F, Ghidoli N, Monti P, Olivieri S, Zaccagnino L, et al. Up-regulation of CD1d expression restores the immunoregulatory function of NKT cells and prevents autoimmune diabetes in nonobese diabetic mice. J Immunol. 2004;172(10):5908-16.

22. Naumov YN, Bahjat KS, Gausling R, Abraham R, Exley MA, Koezuka Y, et al. Activation of CD1d-restricted T cells protects NOD mice from developing diabetes by regulating dendritic cell subsets. Proc Natl Acad Sci U S A. 2001;98(24):13838-43.

23. Beaudoin L, Laloux V, Novak J, Lucas B, Lehuen A. NKT cells inhibit the onset of diabetes by impairing the development of pathogenic T cells specific for pancreatic beta cells. Immunity. 2002;17(6):725-36.

24. Chen YG, Choisy-Rossi CM, Holl TM, Chapman HD, Besra GS, Porcelli SA, et al. Activated NKT cells inhibit autoimmune diabetes through tolerogenic recruitment of dendritic cells to pancreatic lymph nodes. J Immunol. 2005;174(3):1196-204.

25. Wang J, Cho S, Ueno A, Cheng L, Xu BY, Desrosiers MD, et al. Ligand-dependent induction of noninflammatory dendritic cells by anergic invariant NKT cells minimizes autoimmune inflammation. J Immunol. 2008;181(4):2438-45.

26. Lynch L, Nowak M, Varghese B, Clark J, Hogan AE, Toxavidis V, et al. Adipose tissue invariant NKT cells protect against diet-induced obesity and metabolic disorder through regulatory cytokine production. Immunity. 2012;37(3):574-87.

27. LaMarche NM, Kane H, Kohlgruber AC, Dong H, Lynch L, Brenner MB. Distinct iNKT Cell Populations Use IFNgamma or ER Stress-Induced IL-10 to Control Adipose Tissue Homeostasis. Cell Metab. 2020;32(2):243-58 e6.

28. Lynch L, Michelet X, Zhang S, Brennan PJ, Moseman A, Lester C, et al. Regulatory iNKT cells lack expression of the transcription factor PLZF and control the homeostasis of T(reg) cells and macrophages in adipose tissue. Nat Immunol. 2015;16(1):85-95.

29. Liew PX, Lee WY, Kubes P. iNKT Cells Orchestrate a Switch from Inflammation to Resolution of Sterile Liver Injury. Immunity. 2017;47(4):752-65 e5.

30. Goto T, Ito Y, Satoh M, Nakamoto S, Nishizawa N, Hosono K, et al. Activation of iNKT Cells Facilitates Liver Repair After Hepatic Ischemia Reperfusion Injury Through Acceleration of Macrophage Polarization. Front Immunol. 2021;12:754106.

31. Hashimoto D, Asakura S, Miyake S, Yamamura T, Van Kaer L, Liu C, et al. Stimulation of host NKT cells by synthetic glycolipid regulates acute graft-versus-host disease by inducing Th2 polarization of donor T cells. J Immunol. 2005;174(1):551-6.

32. Pillai AB, George TI, Dutt S, Strober S. Host natural killer T cells induce an interleukin-4-dependent expansion of donor CD4+CD25+Foxp3+ T regulatory cells that protects against graft-versus-host disease. Blood. 2009;113(18):4458-67.

33. Leveson-Gower DB, Olson JA, Sega EI, Luong RH, Baker J, Zeiser R, et al. Low doses of natural killer T cells provide protection from acute graft-versus-host disease via an IL-4-dependent mechanism. Blood. 2011;117(11):3220-9.

34. Du J, Paz K, Thangavelu G, Schneidawind D, Baker J, Flynn R, et al. Invariant natural killer T cells ameliorate murine chronic GVHD by expanding donor regulatory T cells. Blood. 2017;129(23):3121-5.

35. Schneidawind D, Baker J, Pierini A, Buechele C, Luong RH, Meyer EH, et al. Third-party CD4+ invariant natural killer T cells protect from murine GVHD lethality. Blood. 2015;125(22):3491-500.

36. Schneidawind D, Pierini A, Alvarez M, Pan Y, Baker J, Buechele C, et al. CD4+ invariant natural killer T cells protect from murine GVHD lethality through expansion of donor CD4+CD25+FoxP3+ regulatory T cells. Blood. 2014;124(22):3320-8.

37. Burrello C, Strati F, Lattanzi G, Diaz-Basabe A, Mileti E, Giuffre MR, et al. IL10 secretion endows intestinal human iNKT cells with regulatory functions towards pathogenic T lymphocytes. J Crohns Colitis. 2022.

38. Venken K, Decruy T, Aspeslagh S, Van Calenbergh S, Lambrecht BN, Elewaut D. Bacterial CD1d-restricted glycolipids induce IL-10 production by human regulatory T cells upon cross-talk with invariant NKT cells. J Immunol. 2013;191(5):2174-83.

39. Hegde S, Chen X, Keaton JM, Reddington F, Besra GS, Gumperz JE. NKT cells direct monocytes into a DC differentiation pathway. J Leukoc Biol. 2007;81(5):1224-35.

40. Hegde S, Jankowska-Gan E, Roenneburg DA, Torrealba J, Burlingham WJ, Gumperz JE. Human NKT cells promote monocyte differentiation into suppressive myeloid antigen-presenting cells. J Leukoc Biol. 2009;86(4):757-68.

41. Hegde S, Lockridge JL, Becker YA, Ma S, Kenney SC, Gumperz JE. Human NKT cells direct the differentiation of myeloid APCs that regulate T cell responses via expression of programmed cell death ligands. J Autoimmun. 2011;37(1):28-38.

42. Terabe M, Matsui S, Noben-Trauth N, Chen H, Watson C, Donaldson DD, et al. NKT cell-mediated repression of tumor immunosurveillance by IL-13 and the IL-4R-STAT6 pathway. Nat Immunol. 2000;1(6):515-20.

43. Terabe M, Matsui S, Park JM, Mamura M, Noben-Trauth N, Donaldson DD, et al. Transforming growth factor-beta production and myeloid cells are an effector mechanism through which CD1d-restricted T cells block cytotoxic T lymphocyte-mediated tumor immunosurveillance: abrogation prevents tumor recurrence. J Exp Med. 2003;198(11):1741-52.

44. Hess NJ, N SB, Bobeck EA, McDougal CE, Ma S, Sauer JD, et al. iNKT cells coordinate immune pathways to enable engraftment in nonconditioned hosts. Life Sci Alliance. 2021;4(7).

45. Muller AM, Florek M, Kohrt HE, Kupper NJ, Filatenkov A, Linderman JA, et al. Blood Stem Cell Activity Is Arrested by Th1-Mediated Injury Preventing Engraftment following Nonmyeloablative Conditioning. J Immunol. 2016;197(10):4151-62.

46. Nicol A, Nieda M, Koezuka Y, Porcelli S, Suzuki K, Tadokoro K, et al. Dendritic cells are targets for human invariant Valpha24+ natural killer T-cell cytotoxic activity: an important immune regulatory function. Exp Hematol. 2000;28(3):276-82.

47. Yang OO, Racke FK, Nguyen PT, Gausling R, Severino ME, Horton HF, et al. CD1d on myeloid dendritic cells stimulates cytokine secretion from and cytolytic activity of V alpha 24J alpha Q T cells: a feedback mechanism for immune regulation. J Immunol. 2000;165(7):3756-62.

48. Liu TY, Uemura Y, Suzuki M, Narita Y, Hirata S, Ohyama H, et al. Distinct subsets of human invariant NKT cells differentially regulate T helper responses via dendritic cells. Eur J Immunol. 2008;38(4):1012-23.

49. Schmid H, Ribeiro EM, Secker KA, Duerr-Stoerzer S, Keppeler H, Dong R, et al. Human invariant natural killer T cells promote tolerance by preferential apoptosis induction of conventional dendritic cells. Haematologica. 2022;107(2):427-36.

50. Kok WL, Denney L, Benam K, Cole S, Clelland C, McMichael AJ, et al. Pivotal Advance: Invariant NKT cells reduce accumulation of inflammatory monocytes in the lungs and decrease immune-pathology during severe influenza A virus infection. J Leukoc Biol. 2012;91(3):357-68.

51. Nagarajan NA, Kronenberg M. Invariant NKT cells amplify the innate immune response to lipopolysaccharide. J Immunol. 2007;178(5):2706-13.

52. Wang X, Bishop KA, Hegde S, Rodenkirch LA, Pike JW, Gumperz JE. Human invariant natural killer T cells acquire transient innate responsiveness via histone H4 acetylation induced by weak TCR stimulation. J Exp Med. 2012;209(5):987-1000.

53. Holzapfel KL, Tyznik AJ, Kronenberg M, Hogquist KA. Antigen-dependent versus -independent activation of invariant NKT cells during infection. J Immunol. 2014;192(12):5490-8.

54. Sharma A, Lawry SM, Klein BS, Wang X, Sherer NM, Zumwalde NA, et al. LFA-1 Ligation by High-Density ICAM-1 Is Sufficient To Activate IFN-gamma Release by Innate T Lymphocytes. J Immunol. 2018;201(8):2452-61.

55. Metelitsa LS, Naidenko OV, Kant A, Wu HW, Loza MJ, Perussia B, et al. Human NKT cells mediate antitumor cytotoxicity directly by recognizing target cell CD1d with bound ligand or indirectly by producing IL-2 to activate NK cells. J Immunol. 2001;167(6):3114-22.

56. Metelitsa LS, Weinberg KI, Emanuel PD, Seeger RC. Expression of CD1d by myelomonocytic leukemias provides a target for cytotoxic NKT cells. Leukemia. 2003;17(6):1068-77.

57. Chen X, Wang X, Besra GS, Gumperz JE. Modulation of CD1d-restricted NKT cell responses by CD4. J Leukoc Biol. 2007;82(6):1455-65.

58. von Gerichten J, Lamprecht D, Opalka L, Soulard D, Marsching C, Pilz R, et al. Bacterial immunogenic alpha-galactosylceramide identified in the murine large intestine: dependency on diet and inflammation. J Lipid Res. 2019;60(11):1892-904.

59. Wieland Brown LC, Penaranda C, Kashyap PC, Williams BB, Clardy J, Kronenberg M, et al. Production of alpha-galactosylceramide by a prominent member of the human gut microbiota. PLoS Biol. 2013;11(7):e1001610.

60. An D, Oh SF, Olszak T, Neves JF, Avci FY, Erturk-Hasdemir D, et al. Sphingolipids from a symbiotic microbe regulate homeostasis of host intestinal natural killer T cells. Cell. 2014;156(1-2):123-33.

61. Kain L, Webb B, Anderson BL, Deng S, Holt M, Costanzo A, et al. The identification of the endogenous ligands of natural killer T cells reveals the presence of mammalian alpha-linked glycosylceramides. Immunity. 2014;41(4):543-54.

62. Kain L, Costanzo A, Webb B, Holt M, Bendelac A, Savage PB, et al. Endogenous ligands of natural killer T cells are alpha-linked glycosylceramides. Molec Immunol. 2015;68(2 Pt A):94-7.

63. Ortaldo JR, Young HA, Winkler-Pickett RT, Bere EW, Jr., Murphy WJ, Wiltrout RH. Dissociation of NKT stimulation, cytokine induction, and NK activation in vivo by the use of distinct TCR-binding ceramides. J Immunol. 2004;172(2):943-53.

64. Paget C, Mallevaey T, Speak AO, Torres D, Fontaine J, Sheehan KC, et al. Activation of invariant NKT cells by toll-like receptor 9-stimulated dendritic cells requires type I interferon and charged glycosphingolipids. Immunity. 2007;27(4):597-609.

65. Salio M, Speak AO, Shepherd D, Polzella P, Illarionov PA, Veerapen N, et al. Modulation of human natural killer T cell ligands on TLR-mediated antigen-presenting cell activation. Proc Natl Acad Sci U S A. 2007;104(51):20490-5.

66. Fox LM, Cox DG, Lockridge JL, Wang X, Chen X, Scharf L, et al. Recognition of lyso-phospholipids by human natural killer T lymphocytes. PLoS Biol. 2009;7(10):e1000228.

67. Facciotti F, Ramanjaneyulu GS, Lepore M, Sansano S, Cavallari M, Kistowska M, et al. Peroxisome-derived lipids are self antigens that stimulate invariant natural killer T cells in the thymus. Nat Immunol. 2012;13(5):474-80.

68. Gately CM, Podbielska M, Counihan T, Hennessy M, Leahy T, Moran AP, et al. Invariant Natural Killer T-cell anergy to endogenous myelin acetyl-glycolipids in multiple sclerosis. J Neuroimmunol. 2013;259(1-2):1-7.

69. Bedard M, Shrestha D, Priestman DA, Wang Y, Schneider F, Matute JD, et al. Sterile activation of invariant natural killer T cells by ER-stressed antigen-presenting cells. Proc Natl Acad Sci U S A. 2019;116(47):23671-81.

70. Brigl M, Bry L, Kent SC, Gumperz JE, Brenner MB. Mechanism of CD1d-restricted natural killer T cell activation during microbial infection. Nat Immunol. 2003;4(12):1230-7.

71. Brigl M, Tatituri RV, Watts GF, Bhowruth V, Leadbetter EA, Barton N, et al. Innate and cytokine-driven signals, rather than microbial antigens, dominate in natural killer T cell activation during microbial infection. J Exp Med. 2011;208(6):1163-77.

72. Godfrey DI, Kronenberg M. Going both ways: immune regulation via CD1d-dependent NKT cells. J Clin Invest. 2004;114(10):1379-88.

73. Stetson DB, Mohrs M, Reinhardt RL, Baron JL, Wang ZE, Gapin L, et al. Constitutive cytokine mRNAs mark natural killer (NK) and NK T cells poised for rapid effector function. J Exp Med. 2003;198(7):1069-76.

74. Watarai H, Sekine-Kondo E, Shigeura T, Motomura Y, Yasuda T, Satoh R, et al. Development and function of invariant natural killer T cells producing T(h)2- and T(h)17-cytokines. PLoS Biol. 2012;10(2):e1001255.

75. Constantinides MG, Bendelac A. Transcriptional regulation of the NKT cell lineage. Cur Opin Immunol. 2013;25(2):161-7.

76. Lee YJ, Holzapfel KL, Zhu J, Jameson SC, Hogquist KA. Steady-state production of IL-4 modulates immunity in mouse strains and is determined by lineage diversity of iNKT cells. Nat Immunol. 2013;14(11):1146-54.

77. Wang H, Hogquist KA. How Lipid-Specific T Cells Become Effectors: The Differentiation of iNKT Subsets. Front Immunol. 2018;9:1450.

78. Lee YJ, Wang H, Starrett GJ, Phuong V, Jameson SC, Hogquist KA. Tissue-Specific Distribution of iNKT Cells Impacts Their Cytokine Response. Immunity. 2015;43(3):566-78.

79. Savage AK, Constantinides MG, Han J, Picard D, Martin E, Li B, et al. The transcription factor PLZF directs the effector program of the NKT cell lineage. Immunity. 2008;29(3):391-403.

80. Eidson M, Wahlstrom J, Beaulieu AM, Zaidi B, Carsons SE, Crow PK, et al. Altered development of NKT cells, gammadelta T cells, CD8 T cells and NK cells in a PLZF deficient patient. PLoS One. 2011;6(9):e24441.

81. Constantinides MG, Picard D, Savage AK, Bendelac A. A naive-like population of human CD1d-restricted T cells expressing intermediate levels of promyelocytic leukemia zinc finger. J Immunol. 2011;187(1):309-15.

82. Gutierrez-Arcelus M, Teslovich N, Mola AR, Polidoro RB, Nathan A, Kim H, et al. Lymphocyte innateness defined by transcriptional states reflects a balance between proliferation and effector functions. Nat Commun. 2019;10(1):687.

83. Gumperz JE, Miyake S, Yamamura T, Brenner MB. Functionally Distinct Subsets of CD1d-restricted Natural Killer T Cells Revealed by CD1d Tetramer Staining. J Exp Med. 2002;195(5):625-36.

84. Lee PT, Benlagha K, Teyton L, Bendelac A. Distinct Functional Lineages of Human Valpha24 Natural Killer T Cells. J Exp Med. 2002;195(5):637-41.

85. Montoya CJ, Pollard D, Martinson J, Kumari K, Wasserfall C, Mulder CB, et al. Characterization of human invariant natural killer T subsets in health and disease using a novel invariant natural killer T cell-clonotypic monoclonal antibody, 6B11. Immunology. 2007;122(1):1-14.

86. Zhou L, Adrianto I, Wang J, Wu X, Datta I, Mi QS. Single-Cell RNA-Seq Analysis Uncovers Distinct Functional Human NKT Cell Sub-Populations in Peripheral Blood. Front Cell Dev Biol. 2020;8:384.

87. Erkers T, Xie BJ, Kenyon LJ, Smith B, Rieck M, Jensen KP, et al. High-parametric evaluation of human invariant natural killer T cells to delineate heterogeneity in allo- and autoimmunity. Blood. 2020;135(11):814-25.

88. O'Reilly V, Zeng SG, Bricard G, Atzberger A, Hogan AE, Jackson J, et al. Distinct and overlapping effector functions of expanded human CD4+, CD8alpha+ and CD4-CD8alpha- invariant natural killer T cells. PLoS One. 2011;6(12):e28648.

89. Chan AC, Leeansyah E, Cochrane A, d'Udekem d'Acoz Y, Mittag D, Harrison LC, et al. Ex-vivo analysis of human natural killer T cells demonstrates heterogeneity between tissues and within established CD4(+) and CD4(-) subsets. Clin Exp Immunol. 2013;172(1):129-37.

90. Kawano T, Cui J, Koezuka Y, Toura I, Kaneko Y, Motoki K, et al. CD1d-restricted and TCR-mediated activation of valpha14 NKT cells by glycosylceramides. Science. 1997;278(5343):1626-9.

91. Carreno LJ, Saavedra-Avila NA, Porcelli SA. Synthetic glycolipid activators of natural killer T cells as immunotherapeutic agents. Clin Transl Immunology. 2016;5(4):e69.

92. Burdin N, Brossay L, Kronenberg M. Immunization with alpha-galactosylceramide polarizes CD1-reactive NK T cells towards Th2 cytokine synthesis. Eur J Immunol. 1999;29(6):2014-25.

93. Miyamoto K, Miyake S, Yamamura T. A synthetic glycolipid prevents autoimmune encephalomyelitis by inducing TH2 bias of natural killer T cells. Nature. 2001;413(6855):531-4.

94. Yu KO, Im JS, Molano A, Dutronc Y, Illarionov PA, Forestier C, et al. Modulation of CD1d-restricted NKT cell responses by using N-acyl variants of alpha-galactosylceramides. Proc Natl Acad Sci U S A. 2005;102(9):3383-8.

95. Schmieg J, Yang G, Franck RW, Tsuji M. Superior protection against malaria and melanoma metastases by a C-glycoside analogue of the natural killer T cell ligand alpha-Galactosylceramide. J Exp Med. 2003;198(11):1631-41.

96. Goff RD, Gao Y, Mattner J, Zhou D, Yin N, Cantu C, 3rd, et al. Effects of lipid chain lengths in alpha-galactosylceramides on cytokine release by natural killer T cells. J Am Chem Soc. 2004;126(42):13602-3.

97. Arora P, Baena A, Yu KO, Saini NK, Kharkwal SS, Goldberg MF, et al. A single subset of dendritic cells controls the cytokine bias of natural killer T cell responses to diverse glycolipid antigens. Immunity. 2014;40(1):105-16.

98. Sullivan BA, Nagarajan NA, Wingender G, Wang J, Scott I, Tsuji M, et al. Mechanisms for glycolipid antigen-driven cytokine polarization by Valpha14i NKT cells. J Immunol. 2010;184(1):141-53.

99. Dangerfield EM, Cheng JM, Knight DA, Weinkove R, Dunbar PR, Hermans IF, et al. Species-specific activity of glycolipid ligands for invariant NKT cells. Chembiochem. 2012;13(9):1349-56.

100. Wang X, Chen X, Rodenkirch L, Simonson W, Wernimont S, Ndonye RM, et al. Natural killer T-cell autoreactivity leads to a specialized activation state. Blood. 2008;112(10):4128-38.

101. Bricard G, Venkataswamy MM, Yu KO, Im JS, Ndonye RM, Howell AR, et al. Alpha-galactosylceramide analogs with weak agonist activity for human iNKT cells define new candidate anti-inflammatory agents. PLoS One. 2010;5(12):e14374.

102. Purbhoo M, Yigit B, Moskowitz D, Lim M, Shapiro I, Alsaraby A, et al. 400 Persistence and tissue distribution of agent-797 – a native allogeneic iNKT cell-therapy drug product. Journal for ImmunoTherapy of Cancer. 2021;9(Suppl 2):A432-A.

103. Trujillo-Ocampo A, Cho HW, Clowers M, Pareek S, Ruiz-Vazquez W, Lee SE, et al. IL-7 During Antigenic Stimulation Using Allogeneic Dendritic Cells Promotes Expansion of CD45RA(-)CD62L(+)CD4(+) Invariant NKT Cells With Th-2 Biased Cytokine Production Profile. Front Immunol. 2020;11:567406.

104. Huijts CM, Schneiders FL, Garcia-Vallejo JJ, Verheul HM, de Gruijl TD, van der Vliet HJ. mTOR Inhibition Per Se Induces Nuclear Localization of FOXP3 and Conversion of Invariant NKT (iNKT) Cells into Immunosuppressive Regulatory iNKT Cells. J Immunol. 2015;195(5):2038-45.

105. Iwamura C, Nakayama T. Role of CD1d- and MR1-Restricted T Cells in Asthma. Front Immunol. 2018;9:1942.

106. Paget C, Trottein F. Role of type 1 natural killer T cells in pulmonary immunity. Mucosal Immunol. 2013;6(6):1054-67.

107. van Dieren JM, van der Woude CJ, Kuipers EJ, Escher JC, Samsom JN, Blumberg RS, et al. Roles of CD1d-restricted NKT cells in the intestine. Inflamm Bowel Dis. 2007;13(9):1146-52.

For Chapter V

1. Chou, Jennifer P et al. “Prostaglandin E2 promotes features of replicative senescence in chronically activated human CD8+ T cells.” *PloS one* vol. 9,6 e99432. 11 Jun. 2014, doi:10.1371/journal.pone.0099432

2. Christoph Herbel, Nikolaos Patsoukis, Jessica D Weaver, Vassiliki A. Boussiotis; Prostaglandin E2 Alters the Differentiation and Function of Antigen-Specific T Cells By Targeting the Metabolic Gene Regulatory Network Downstream of mTORC1. *Blood* 2016; 128 (22): 552. doi: https://doi.org/10.1182/blood.V128.22.552.552

3. Maas-Bauer, Kristina et al. “Invariant natural killer T-cell subsets have diverse graft-versus-host-disease-preventing and antitumor effects.” Blood vol. 138,10 (2021): 858-870. doi:10.1182/blood.2021010887

4. Sag, Duygu et al. “IL-10-producing NKT10 cells are a distinct regulatory invariant NKT cell subset.” *The Journal of clinical investigation* vol. 124,9 (2014): 3725-40. doi:10.1172/JCI72308

5. Burrello, Claudia et al. “IL10 secretion endows intestinal human iNKT cells with regulatory functions towards pathogenic T lymphocytes.” *Journal of Crohn's & colitis*, jjac049. 31 Mar. 2022, doi:10.1093/ecco-jcc/jjac049

6. LaMarche, Nelson M et al. “Distinct iNKT Cell Populations Use IFNγ or ER Stress-Induced IL-10 to Control Adipose Tissue Homeostasis.” *Cell metabolism* vol. 32,2 (2020): 243-258.e6. doi:10.1016/j.cmet.2020.05.017

7. Khurana, Priya et al. “Distinct Bioenergetic Features of Human Invariant Natural Killer T Cells Enable Retained Functions in Nutrient-Deprived States.” *Frontiers in immunology* vol. 12 700374. 9 Aug. 2021, doi:10.3389/fimmu.2021.70037